Optimization of CO_2 Flooding Strategy to Enhance Heavy Oil Recovery

A Thesis

Submitted to

the Faculty of Graduate Studies and Research

in Partial Fulfillment of the Requirements

for the Degree of

Master of Applied Science

in

Petroleum Systems Engineering

University of Regina

By

Tuo Huang

Regina, Saskatchewan

July, 2015

UNIVERSITY OF REGINA

FACULTY OF GRADUATE STUDIES AND RESEARCH

SUPERVISORY AND EXAMINING COMMITTEE

Tuo Huang, candidate for the degree of Master of Applied Science Peteroleum Systems Engineering**,** has presented a thesis titled, ***Optimization of CO_2 Flooding Strategy to Enhamce Heavy Oil Recovery,*** in an oral examination held on May 29, 2015. The following committee members have found the thesis acceptable in form and content, and that the candidate demonstrated satisfactory knowledge of the subject material.

External Examiner:	Dr. Adisorn Aroonwilas, Industrial Systems Engineering
Supervisor:	Dr. Fanhua Zeng, Petroleum Systems Engineering
Committee Member:	Dr. Gang Zhao, Peetroleum Systems Engineering
Committee Member:	Dr. Teeradet Supap, Adjunct
Chair of Defense:	Dr. Allen Herman, Department of Mathematics & Statistics

ABSTRACT

Heavy oil is a significant energy resource around the world. In Canada, there are tremendous heavy oil reserves lying in the north of the provinces of Alberta and Saskatchewan. The key point for heavy oil recovery is to increase the mobility of heavy oil in the reservoir condition. The most effective methods of heavy oil recovery are thermal methods such as steam flooding, cyclic steam stimulation (CSS), steam-assisted gravity drainage (SAGD) and in-situ combustion for the great heavy oil viscosity reduction by heat. However, thermal methods are proving to be unsuitable for most of the heavy oil reservoirs in Canada because of the thin net-pay zones, large depths and other rock, fluid and geological conditions. Therefore, cold production methods are mostly considered.

In recent years there has been more development of solvent injection methods. CO_2 is considered one of the most promising solvents used in both light and heavy oil for its high solubility. In light oil recovery, the production pressure in CO_2 flooding is kept above the minimum miscible pressure in order to maintain the miscibility. Although in heavy oil recovery, CO_2 miscibility can hardly be reached because of the high oil viscosity, but the oil recovery can still be stimulated to a great extent by CO_2 injection.

Different CO_2 flooding strategies can significantly affect the recovery factor. In this study, different injection and pressure control schemes were tested by 1-D core-flooding

experiments to obtain an optimized one. Field data, oil samples and brine from a heavy oil field in north China were used for the core-flooding experiments. Experimental results indicated that a lower CO_2 injection rate led to a higher recovery factor from 31.1% to 36.7%. In terms of the effects of different production strategies, a constant production pressure at the production port yielded a recovery factor of 31.1%, while a pressure depletion at the production port yielded 7% more oil recovery; and the best pressure control scheme was that in which the production pressure was kept constant during the CO_2 injection period, then the model pressure was depleted with the injector shut-in, yielding a recovery factor of 42.5% of the initial OOIP.

Numerical simulations were conducted to history match the experimental results. The same oil relative permeability curve was used to match the experimental results to all tests. Different gas relative permeability curves were obtained when the production pressure schemes were different. A much lower gas relative permeability curve and higher critical gas saturation were achieved in the best pressure control scheme case compared to other cases. The lower gas relative permeability curve indicated that foamy oil was formed in the pressure depletion processes.

A 3-D reservoir model was built by Computer Modeling Group (CMG) software based on field data and relative permeability curves from history match of the tests. Different strategies, including different injection and production schemes and different injection materials were used, and the better results were chosen for analysis.

ACKNOWLEDGEMENTS

I would like to acknowledge my academic supervisor, Dr. Fanhua (Bill) Zeng, for his strong support, excellent guidance, and continuous encouragement throughout my graduate and thesis studies.

I would like to thank the following team members from Dr. Zeng's research group, Hongyang Wang, Sam Hong, Xiang Zhou and Xiaolong Peng for their support, and other group members for their technical discussions and assistance, and most importantly, their encouragement and friendship to me.

Finally, I would like to express great appreciation to the Petroleum Technology Research Center (PTRC) for the research fund to Dr. Zeng.

DEDICATION

To my dear parents, Mrs. Jinfeng Lu and Dr. Xue Huang, for their constant love, unconditional support and endless encouragement.

TABLE OF CONTENTS

LIST OF TABLES

LIST OF FIGURES

CHAPTER 1 INTRODUCTION

1.1 Heavy oil

With global energy demands, petroleum resources are becoming more and more important. However, excessive consumption is causing conventional oil resources to keep declining and now they are nearly depleted. Fortunately, the world's unconventional resources are significant, even several times greater than conventional oil. Heavy oil, one kind of unconventional petroleum resource, has drawn a great deal of attention worldwide. Heavy oil and extra-heavy oil, are defined as high viscosity (higher than 100 cp), low American Petroleum Institute (API) gravity (lower than 22° API) oil chemically characterized by its content of asphaltenes (Meyer et al., 2003). The technically recoverable heavy oil in the world is 434.4 billion barrels according to the survey by the U.S. Geological Survey (USGS) in 2003. Canada and Venezuela are the two countries that have the largest heavy oil deposits. The two most prolific regions are Alberta in Canada and the Orinoco Belt in Venezuela (Meyer et al., 1998). Canada has total heavy oil in-place of over 2.2 trillion barrels, and over 200 billion barrels are recoverable based on current technology (Dusseault, 2001). Heavy oil has become a considerable alternative energy resource.

1.2 Heavy Oil Recovery Methods

Primary oil recovery methods are not suitable for heavy oil because of its nearly non-mobility characteristic and can only recover at most 10% of the original oil in place (OOIP) (Brook et al., 1998). Water flooding is used in some of the heavy oil projects in Canada for its low cost and easy operation. However, its performance is not satisfactory because of the high mobility ratio between water and heavy oil. Low viscosity water can hardly displace high viscosity heavy oil. Water is easy to breakthrough and causes a significant production water-oil ratio (WOR) (Nasehi et al., 2010). Only oil that is moderately heavy with a viscosity range from 500 cp to 4000 cp can be recovered with water flooding and it still has a declining recovery factor as time goes by (Brooks et al., 1998).

Enhanced oil recovery (EOR) methods are more suitable for heavy oil recovery than water flooding. Currently, two kinds of EOR methods are used, thermal and non-thermal. Thermal methods aim to reduce the heavy oil viscosity by heating the heavy oil itself or the formation for the viscosity is very sensitive to temperature. The commonly considered thermal EOR methods in heavy oil are steam flooding, cyclic steam stimulation (CSS) (Vittoratos et al., 1990), steam-assisted gravity drainage (SAGD) (Butler et al., 1981) and in-situ combustion (ISC) (Ramey, 1971). However, most of the heavy oil reservoirs in Canada are not suitable for thermal methods because of the thin pay layers. Thermal

methods used in a thin pay layer reservoir can lead to high heat loss to overburden and underburden; a too deep and high pressure reservoir can lead to a high vapour point of water and heat lost to wellbore; heating a carbonate reservoir can lead to formation damage (Rojas et al., 1991). Moreover, high water usage is another big issue due to global water shortage.

In comparison, non-thermal methods are more suitable for this kind of heavy oil reservoir. They have the advantage of low energy cost and wide adaptability and have been developed and applied more in recent years. Cold heavy oil production with sand (CHOPS) is a non-thermal method and has been successfully used in Alberta and Saskatchewan unconsolidated heavy oil reservoirs with recovery factors between 5% and 15% (Du et al., 2013; Istchenko and Gates, 2011). Solvent based non-thermal methods are also well known, such as vapor extraction (VAPEX) (Butler and Mokrys, 1992) and cyclic solvent injection (CSI) (Lim et al., 1995). The main mechanism of these non-thermal methods is to stimulate oil mobility and reduce heavy oil viscosity by solvent dissolution.

1.3 CO_2 injection

CO_2, currently one of the biggest solvents concerned, is proved to be effective in both laboratories and the field, especially for heavy oil. In the 1950s, researchers started to perform CO_2 flooding experiments in laboratories and observed a high solubility of CO_2 in

oil that can effectively reduce oil viscosity at a relatively high pressure (Johnson et al., 1952; Besean et al., 1959; Holm, 1959, 1987). The earliest reported field pilot test was the Mead Strawn Field in 1964 which consisted of the injection of a small slug of CO_2 followed by an injection of carbonated water and brine; it gave as much as 50 percent more oil production than by conventional water flooding (Holm et. al., 1971). Over half a century's development, CO_2 EOR techniques have become more and more mature. A survey in 1998 showed that the miscible CO_2 recovery method had already led to the production of over 179,000 barrels of oil per day （BOPD) at that time (Moritis, 1998). And now, more CO_2 EOR processes are being developed, such as continuous CO_2 injection, water-CO_2 mixture injection, CO_2 injection followed by water injection, CO_2 injection followed by Water Alternating Gas (WAG) injection, huff and puff processes, etc.(Shi et al., 2008).

No matter which process is used, the key point is the high solubility of CO_2 in oil. Although CO_2 miscibility can hardly be reached in heavy oil cases, oil recovery can still be greatly enhanced. The most important mechanism of CO_2 methods in heavy oil recovery is viscosity reduction. It is reported that, even though CO_2 is not fully miscible in heavy oil, partially dissolved CO_2 can still reduce heavy oil viscosity by a factor of 10 (Rojas et al., 1991). Oil swelling is another important factor in CO_2 EOR methods. Miller and Jones (1981) indicated that one barrel of heavy oil with 17°API can dissolve more than 700 standard cubic feet (scf) CO_2 and has a volume increase of 10% to 30% in certain pressures

and temperatures (Miller et al., 1981). As the oil volume increases, and pore volume remains constant, extra oil is expelled from the porous media which leads to oil recovery enhancement on a large scale. What is more, this swelling effect makes a great contribution to the recovery of residual oil which was impossible to consider before (Moortgat et al., 2013).

Of course, there are other factors that contribute to enhancing heavy oil recovery by CO_2 methods, such as density change of oil and water, interfacial tension reduction, improvement of formation permeability and so on. These are always considered as subordinate factors compared with the two introduced above and always tend to be neglected. However, solution gas drive, which is one of the factors that was neglected before, has been found to be important in recent years. The reason for that is a phenomenon observed under solution gas drive which is called “foamy oil”. When pressure decline occurs in the oil-solution gas phase, little gas bubbles are generated from the oil, trapped and dispersed in the oil phase. This gas-liquid two-phase fluid is known as foamy oil. The existence of foamy oil flow is believed to be one of the most influential factors in stimulating high recovery in many heavy oil reservoirs in Canada and Venezuela (Maini, 2001). The effect of foamy oil can be affirmed and can be utilized in EOR methods. Due to high dissolution into the oil, slow desorbing when depressurizing and the effect of extraction, CO_2 is expected to generate high quality foamy oil (Or et al., 2014; Claridge et al., 1995).

1.4 Thesis objective

The objective of this thesis is to investigate the performance of different CO_2 injection categories in improving oil recovery in heavy oil reservoir development, as follows:

(1) Test physical properties of CO_2 dissolved heavy oil under different pressures using PVT tests.

(2) Test the performance of different CO_2 injection categories using core-flooding tests, including different injection rates, different production pressure control schemes and different CO_2 purity.

(3) Through core-flooding tests, investigate the characteristics and performance of foamy oil flow.

(4) Investigate relative permeability change of CO_2 in the reservoir under different categories.

(5) Test performance of different categories on a large scale by simulating a numerical reservoir model.

1.5 Thesis outline

This thesis is composed of five chapters. In the first chapter, a brief introduction of the research background and objective of this thesis is presented. Chapter 2 provides a comprehensive literature review of the information and knowledge on research backgrounds, including mechanisms of CO_2 in EOR methods and foamy oil flow. Chapter

3 describes the laboratory experiment studies, including experimental materials, experimental procedures, and discussion of the experimental results. Chapter 4 involves the components of using numerical simulations to history match the physical experiments and predict reservoir model heavy oil recovery. The last chapter summarizes the scientific discoveries from the research and gives some recommendations for future studies.

CHAPTER 2 LITERATURE REVIEW

2.1 Gas injection

Gas injection or gas flooding is an established method to enhance oil recovery beyond the primary oil recovery methods (Jhaveri et al., 2014; Craig and Bray, 1971). Over ninety projects had been developed to improve oil recovery by air and gas injection as early as 1917 (Craig and Bray, 1971).

2.1.1 Miscible gas injection

When referring to gas injection, the concept of miscibility must be introduced. Miscible flooding can be defined as a condition when there is no phase boundary or interface between displaced and displacing substances (Craig and Bray, 1971). Under this condition, capillary forces do not exist. Another easier way to define miscibility is to distinguish it from solubility. Solubility is defined as the ability of a limited amount of one substance to mix with another to form a single homogeneous phase, while miscibility is the ability of two or more substances to form a single homogeneous phase no matter in what kind of proportions (Holm, 1986). Miscible displacement in oil reservoirs is so important because when miscibility is achieved, the interfacial tension (IFT) between oil and displacement substances is eliminated, and the residual oil saturation will be zero in the swept region (Holm, 1986). Theoretically, all the oil can be recovered from the

reservoir when miscibility is achieved. The most important factor in miscibility is minimum miscibility pressure (MMP). MMP is the minimum pressure when reservoir crude oil is miscible with the displacement fluid. Miscible flooding has been one of the most promising techniques to stimulate oil recovery since the 1950s (Thomas et al., 1994; Hall and Geffen, 1957; Kehn et al., 1958; Whorton and Kieschnick, 1950; Stone and Crump, 1956)

2.1.2 Immiscible gas injection

In the case of heavy oil reservoirs, miscible gas flooding can hardly be achieved due to their high viscosity, low API, and low reservoir pressure. However, gas injection still appears to be a practical EOR method (Zhang et al., 2006). Immiscible gas flooding is widely used in heavy oil reservoirs. Although miscibility cannot be achieved, the effect of viscosity reduction, oil swelling, and solution gas drive by immiscible gas can still make a significant contribution to heavy oil recovery. A natural gas injection heavy oil project in the Orinoco Oil Belt, Venezuela in operation since 1963 has proved that high viscosity is not necessarily a limiting factor in oil production. In this project, the cumulative recovery factor has been 32% of OOIP and the estimated final recovery factor could reach 45% of OOIP (Garcia, 1983).

The most important mechanism of immiscible gas injection methods in heavy oil is viscosity reduction. As high viscosity is the main challenge for heavy oil recovery, gas

solvent injection to reduce heavy oil viscosity is the most efficient mechanism. The oil swelling effect is also important. When gas is dissolved in heavy oil, the volume of heavy oil expands. As the oil volume increases, and pore volume remains constant, extra oil is expelled from the porous media which leads to oil recovery enhancement on a large scale (Miller et al., 1981). Also, IFT is reduced when gas is dissolved in heavy oil, even though it cannot be reduced to zero. Solution gas drive is another important mechanism in which the foamy oil flow phenomenon has proved to be one of the major reasons for high oil recovery in some gas injection developed heavy oil reservoirs (Alshmakly and Maini, 2010).

Many kinds of gas have been investigated and proved to be suitable for gas injection in heavy oil reservoirs, such as methane, ethane, propane, fuel gas, carbon dioxide, etc (Spivak and Chima, 1984; Zhang et al., 2000; Dong et al., 2006; Du et al., 2013; Sahin et al., 2007).

2.2 CO_2 characteristics

When we mention CO_2, the first thing that comes to mind is that it is one important component of the atmosphere. Also, CO_2 is well known as a greenhouse gas that is primarily responsible for global warming. It is reported that the concentration of CO_2 in the atmosphere increased from 280 parts per million by volume (ppmv) in around 1860 to 316 ppmv in 1958 and rapidly to 369 ppmv in 2005 (Wang et al., 2011). CO_2 does not play a good role in the eyes of most people. Nevertheless, CO_2 is proved to be one of the

most important solvents in the petroleum field, effective in both laboratories and the field, especially for heavy oil.

In the 1950s, investigators (Johnson et al., 1952; Besean et al., 1959; Holm, 1959) started to use CO_2 in laboratory experiments. They observed a high solubility of CO_2 in oil, and at high pressure, it could effectively reduce oil viscosity, and displacement efficiency was improved. Moreover, with CO_2 dissolution, the oil would swell a lot. In addition, residual oil would be highly swollen, and the residual oil saturation was lower than in the absence of CO_2. (Johnson et al., 1952; Besean et al., 1959; Holm, 1959, 1987). The earliest reported field pilot test was the Mead Strawn Field in 1964. The test consisted of injection of a small slug of CO_2 followed by carbonated water and brine injection. It finally gave as much as 50 percent more oil production than by conventional water flooding (Holm et. al., 1971). Over half a century's development, CO_2 EOR techniques have become more and more mature. A survey in 1998 showed that the miscible CO_2 recovery method had already led to a production of over 179,000 barrels of oil per day (BOPD) (Moritis, 1998).

The mechanism of CO_2 displacing oil from porous rocks can be summarized as follows (Holm and Josendal, 1974):

1) Promotes swelling
2) Reduces oil viscosity
3) Highly soluble in water
4) Exerts an acidic effect on rock

5) Vaporizes and extracts portions of crude oil

6) Transports chromatographically through porous rock

Under miscible flooding, all these CO_2 mechanisms can be fully effective. CO_2 mixes with oil by three mass transfer mechanisms:

1) Solubility

2) Diffusion

3) Dispersion

of which solubility accounts for the greater part (Dyer and Farouq Ali, 1989; Bon et al., 2005). With miscible flooding, the IFT between CO_2 and resident oil is reduced to zero eliminating the capillary pressure, which leads to theoretically zero percent residual oil saturation (Holm, 1986).

As these mechanisms are well-known, many CO_2 based EOR methods or processes are proposed, such as continuous CO_2 gas injection, injection of CO_2 gas or liquid slug flowed by continuous water injection, injection of water-CO_2 mixture, CO_2 gas or liquid slug followed by water alternating CO_2 gas injection (WAG), etc. (Shi and Kantzas, 2008).

As heavy oil has high viscosity and low API, it is hard for CO_2 to achieve miscibly. Therefore, IFT and capillary pressure are not zero, resulting in vestigial residual oil (Ghedan, 2009). However, CO_2 immiscible flooding still makes a great contribution to oil recovery by several mechanism factors (Danesh, 1998; Srivastava, 2000):

1) Lower interfacial tensions

2) Viscosity reduction

3) Oil swelling

4) Improvement of formation permeability

5) Solution gas flooding

6) Density change of oil and water

Of these, viscosity reduction, oil swelling, lower interfacial tensions and solution gas flooding are the greater contributory factors and will be introduced below.

2.2.1 Solubility

The high solubility of CO_2 in oil is the key to CO_2 EOR methods, even in heavy oil. It is reported that the solubility of CO_2 in oil decreases as oil API decreases, or viscosity increases (Chung, 1988).

Figure 2-1 shows the relationship between the solubility of CO_2 in oil and temperature, and pressure. It needs to be mentioned that the solubility of CO_2 in oil is only sensitive when CO_2 is in the gas phase. This can be seen when comparing the trend of the 75°F curve of pressure below 1000 psia and above, because at this temperature the CO_2 is liquefied when pressure is greater than 1000 psia. Also, the figure shows that the 200°F curve crosses with the 140°F and 75°F curves at about 3000 psia and 4000 psia respectively. That is because, at high pressure, liquids become denser, the molecules of liquids are

compressed much closer to each other, and leave less room for gas molecules. Therefore, at high pressure, the solubility of gasses may increase as the temperature increases. But at lower pressure, although the space between liquid molecules is more than enough, the gas molecules hold more energy and become volatile at higher temperature, which leads to a decrease in the solubility of the gas (Chung, 1988).

Figure 2-2 is an interesting but effective method to predict the solubility of CO_2 in heavy oil with different API under different pressure and temperature conditions. As the line in the figure shows, the solubility of CO_2 in 17°API heavy oil under 130°F and 1200 psia is approximately 380 standard cubic feet/barrel (SCF/bbl) (Chung, 1988).

Chung (1988) also stated that the solubility of CO_2 in live oil is lower than in dead oil, as shown in Figure 2-3. A live oil saturated with CH_4 (methane) has less room for CO_2 to dissolve. But as CO_2 is injected in the live oil, CH_4 will be released from the heavy oil as the solution gas is stripped by CO_2.

2.2.2 Viscosity reduction

When CO_2 dissolves in heavy oil, the oil viscosity is largely reduced. This is the most important effect of CO_2 immiscible flooding on heavy oil. Even at a very low pressure, CO_2 can still greatly reduce the heavy oil viscosity. How much the viscosity is reduced depends on the quantity of CO_2 dissolved, the dead oil viscosity, temperature and pressure (Chung, 1988). It is found that the magnitude of oil viscosity reduction is a linear

function of CO_2 concentration (Enayati et al., 2008). Figure 2-4 shows the viscosity change as a function of

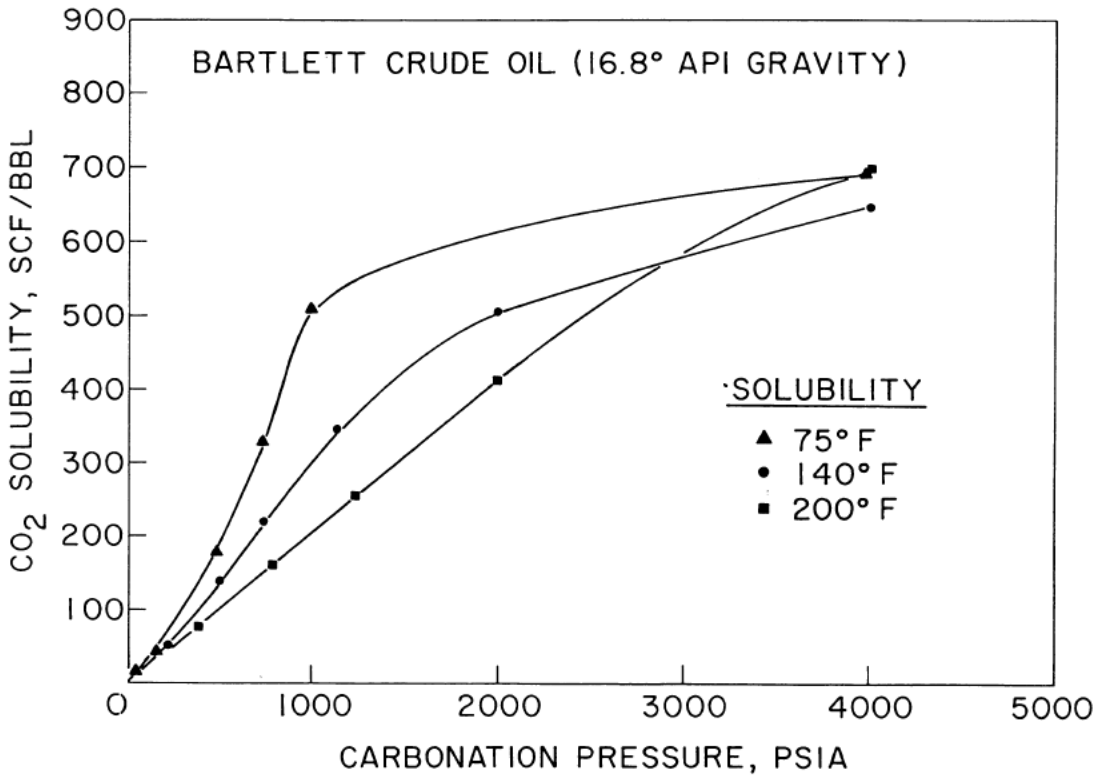

Figure 2-1 Solubility of oil with 17°API at 75°F, 140°F, and 200°F (Chung, 1988; Miller and Jones, 1981)

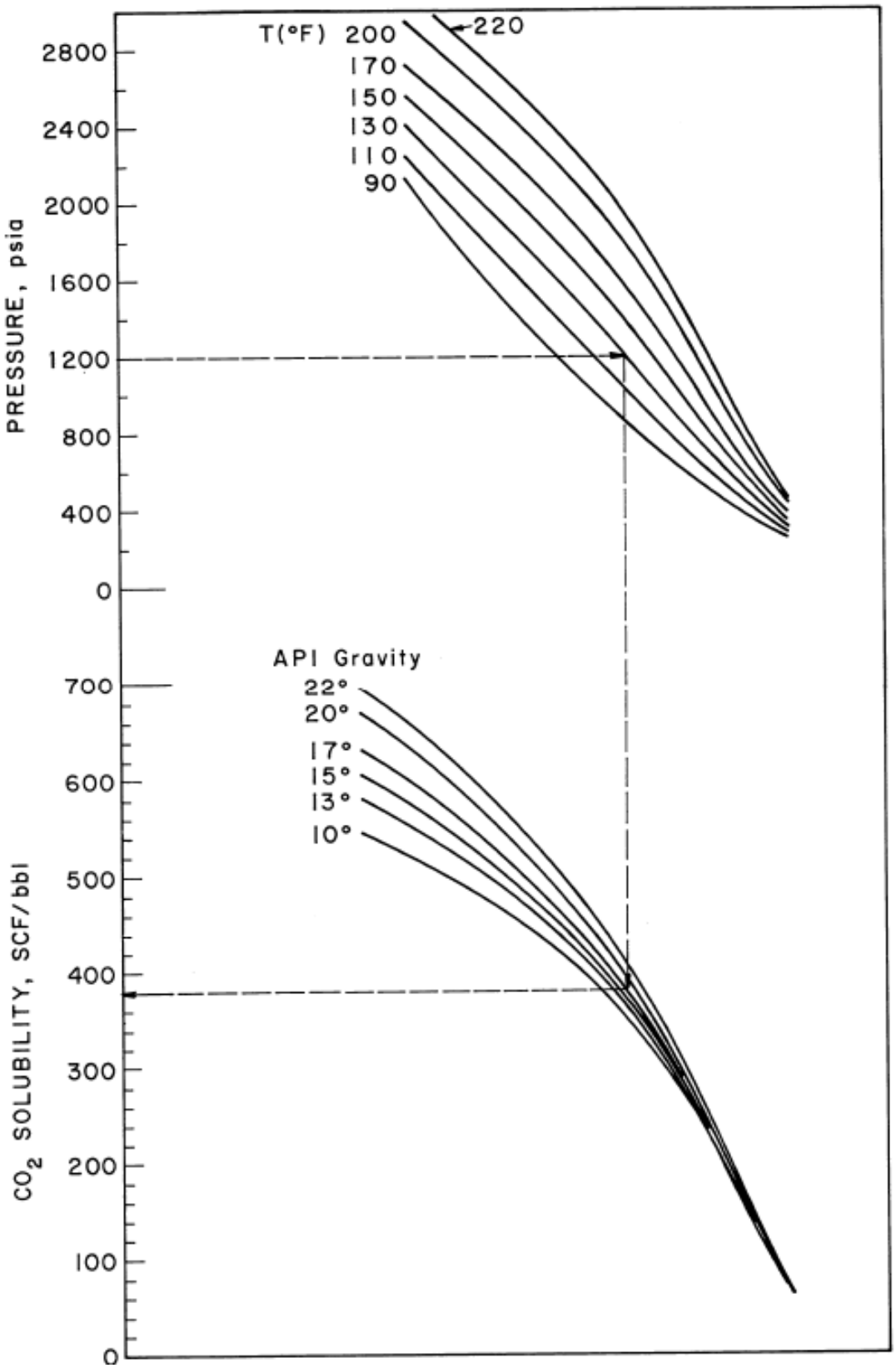

Figure 2-2 A prediction method of CO_2 solubility in heavy oil (Chung, 1988)

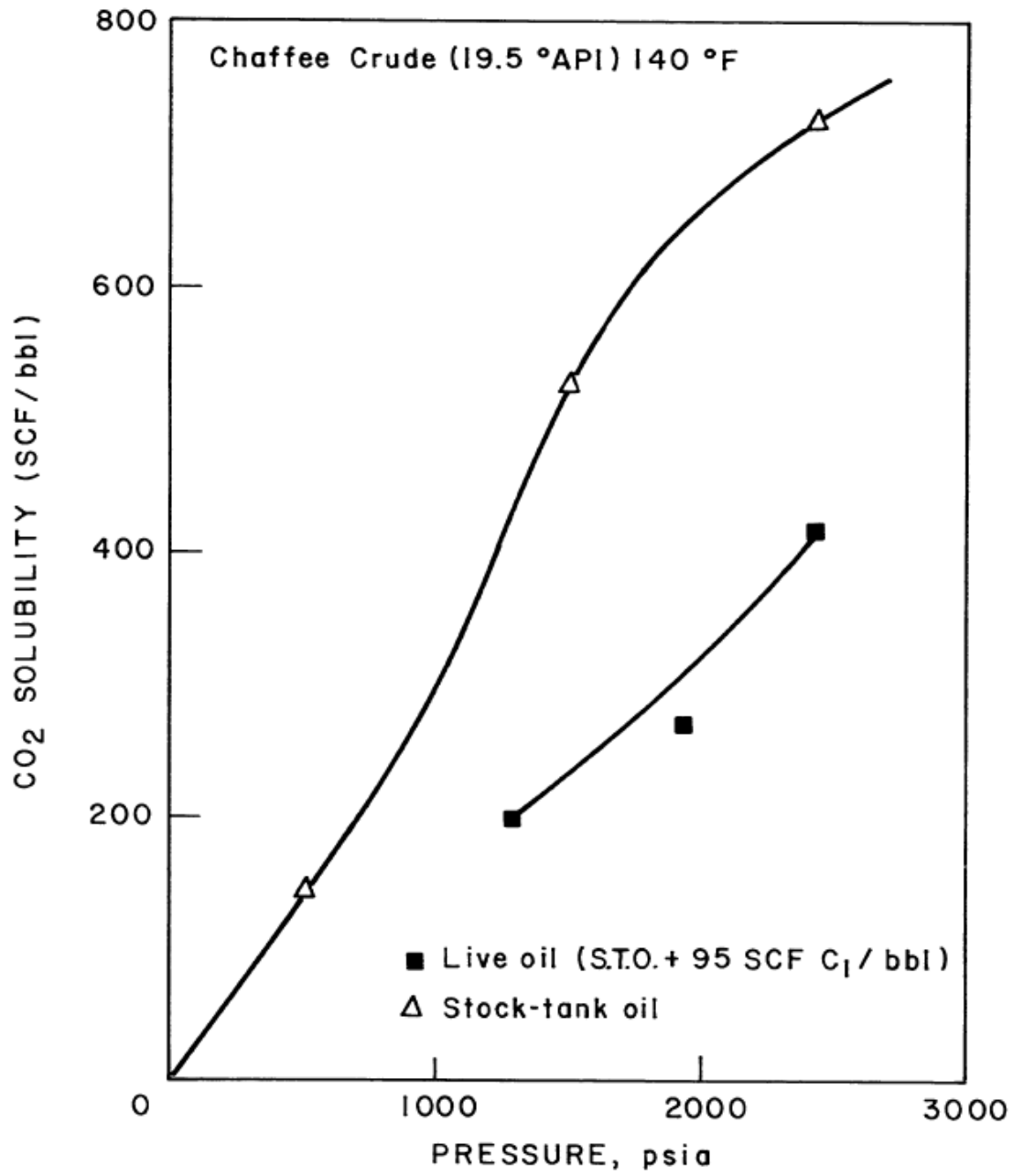

Figure 2-3 CO_2 solubility in dead and live oil (Chung, 1988)

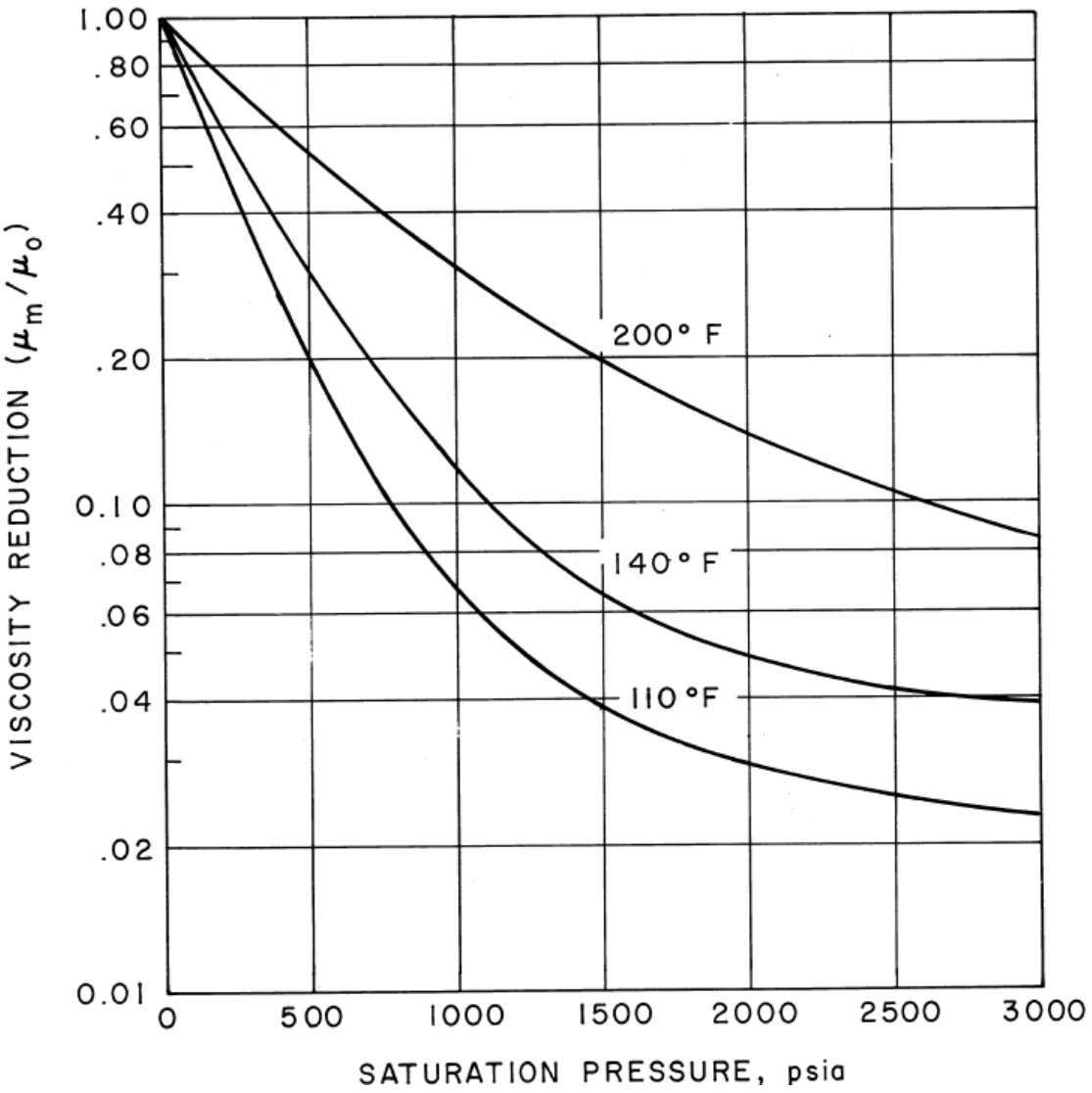

Figure 2-4 Viscosity reduction as functions of temperature and CO_2-saturated pressure

(Chung, 1988)

saturated pressure at three different temperatures. This figure can be used as a simple way to estimate the viscosity reduction, but only roughly. As can be seen in the figure, viscosity reduces faster at relatively lower pressure and temperature. In high pressure conditions, the viscosity reduction is no longer as significant as before and needs to be heated to a higher temperature for further reduction (Chung, 1988; Chung et al., 1988). Other investigators have also evaluated the ability of CO_2 to reduce the oil viscosity when dissolved in (Kantar et al., 1985; Huang et al., 1987; Hatzignatiou and Lu, 1994).

Different mathematical correlations have been developed to estimate the oil viscosity change with gas dissolution. Shu (1984) indicated that the Lederer (1933) equation was excellent in representing high viscosity ratio systems such as heavy oil and CO_2. The Lederer equation is:

$$\ln \mu_m = X_O \ln (\mu_O) + X_S \ln(\mu_S) \qquad 2.1$$

where

$$X_S = \frac{V_S}{\alpha V_O + V_S} \qquad 2.2$$

and

$$X_O = 1 - X_S \qquad 2.3$$

In the equation, V is volume fraction; μ is viscosity; subscripts O, S and m stand for heavy oil, CO_2 and the mixture, respectively; and α is an empirical parameter which needs to be determined by data.

Shu (1984) developed a correlation for α as:

$$\alpha = \frac{17.04(\gamma_O - \gamma_S)^{0.5237}\gamma_O^{3.2745}\gamma_S^{1.6316}}{\ln(\mu_O/\mu_S)} \quad 2.4$$

where γ_s and γ_o are specific gravities of the solvent and heavy oil. This correlation is based on data of organic solvents mixed with heavy oil or bitumen and cannot be applied to CO_2 and heavy oil systems.

Chung (1988) developed a correlation for α with function of temperature, pressure and specific gravity:

$$\alpha = 0.255\gamma^{-4.16}T_r^{1.85}\left[\frac{e^{7.36} - e^{7.36(1-p_r}}{e^{7.36}-1}\right] \quad 2.5$$

where T_r = T/547.57 and P_r = p/1071 are reduced temperature and pressure, respectively; γ is the specific gravity; 547.57 and 1071 are the critical temperature and pressure, T is in °R; and p is in psia.

Other correlations have also been developed, such as those by Chew and Connally Jr. in 1959, Simon and Graue in 1965, Lobe in 1973, Beggs and Robinson in 1975, Mehrotra and Svrcek in 1982, and Emera and Sarma in 2008.

2.2.3 Swelling effect

Oil swelling is another important factor in CO_2 EOR methods. Miller and Jones (1981) indicated that one barrel of heavy oil with 17°API can dissolve more than 700 standard cubic feet (scf) CO_2 and has a volume increase of 10% to 30% in certain pressures and temperatures.

The mechanism of the swelling effect to stimulate oil recovery is simple. As CO_2 is

dissolved in oil in the reservoir, the volume of the oil increases. And the increased volume of oil will enter more pore space than before, and connect with the discontinuous oil droplets which were trapped in pores. Once they are connected, the trapped droplets merge with the flowing phase and become able to flow freely. What is more, this swelling effect makes a great contribution to recovering residual oil which was impossible to consider before. (Moortgat et al., 2013)

The magnitude of the oil swelling when the CO_2 dissolves is controlled by the swelling factor, which is the ratio of the volume of CO_2 in saturated oil at the saturation pressure and reservoir temperature to the original volume at the same temperature and one atmosphere pressure (Welker and Dunlop, 1963; Chung, 1988). The swelling factor has a direct linear relationship with CO_2 solubility in oil before reaching bubble point pressure (Dyer and Farouq, 1989). Therefore, as introduced above, when oil API increases, the oil swelling efficiency is greater because the solubility of CO_2 in lighter oil is higher.

Figure 2-5 shows the linear relationship between the swelling factor and CO_2 solubility conducted by Welker and Dunlop's correlation (1963):

$$\mathrm{SF} = 1.0 + (0.35R_{SC})/1000 \qquad 2.6$$

where R_{sc} is the solubility.

This correlation has apparent defects. First of all, it is not suitable for mixture gasses. Second, it does not mention other factors such as oil properties and molecular size (Simon and Graue, 1965). Therefore, other correlations by other researchers were

obtained.

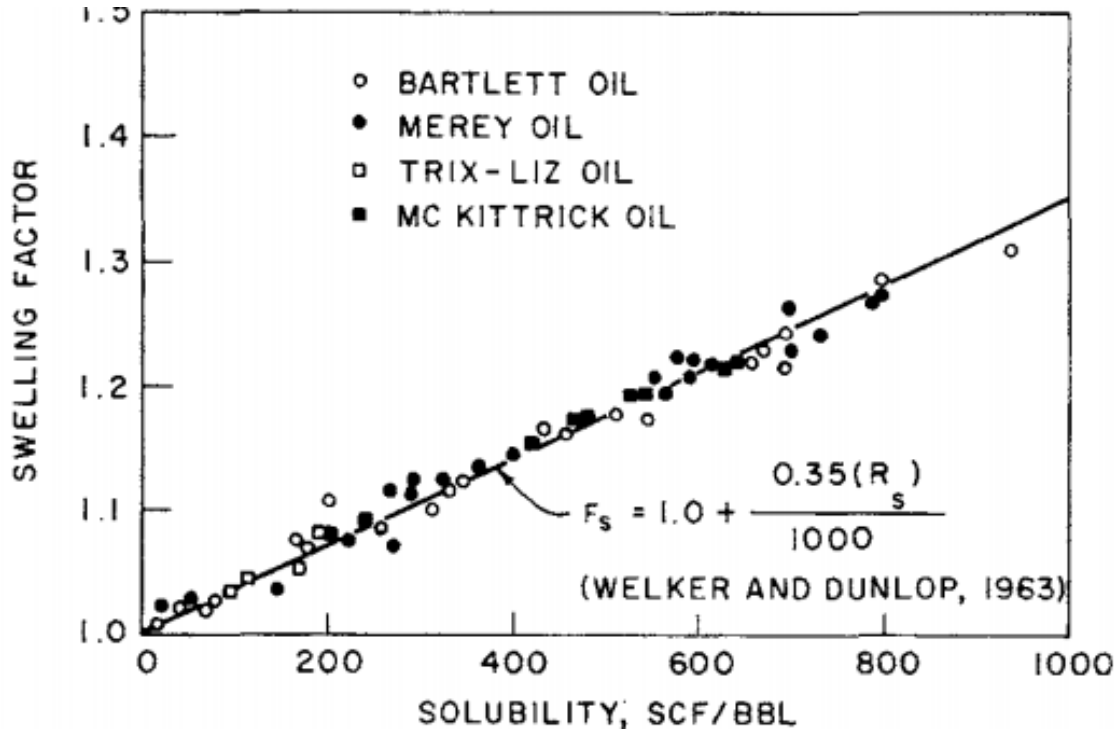

Figure 2-5 Welker and Dunlop's correlation between swelling factor and solubility (Welker and Dunlop, 1963; Chung et al., 1988)

Teja and Sandler (1980) developed a correlation:

$$\mathrm{SF} = \frac{V_{m2}}{V_{m1}} \times \frac{1}{1-R_s} \qquad 2.7$$

where V_{m1} is the molar volume of CO_2 saturated oil at saturation temperature and atmospheric pressure; V_{m2} is the molar volume of CO_2 saturated oil at saturation temperature and saturation pressure; and R_s is CO_2 solubility.

In 2008, Emera and Sarma reported a swelling factor correlation. For heavier oil with molecular weight (MW) larger than or equal to 300:

$$\mathrm{SF} = 1 + 0.3302\mathrm{Y} - 0.8417Y^2 + 1.5804Y^3 - 1.074Y^4 \qquad 2.8$$

where

$$\mathrm{Y} = 1000 \times \left\{ \left[\left(\frac{n}{MW} \right) \times sol(mole\ fraction)^2 \right]^{\exp\left(\frac{n}{MW}\right)} \right\} \qquad 2.9$$

For lighter oil with MW smaller than 300:

$$\mathrm{SF} = 1 + 0.48411\mathrm{Y} - 0.9928Y^2 + 1.6019Y^3 - 1.2773Y^4 + 0.48267Y^5 - 0.06671Y^6 \qquad 2.10$$

where n is oil specific gravity; the "sol (mole fraction)" is the solution gas solubility mole fraction, and here is the solubility of CO_2 in the mole fraction.

2.3 Foamy oil flow

Solution gas drive, which was previously one of the neglected factors, has been found to be important in recent years. The reason for this is a phenomenon observed under solution gas drive which is called "foamy oil".

In several heavy oil reservoir development projects in Canada and Venezuela, the recovery factor of the primary recovery process showed unexpected anomalous performances which were much higher than expected. When the production sample at the wellhead was collected, the container for collecting the sample appeared to be nearly empty. Less than 20% of its volume was filled with oil when opened in the laboratory several days later (Smith, 1988). Investigators have studied this phenomenon in the past several decades and the most significant factor for this has been believed to be the performance of foamy oil flow.

When pressure decline happens in the oil-solution gas phase, little gas bubbles are generated from the oil, trapped and dispersed in the oil phase. This gas-liquid two-phase fluid is known as foamy oil.

In the normal primary production process in conventional oil reservoirs, the main drive mechanism is the pressure differential between the reservoirs and the well bottom hole. Pressure decline is always faster than fluid injection. The gas-oil ratio (GOR) rises from being initially low to much higher. The production rate declines fast and the total recovery factor is normally less than 25% (Sheng, 1999). These are characteristics of primary conventional oil reserve developments. For conventional oil or lighter oil, solution gas will evolve out rapidly when pressure drop occurs, and the gas will form a continuous phase quickly with high mobility. That will lead to high production GOR and higher reservoir pressure drop and then, a low recovery factor.

With heavy oil, when gas releases from live oil, the viscosity rises a lot, which should lead to a recovery factor of less than 5% (Sheng et al., 1996). However, as mentioned before, the field performances showed much better results such as low production GOR, better reservoir pressure maintenance, and a higher oil recovery factor. This is very different from the understanding of conventional solution gas drives. That is the contribution of foamy oil flow.

There are two main non-equilibrium mechanisms in foamy oil flow (Maini, 1999). The first is supersaturation. This is the gas saturation difference between the equilibrium state and the instantaneous state. This non-equilibrium happens because of the high viscosity of heavy oil which affects the gas bubble nucleation and growth. Another non-equilibrium is the fluid distribution in the porous media. According to capillary force and interfacial tension theory, the fluid distribution in the porous media is not going to change, and gas will not flow until the continuous phase forms. However, this may be different here, for high viscosity and high pressure drop, bubbles can move due to local high capillary pressure.

There are several foamy oil solution gas drive mechanisms:

2.3.1 Pseudo bubble point

A pseudo bubble point concept is proposed (Kraus et al., 1993; Mastmann et al., 2001). The pseudo bubble point is a concept for foamy oil only. It is lower than the true

equilibrium bubble point. The true bubble point is totally in a state of equilibrium, and the pressure of the first gas bubble of the solution gas phase evolves out from oil as a free gas phase, while in foamy oil, due to the high viscosity, the gas bubble cannot evolve out and coalesce to form a free gas phase when pressure drops below the true bubble point. The bubbles are trapped in the oil phase and form gas-in-oil dispersion. As the pressure keeps dropping, the bubbles will finally coalesce together to a free gas phase, and this pressure is the pseudo bubble point pressure.

In the time of pressure drop from true bubble point to pseudo bubble point, trapped bubbles will expand due to the high compressibility which will lead to expend of oil. This is a possible reason for high oil recovery observed in solution gas driven heavy oil fields.

Researchers measured the pseudo bubble point under different conditions and found that the difference between the true bubble point and pseudo bubble point increased when the fluid flow velocity was higher.

2.3.2 Critical gas saturation

There are several theories to describe how the gas bubble dispersion forms. The first is that the micro gas bubbles, which are even smaller than pore throats, are generated by nucleation (Smith, 1988; Geilikman et al., 1995; Arora, 2001). The theory considers that the micro gas bubbles are not able to grow larger as the pressure drops. Another theory is that the dispersion is formed by the break-up of larger gas bubbles into small bubbles

(Bora et al., 1997; Maini, 2003).

Foamy oil is a non-Darcy two-phase flow (Sarma and Maini, 1992). The production GOR in this kind of reservoir is very low and even the pressure is low until the bubbles grow and coalesce together to form a continuous free gas phase. In this period, the gas mobility is very low. And the minimum gas saturation when the continuous free gas phase forms is the critical gas saturation (Maini et al., 1993).

Critical gas saturation is associated with the gas mobility in the reservoir. Gas mobility in the heavy oil reservoir solution gas drive process is much lower than in light oil reservoirs, which leads to high reservoir performance (Pooladi-Darvish and Firoozabadi, 1999). And the gas relative permeability is very small (Tang and Firoozabadi., 1999). The gas relative permeability is associated with oil viscosity as it decreases when the oil viscosity increases.

2.3.3 Capillary number effect

Sand pack pressure depletion experiments were done by Ostos and Maini (2003) to test the effect of capillary number and viscous force. They found that the capillary number would act differently in three stages. When oil is being produced as foamy oil, a high capillary number appears, and at the same time, the gravity force has little effect on oil production; when foamy oil is diminishing, the gravity force affects the oil production more and a medium capillary number is obtained; lastly, a low capillary number appears

when the oil production is affected mainly by gravity force.

2.3.4 Viscosity of the gas-in-oil dispersion

In 1995, Claridge and Prats (1995) assumed that the gas bubbles dispersed in the oil phase would adsorb asphaltene molecules to the gas bubble surface to form a rigid coating. This coating can prevent bubbles from further growing or coalescencing. And as asphaltene is adsorbed, the oil viscosity is reduced. However, this theory is not supported by any experimental evidence. In contrast, Alshmakhy and Maini (2010) measured the foamy oil viscosity in many ways and found that with more gas dispersions in oil, the viscosity rises, so viscosity reduction is not the characteristic of foamy oil flow and does not contribute to improving heavy oil recovery.

CHAPTER 3 EXPERIMENTAL

3.1 PVT tests

3.1.1 Introduction

To better analyze the results of the core-flooding tests and provide data for the following numerical simulations, the physical properties of the heavy oil sample with CO_2 should be understood. Also for the following simulations, the heavy oil components data is needed as the components of the heavy oil sample cannot be tested by our current equipment. However, a simulation by CMG Winprop can give a pseudo-component result by inserting the pressure-volume-temperature (PVT) properties of heavy oil. In those circumstances, a series PVT tests is necessary.

3.1.2 Materials, Equipment and Procedures

A gas oil ratio for each PVT test was calculated and simulated. Live oil of a heavy oil sample and purities of 99.99% CO_2 were prepared based on the current gas oil ratio ahead of each PVT test. A certain volume of the heavy oil sample and CO_2 was injected into the cylinder of live oil equipment. The temperature and pressure were set at the reservoir condition (11 MPa and 55℃). The cylinder of live oil equipment was rotated for 12 hours to make the live oil equilibrium perfectly.

Once the live oil was prepared, it was transferred into the PVT cell of the PVT equipment

system. The PVT cell is housed in an air bath which can produce a temperature as high as 150℃; in these tests, it was set to 55℃. There is a floating piston in the PVT cell to isolate the test sample and hydraulic oil. Pressure can be supplied and held automatically by a high pressure-sensitive pump connected on the hydraulic oil side. There are pressure and temperature sensors in the PVT cell to measure the current pressure and temperature of the inner cell, and also a piston position sensor can be used to read the piston shifting distance, and then the swelling volume of the live oil can be calculated. There is also a magnetic rotor at the end of the PVT cell to stir the test sample, which can make the test sample reach equilibrium faster.

After the live oil was transferred into the cell, the pressure was raised by pumping in hydraulic oil. Then the pump was controlled to depressurize step by step. The depressurizing value for each step could at first be as large as 2 MPa. A long enough equilibration time for each step is necessary. As the sample volume increased abruptly after a few steps, indicating the appearance of free gas, a smaller value was used to depressurize for another few steps. Volume and pressure were recorded for each step.

The falling-ball method was used to measure the viscosity of live oil under reservoir temperature and bubble point pressure obtained from each test.

Between each test, all the equipment was thoroughly cleaned with kerosene and water and then dried by air blowing.

3.1.3 Results and Analysis

Four PVT tests were completed under different volumes and GOR (cm3/cm3). The GORs were 12.46, 24.74, 51.71 and 106.21 respectively. Each test gave a series of pressure and volume data. Introducing the data into the curve of pressure vs. volume, a two-stage curve was obtained, and the joint point is the bubble point. By generating trend lines and trend equations, the pressure value of the bubble point could be calculated. The results of each test are shown in Table 3-1, Table 3-2, Table 3-3, Table 3-4, Figure 3-2, Figure 3-3, Figure 3-4, Figure 3-5. Finally the concluded results are shown in Table 3-5 with additional mass gas oil ratio, volume factor, density and viscosity data. Density and viscosity were tested by the additional equipment in the PVT cell.

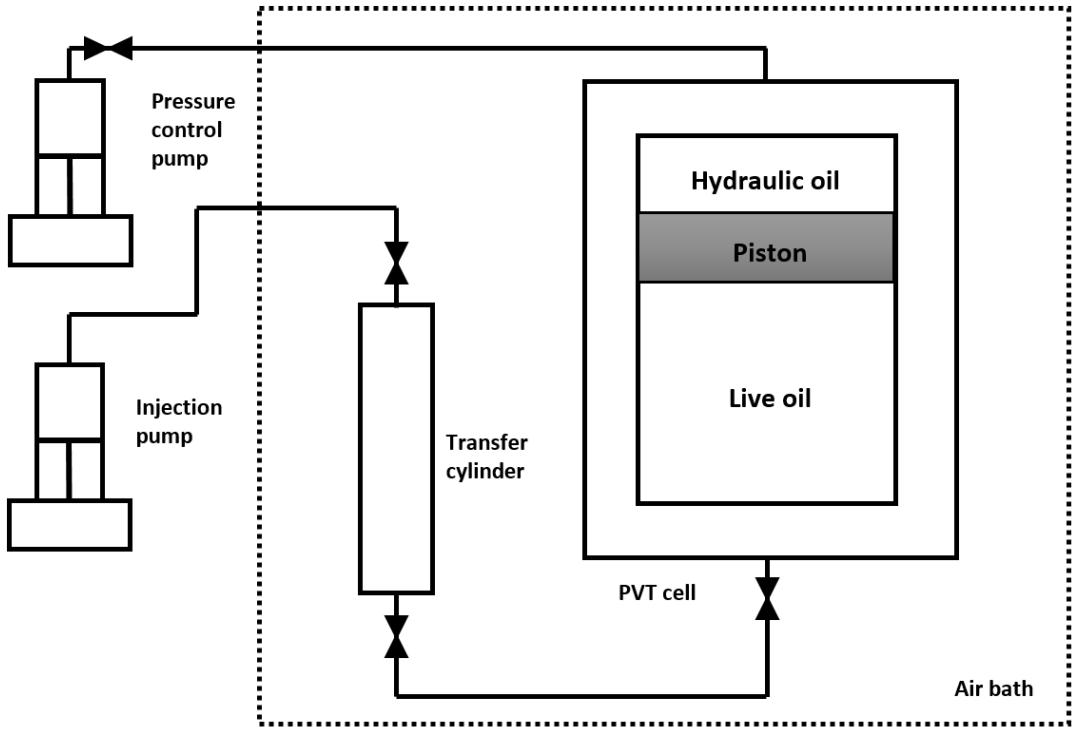

Figure 3-1 Schematic diagram of PVT tests equipment system

Table 3-1 Result data of PVT test with gas oil ratio of 12.46 cm^3/cm^3

P(MPa)	v	P(MPa)	v
20.48	26.63	7.85	28.14
18.54	26.84	5.94	28.4
16.52	27.08	2.73	36.35
14.89	27.28	2.42	43.54
13.02	27.49	1.92	51.4
11.21	27.73	1.58	58.72
9.94	27.88	1.2	66.28

Table 3-2 Result data of PVT test with gas oil ratio of 24.74 cm^3/cm^3

P(MPa)	v	P(MPa)	v
26.69	80.74	10.82	83.19
24.62	81.02	8.58	83.56
22.74	81.3	6.72	83.9
20.84	81.62	4.78	91.55
18.96	81.88	4.34	99.3
16.74	82.26	4.02	107.4
14.72	82.55	3.77	115.06
12.68	82.91	3.53	122.74

Table 3-3 Result data of PVT test with gas oil ratio of 51.71 cm^3/cm^3

P(MPa)	v	P(MPa)	v
28.11	136.77	12.43	139.89
26.52	137.04	10.87	140.22
24.47	137.45	8.51	140.77
22.41	137.87	7.29	148.81
20.26	138.27	6.74	156.27
18.58	138.65	6.16	163.88
16.33	139.06	5.53	171.35
14.38	139.51	5.01	178.91

Table 3-4 Result data of PVT test with gas oil ratio of 106.21 cm^3/cm^3

P(MPa)	v	P(MPa)	v
24.26	218.71	10.29	248.33
22.67	219.8	10.01	255.75
20.51	221.29	9.71	263.51
18.6	222.62	9.41	271.51
16.45	224.11	9.12	279.18
14.58	225.41	8.83	286.74
12.68	226.72		

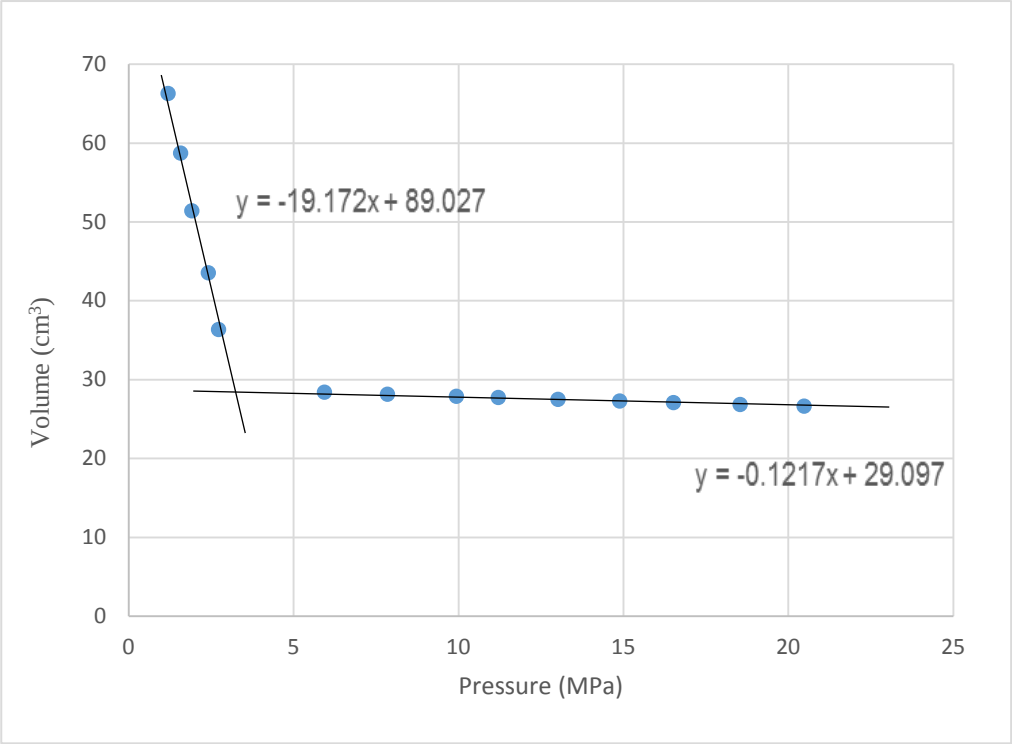

Figure 3-2 Result curve of PVT test with gas oil ratio of 12.46 cm^3/cm^3

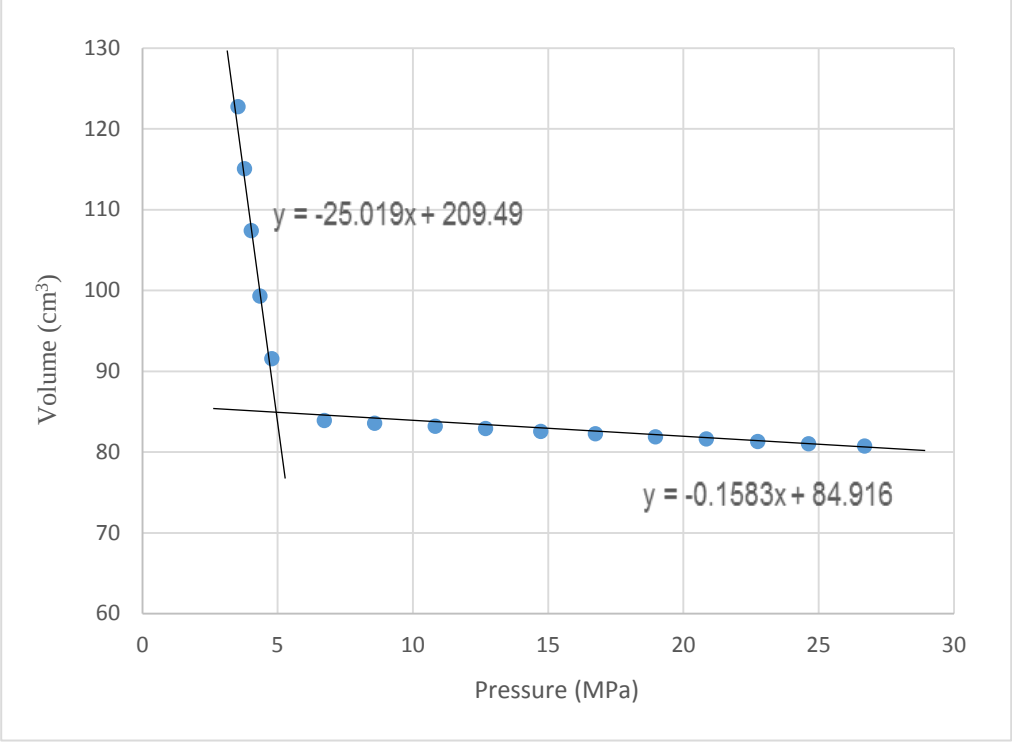

Figure 3-3 Result curve of PVT test with gas oil ratio of 24.74 cm^3/cm^3

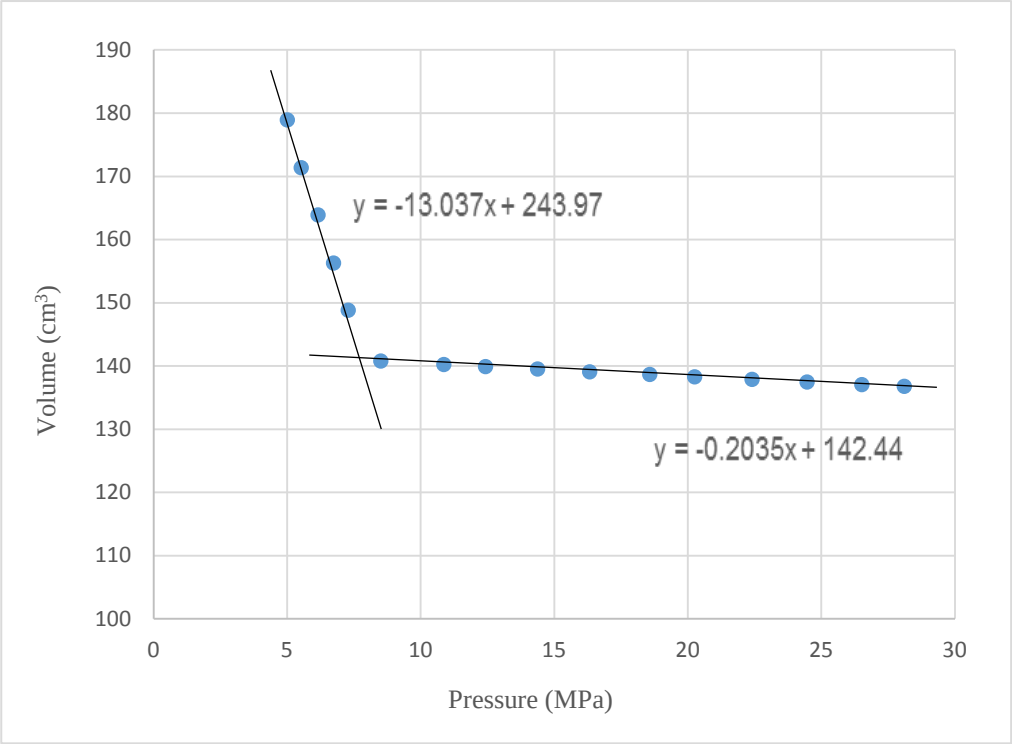

Figure 3-4 Result curve of PVT test with gas oil ratio of 51.71 cm^3/cm^3

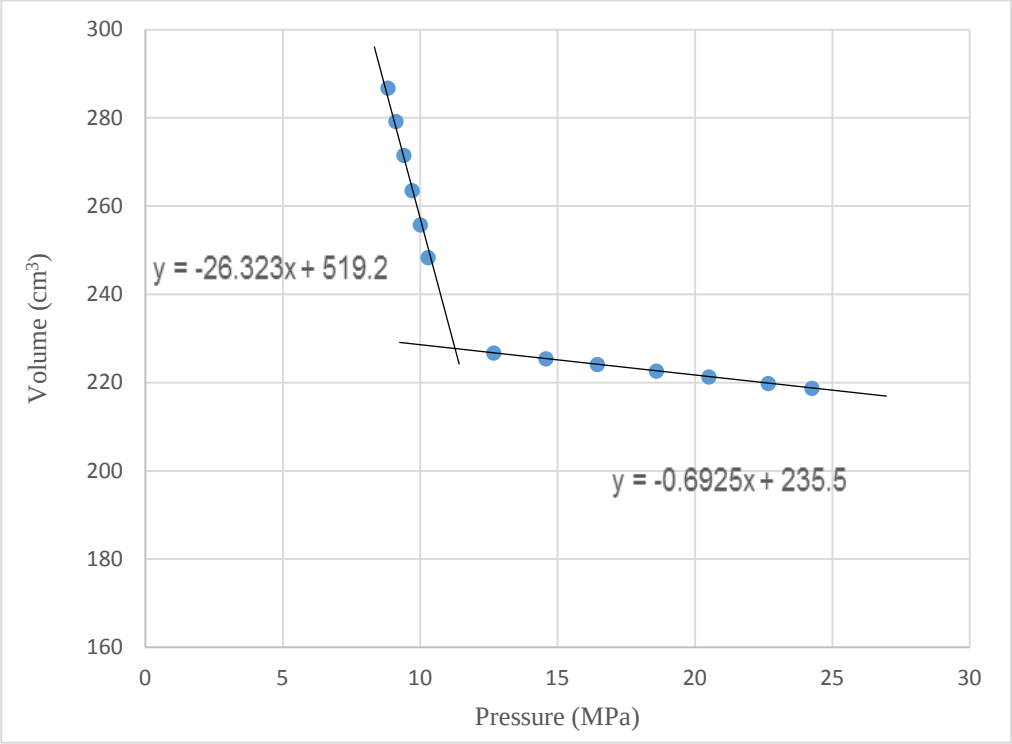

Figure 3-5 Result curve of PVT test with gas oil ratio of 106.21 cm^3/cm^3

Table 3-5 Final result of PVT tests

Saturation Pressure, MPa	Volume Gas Oil Ratio, cm^3/cm^3	Mass Gas Oil Ratio, cm^3/g	Formation Volume Factor	Density, g/cm^3	Viscosity, cp
0	0	0	1	0.93	528.42
3.14	12.46	13.20	1.04	0.90	223.69
4.99	24.74	26.21	1.10	0.87	153.08
7.91	51.71	54.78	1.17	0.85	56.17
11.07	106.21	112.51	1.32	0.81	28.73

3.2 Core-flooding tests

3.2.1 Introduction

Six core-flooding tests were designed based on the research aims. All the tests had the same quantity of injection gas which was five times the pore volume (PV) of each core. Two of the tests had constant production pressure but different gas injection rates; another two were designed to have depletion production pressure schemes; the fifth test was the flue gas test and the last one was a “multi-pressure-control” scheme test.

3.2.2 Materials

In this study, the heavy oil sample and brine sample from the same area were kindly offered by an oil field in North China. The physical properties of the heavy oil were tested by PVT tests beforehand. The reservoir property parameters were all based on field data from the oil field. Reservoir pressure was 11 MPa. The average permeability of the reservoir was 1500 mD and reservoir temperature was 55℃. The reservoir had already been developed with water flooding methods for many years with the water cut reaching 90%. The core suitable for the core holder is a cuboid with length around 30 cm and 4.5 cm for both four sides of the cross section. The sandstone cores were made artificially with the above parameters shown (Figure 3-6). The CO_2 gas used in the experiments had a purity of 99.99 mol.%.

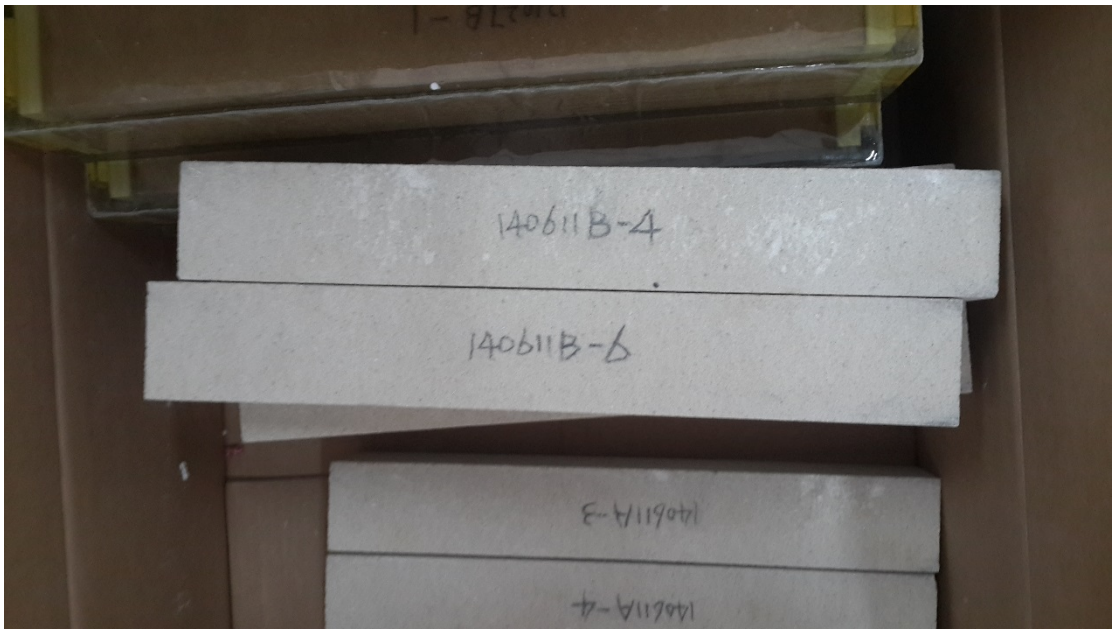

Length: 30 cm

Width: 4.5 cm

Figure 3-6 Artificial sandstone cores

3.2.3 Experimental setup

All the six tests were done in the same equipment system for better consistency. This core-flooding system consists of three parts: material injection, the reservoir model and production collection.

The material injection part plays an important role both in the preparation and experimental procedures. It consists of injection pumps, a heavy oil sample transfer cylinder, a brine sample transfer cylinder, an injection gas cylinder, a pneumatic valve group and pressure transducers. The injection pump used in these series of tests is a double pump system which can provide large volume continuous injection. Every transfer cylinder is equipped with one pressure transducer and one pneumatic valve. The pump, transducers, and valves are all controlled and monitored by computer. All the pieces of this part except the pump are placed in a large air bath.

The reservoir model is the most important part. It consists of a core holder, pressure transducers, and an overburden supply pump. Two pressure transducers are connected on both sides of the core holder. The overburden supply pump can maintain the overburden pressure for value higher than the core pressure. All pieces of this part are in the air bath.

The production collection part consists of a high pressure back pressure regulator (BPR), a production pressure control pump, a valve, sample collection tubes, and a gas flow meter. This equipment is placed in a separate air bath. The reason for that is to hold the temperature of reservoir model part constant. The whole system is shown in Figure

3-7.

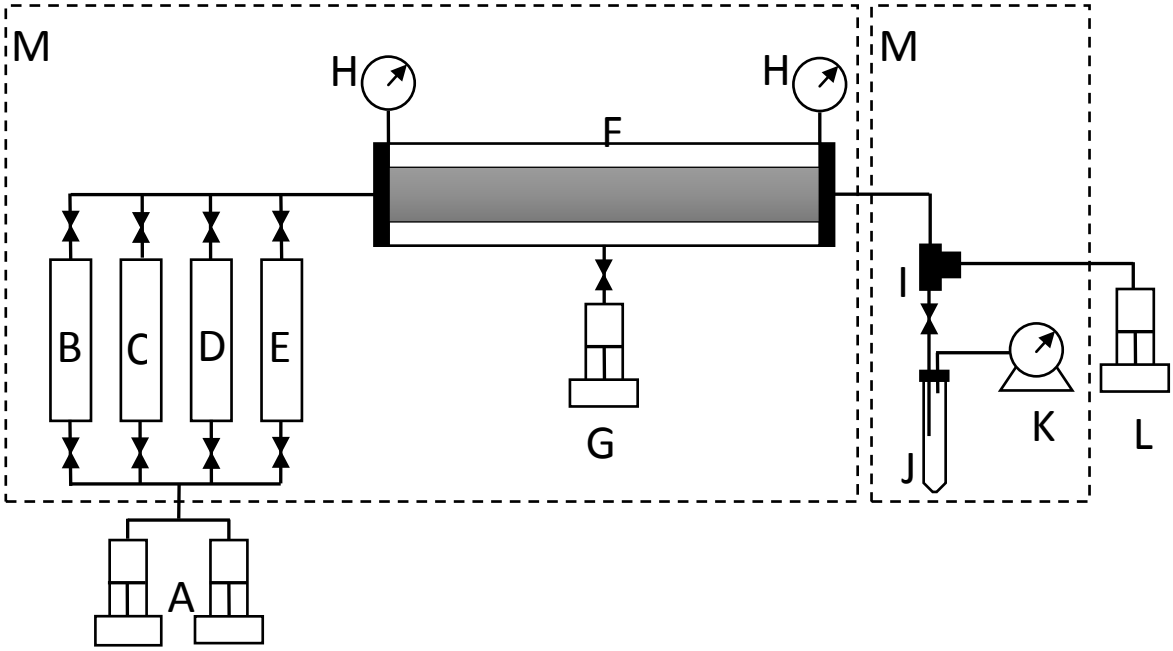

A. Injection Pump
B. Heavy oil Cylinder
C. Brine Cylinder
D. CO_2 Cylinder
E. Flue Gas Cylinder
F. Core-Holder
G. Overburden Supply Pump
H. Pressure Transducer
I. Back Pressure Regulator
J. Sampling Tube
K. Gas Flow Meter
L. Production Pressure Control Pump
M. Air bath

Figure 3-7 Schematic diagram of the core-flooding system

3.2.4 Experimental preparation

3.2.4.1 Material preparation

The materials were transferred into the corresponding transfer cylinders ahead of time. The brine was filtered twice before transfer to make sure no solid impurities. The heavy oil sample was transferred into the cylinder directly. CO_2 preparation was a little complex. Because the CO_2 resource cylinder did not have enough pressure compared to what we needed, a compress process by pump and another transfer cylinder had to be used. The CO_2 transfer cylinder was set to the required volume which was five times pore volume and was vacuumed beforehand. After all these materials had been transferred, all the transfer cylinders had to be placed in the air bath and heated to the test temperature.

3.2.4.2 Porosity Measurement

After installation into the core holder, the core had to be saturated with brine, and the porosity measurement was completed at the same time. The overburden pressure was applied, and the core was vacuumed with a vacuum pump. After being vacuumed for two hours, all the valves of the core holder were shut. A burette filled with brine was connected to the core holder. The valve which connected the burette was opened, and the brine was imbibed into the core holder. Once the reading on the burette stopped changing, it was recorded. The reading for the dead volume of the core holder was subtracted and the pore volume (PV) of the core was determined. The porosity was then determined as

the ratio of the PV to the core volume. Following this the core holder was placed in the air bath to be heated to the test temperature. The core holder was connected into the system with the transfer cylinders and transducers.

3.2.4.3 Permeability measurement

After the core holder was connected to the system and heated to the test temperature, the permeability of the core was measured. The valves of the injection pump and brine cylinder were opened. Brine was injected into the core at different flow rates. Pressure changes were monitored by pressure regulators. The permeability of the core was determined by steady-state flow of Darcy's Law. The permeability measurement processes were controlled and calculated by an automatic computer program.

3.2.4.4 Initial oil saturation

After the permeability measurement, the heavy oil sample needed to be saturated into the core. The valves of the injection pump and heavy oil cylinder were opened. The production pressure control pump at the production side was set to the designed reservoir pressure. Then the heavy oil was injected into the core at a constant rate of 0.3 ml/min. The water and oil produced from the production side were collected by 1000 ml graduate cylinder. When heavy oil was produced, the injection process still continued until no more water produced. The ratio of water production to the PV is the initial oil saturation and the ratio of the volume of water remaining in the core to the PV is the connate water

saturation.

Table 3-6 Porosities, permeabilities and initial oil saturations for the six tests

	Test #1	Test #2	Test #3	Test #4	Test #5	Test #6
Porosity (%)	29.07	29.25	29.36	29.11	28.61	28.72
Permeability (mD)	1551	1753	1551	1492	1682	1587
Initial oil saturation (%)	73.02	76.52	69.43	69.16	77.88	74.27

3.2.4.5 Water flooding process

Because the reservoir was developed with the water flooding method before, and the water cut was 90%, a water flooding process needed to be done before the test. The valves of the injection pump and brine cylinder were opened. The production pressure control pump was set to the reservoir pressure. Then the brine was injected into the core at a constant flow rate of 0.3 ml/min. The water and oil produced from the production side were collected using a 1000 ml graduate cylinder. The volume of heavy oil and the water production volume were recorded at regular intervals. When 90% water production was reached in one time interval, water flooding was completed and stopped. The total heavy oil production was recorded.

3.2.5 Experimental tests

3.2.5.1 Constant production pressure tests

Tests #1, #2 and #5 were done with constant production pressure. Tests #1 and #2 were CO_2 injection cases with constant gas injection rates of 7 ml/min and 2ml/min respectively. Test #5 was the flue gas (20% CO_2 and 80% N_2) injection case with a constant gas injection rate of 7 ml/min. When the tests started, the injection pump started to inject gas into the core at a designated rate. The pressure of each side of the core holder was recorded once per minute by computer through pressure transducers. Liquid

production samples were collected using test tubes. The tubes were changed every time period. The time periods at the beginning of the test were long because there was little liquid production. The frequency of changing the tubes was increased when the gas broke through, which was the peak of liquid production. When the peak passed, the frequency could be reduced to a constant time period. The time, test tube number and gas flow meter readings were recorded each time the tubes were changed.

3.2.5.2 Production pressure depletion tests

Tests #3 and #4 were done with a production pressure depletion scheme. Test#3 had a constant gas injection rate of 2 ml/min. The production pressure depleted uniformly from the reservoir pressure (11MPa) to 8 MPa in the period when 5 PV gas were injected up. Test #4 had a constant gas injection rate of 7 ml/min. The production pressure depleted from the reservoir pressure (11MPa) to 5 MPa in the period when 5 PV gas were injected up. Pressures were recorded every minute as well. The sample collection and gas recording methods were all the same as before.

3.2.5.3 Multi-pressure-control scheme test

Test #6 was the multi-pressure-control test. The test was a cyclic test with four cycles in total. Each cycle had two stages. The first stage was at constant production pressure with a constant injection rate of 7 ml/min; 1.25 PV CO_2 was injected at this stage. The second stage was the production pressure depletion process with the injection well shut.

The production pressure depleted from 11 MPa to 5 MPa uniformly. The depletion time depended on the time it took to inject 5 PV gas with a rate of 7 ml/min. After the depletion stage, the valve of the injection well was opened, and the model pressure rose back to 11 MPa instantaneously. Then the next cycle followed. Pressures were recorded every minute as well (Figure 3-8).

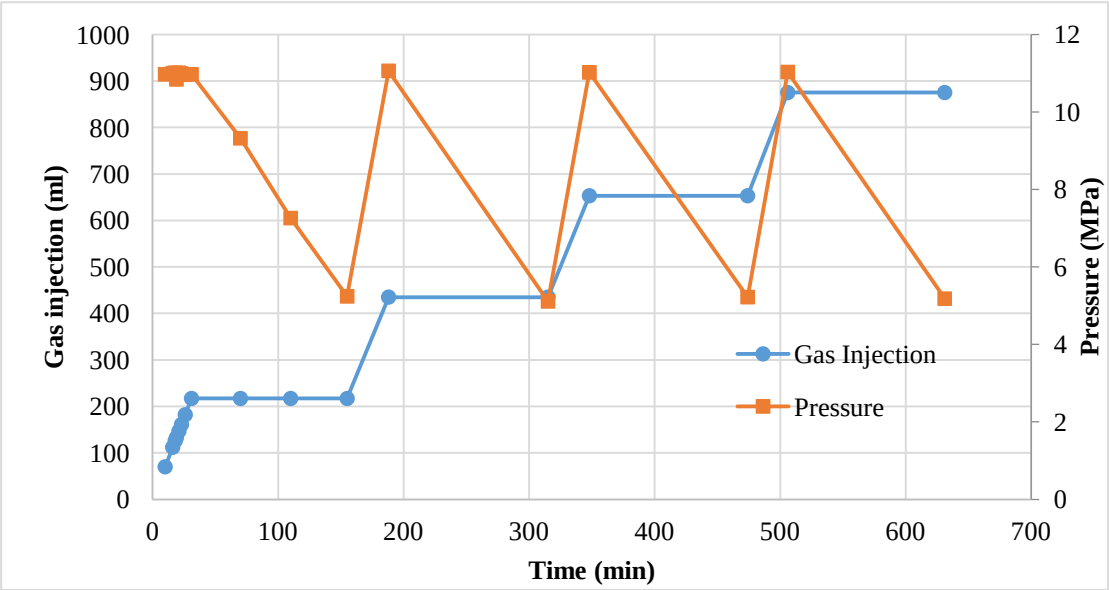

Test #6 was the multi-pressure-control test. The test was a cyclic test with four cycles in total. Each cycle had two stages. The first stage was at constant production pressure with a constant injection rate of 7 ml/min; 1.25 PV CO_2 was injected at this stage. The second stage was the production pressure depletion process with the injection well shut. The production pressure depleted from 11MPa to 5 MPa uniformly. The depletion time depended on the time it took to inject 5 PV gas with a rate of 7 ml/min. After the depletion stage, the valve of the injection well was opened, and the model pressure rose back to 11 MPa instantaneously. Then the next cycle followed.

Figure 3-8 Curves of gas injection volume and pressure for test #6

Table 3-7 Schemes of core-flooding tests

Test#	1	2	3	4	5	6
Injection Gas	CO_2	CO_2	CO_2	CO_2	Flue Gas	CO_2
Injection Volume（PV）	5	5	5	5	5	5
Injection Rate (ml/min)	7	2	2	7	7	7
Production Pressure Scheme	Constant 11 MPa	Constant 11 MPa	Depletion 11 to 8 MPa	Depletion 11 to 5 MPa	Constant 11 MPa	Constant/ Depletion

3.2.6 Core-flooding results and discussion

3.2.6.1 General analysis

After all the tests had been done, the experimental data was collected and analyzed. The test that had the lowest recovery factor was test #5 which was the flue gas case. And the highest recovery factor case was test #6 which was the multi-pressure-control scheme case. Obviously, CO_2 flooding is really effective even after water flooding to 90% water cut.

During the tests, several phenomena could be observed. At the beginning of the injection, the pressure of the injector rose slowly, but some time was needed for the pressure to transmit to the other side of the core. For the constant production pressure tests, the pressure at the producer did not change at this time, and no liquid was produced. For the production pressure depletion tests, because the bottomhole pressure decreased, the pressure at the producer dropped. And little liquid was produced, most of which was water. No gas was produced during this period in either the constant or the depleted production pressure cases. When the pressure had transmitted to the other end of the core, more fluid was produced, which was mostly water. Only a little heavy oil was produced, and the amount was too small to read the volume from the test tube. After several minutes, more heavy oil was produced, accompanied by some water and gas. Soon, the peak of the heavy oil production rate was reached. A large amount of heavy oil erupted from the

production well, accompanied by a lot of gas. Hardly any water was produced this time. After the peak of production rate, a large amount of gas was produced, and the production rate was stable. The heavy oil production rate soon started to drop and went stable. At the later stage of the tests, the oil production and production rate were small but the gas production and the production rate remained stable.

From the phenomena we observed, we have an analysis of the whole process. At the beginning of the tests, the injected gas tended to move from the injector towards the producer. However, the pressure differential in the core had just built up and pressure had not yet transmitted to the producer. Therefore, there was no effect on the production well. As more gas kept being injected, pressure was transmitted to the producer. When the producer pressure was higher than the BPR, which held the pressure of the production pressure control pump, fluid started to be produced.

In the water flooding process before each test, water broke through and formed water channels in the core. When it came to the gas flooding process, the gas tended to flow through the channels rather than other passes. Therefore, before the gas broke through, almost 99% percent of production was water which all came from the water channels. At the same time, CO_2 in the injected gas flowed through the channels, spread away and dissolved in the heavy oil around the channels. This heavy oil had high mobility and flowed through the channel driven by the injected gas. As all the water in the channels was pushed out and the gas broke through, this heavy oil erupted from the producer and

led to the peak rate of oil production.

After the breakthrough, the channels were filled with gas; there was little time for the CO_2 to dissolve in the heavy oil in a larger range, which led to the drop in heavy oil production.

3.2.6.2 Comparison of different injection gasses

Test #1 vs. test #5

Test #1 was the case with pure CO_2 while test #5 was with flue gas which is 20% CO_2 and %80 N_2. All other conditions were the same: the same gas injection rate, the same constant production pressure, etc. The comparison between these two tests can prove the significant effect of CO_2 on heavy oil recovery.

Test #1 had a total recovery factor of 31.1%, nearly double that of test #5, which was 16.9%. This result clearly demonstrates the effect of CO_2 on heavy oil recovery.

Figure 3-9 is the curves of time vs. oil production rate of tests #1 and #5. It is obvious from the curves that the oil production rate of test #5 is lower than that of test #1 in early stage and tends to be the same in the later stage. The peak oil production rate of test #1 is higher than that of test #5. In test #5, 80% of the injected gas was N_2, which cannot dissolve in heavy oil at all. The only function of N_2 in test #5 was to provide differential pressure to offer enough displacement efficiency. Therefore, the total quantity of heavy oil with CO_2 dissolved in test #1 was far more than in test #5, which led to the higher

heavy oil recovery rate in the early stage. In the later stage, there was enough CO_2 in the core in both tests; the heavy oil in the gas spread range was fully saturated with CO_2. The free CO_2 in test #1 only had the function of providing differential pressure, just like N_2 and free CO_2 in test #5. Therefore, the later stage heavy oil recovery rates were the same in both tests.

As shown in Figure 3-9 and Figure 3-10, test #5 produced heavy oil earlier than test #1 and the peak of the heavy oil production rate of test #5 also came earlier than that of test #1. The reason for this is that at the earlier stage, more CO_2 was dissolved in the core in test #1 while there was not enough CO_2 to saturate the heavy oil in test #5. The remaining free gas in the core in test #5 was much greater than that in test #1, which led to higher differential pressure in test #5, as Figure 3-11 shows. But more CO_2 gas was dissolved in heavy oil in test #1 which led to more heavy oil was produced.

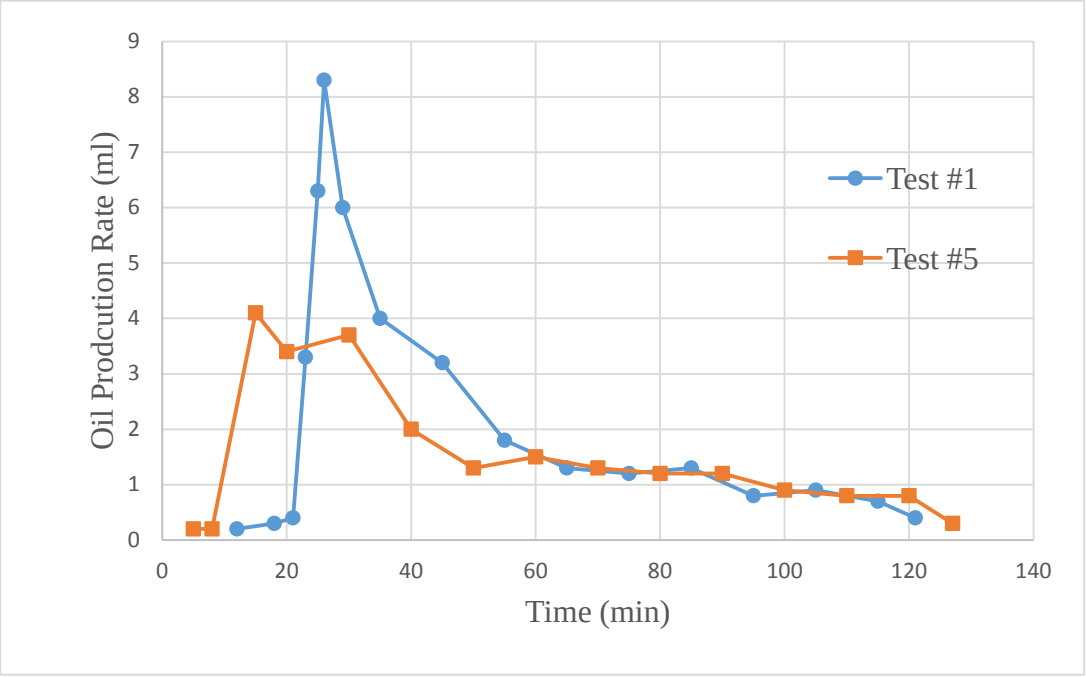

Test#	1	5
Injection Gas	CO_2	20% CO_2
Injection Volume（PV）	5	5
Injection Rate (ml/min)	7	7
Production Pressure Scheme	Constant 11 MPa	Constant 11 MPa

Figure 3-9 Curves of oil production rates for test #1 and test #5

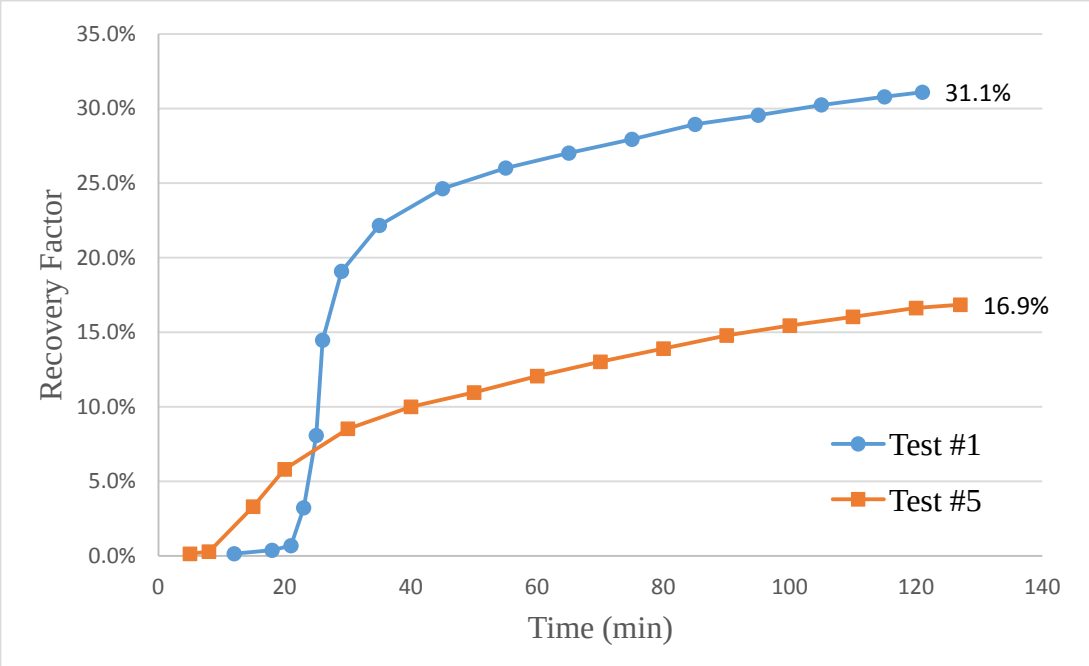

Test#	1	5
Injection Gas	CO_2	20% CO_2
Injection Volume（PV）	5	5
Injection Rate (ml/min)	7	7
Production Pressure Scheme	Constant 11 MPa	Constant 11 MPa

Figure 3-10 Curves of recovery factors for test #1 and test #5

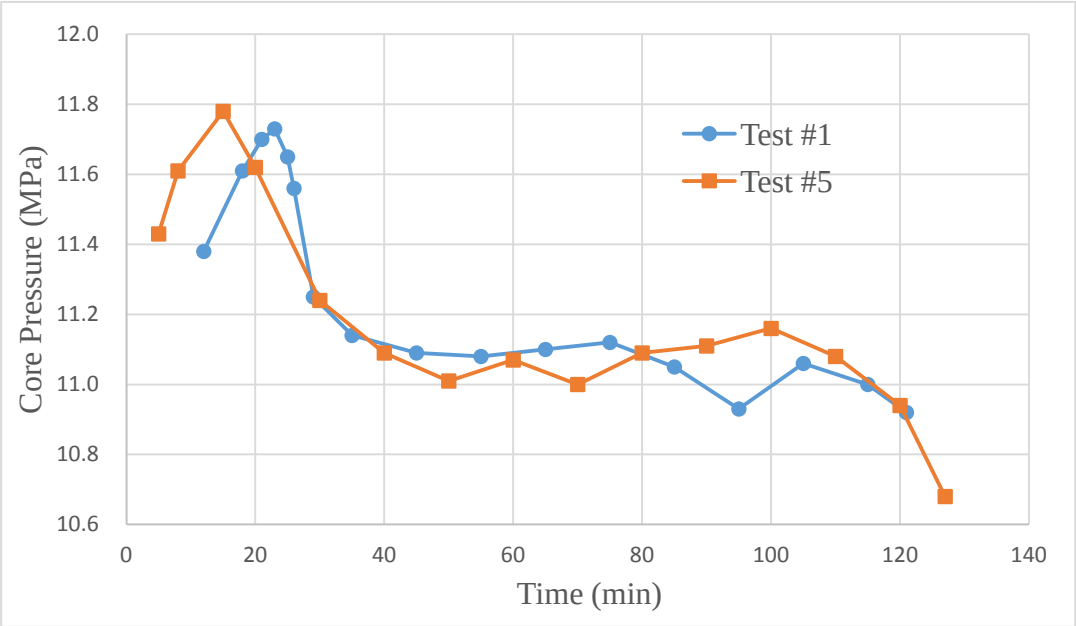

Test#	1	5
Injection Gas	CO_2	20% CO_2
Injection Volume（PV）	5	5
Injection Rate (ml/min)	7	7
Production Pressure Scheme	Constant 11 MPa	Constant 11 MPa

Figure 3-11 Curves of core pressures for test #1 and test #5

3.2.6.3 Comparison of different production pressure schemes

Test #2 vs. test #3

Test #2 was the constant production pressure case, and test #3 was the depleted production pressure case. Both of them had pure CO_2 injected with an injection rate of 2 ml/min. The comparison between these two tests proves the effect of depleted production pressure and foamy oil flow on oil production.

Tests #3 had a total recovery factor of 39.0% while test #2 had 36.7%. The gap between these two tests is obvious. From Figure 3-12 and Figure 3-13 we can clearly see that the recovery efficiency of the depleted production pressure scheme (test #3) is better than that of the constant production pressure scheme (test #2). The oil production rate of test #3 is higher than that of test #2 from the beginning of the production. Moreover, the oil production peak rate of test #3 was achieved earlier than for test #2. From the beginning of the tests, the differential pressure in test #2 was provided only by gas injection while in test #3, the differential pressure was provided by the combined contributions of both gas injection and production pressure depletion. Therefore, the displacement efficiency of test #3 is better than that of test #2 and can lead to earlier heavy oil production. In addition, production pressure depletion in test #3 is beneficial for the achievement of foamy oil flow.

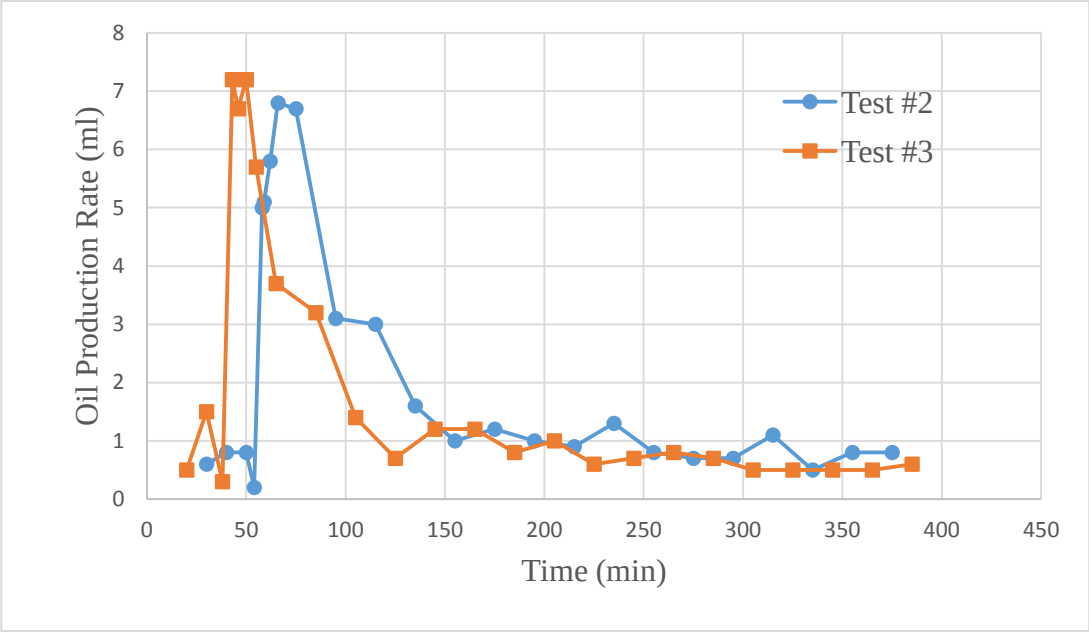

Test#	2	3
Injection Gas	CO_2	CO_2
Injection Volume（PV）	5	5
Injection Rate (ml/min)	2	2
Production Pressure Scheme	Constant 11 MPa	Depletion 11 to 8 MPa

Figure 3-12 Curves of oil production rates for test #2 and test #3

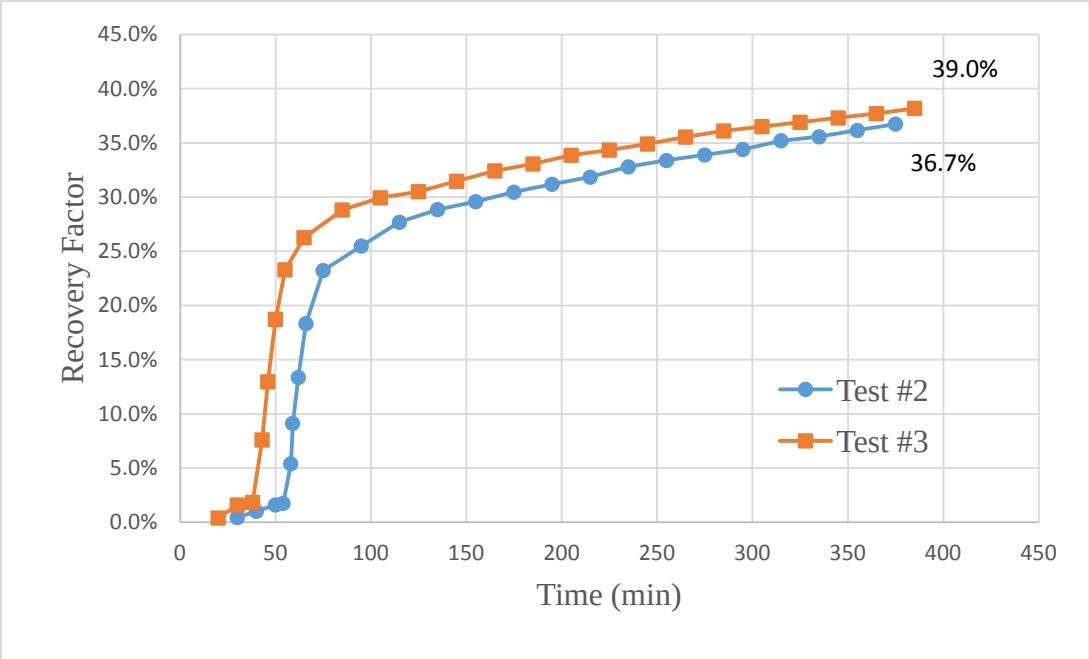

Test#	2	3
Injection Gas	CO_2	CO_2
Injection Volume（PV）	5	5
Injection Rate (ml/min)	2	2
Production Pressure Scheme	Constant 11 MPa	Depletion 11 to 8 MPa

Figure 3-13 Curves of recovery factors for test #2 and test #3

Test #1 vs. test #4

Test #1 was the constant production pressure case, and test #4 was the depleted production pressure case. Both of them had pure CO_2 injected with an injection rate of 7 ml/min. Test #1 had a recovery factor of 31.1% while test #4 had 38%.

From Figure 3-14 and Figure 3-15 we can find that the difference between these two cases is even larger than between the previous two. The oil production rate of test #4 is far greater than that of test #1 and the difference between peak rates is much greater than in the last comparison. This is because, as the injection rate was greater, the total time was shorter, which led to a greater pressure depletion rate in test #4. The greater depletion rate made the differential pressure greater in the early stage and then made the production rate greater and production rate peak earlier.

Moreover, a greater production depletion pressure can create foamy oil better. The efficiency of the foamy oil flow on the heavy oil production rate and the total oil production factor is more obvious, especially from the period after the oil production rate peaks.

3.2.6.4 Comparison of different gas injection rates

Test #1 vs. test #2

Test #1 had a gas injection rate of 7 ml/min and test #2 had a rate of 2 ml/min. Both of them had pure CO_2 injected with constant production pressure. From a comparison between these two tests an analysis can be done of the effect of the injection rate on the

constant

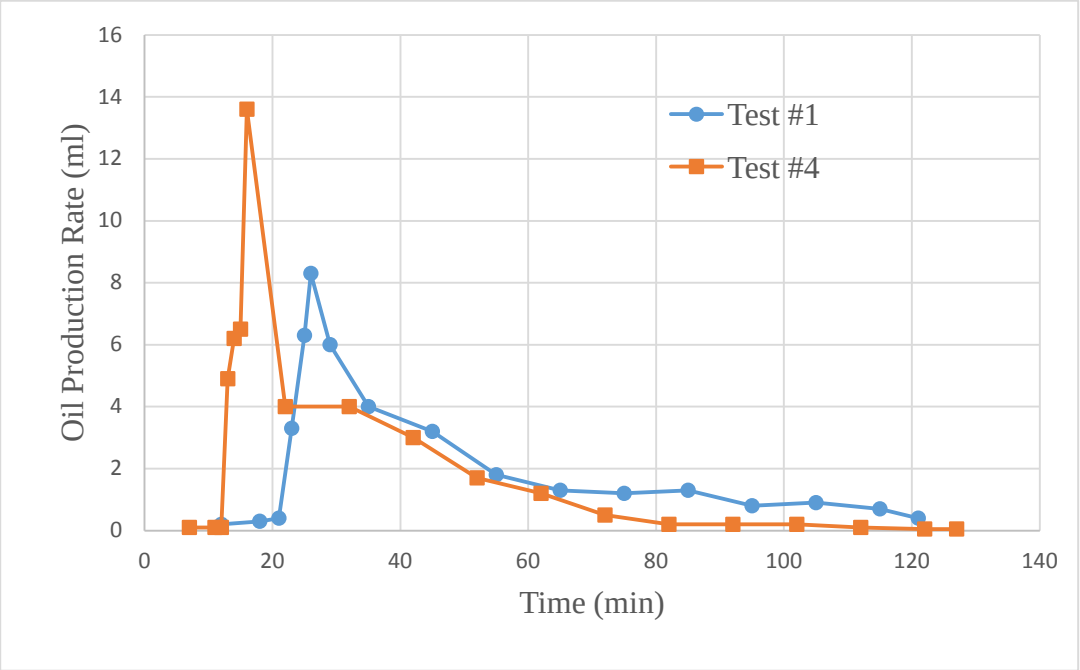

Test#	1	4
Injection Gas	CO_2	CO_2
Injection Volume（PV）	5	5
Injection Rate (ml/min)	7	7
Production Pressure Scheme	Constant 11 MPa	Depletion 11 to 5 MPa

Figure 3-14 Curves of oil production rates for test #1 and test #4

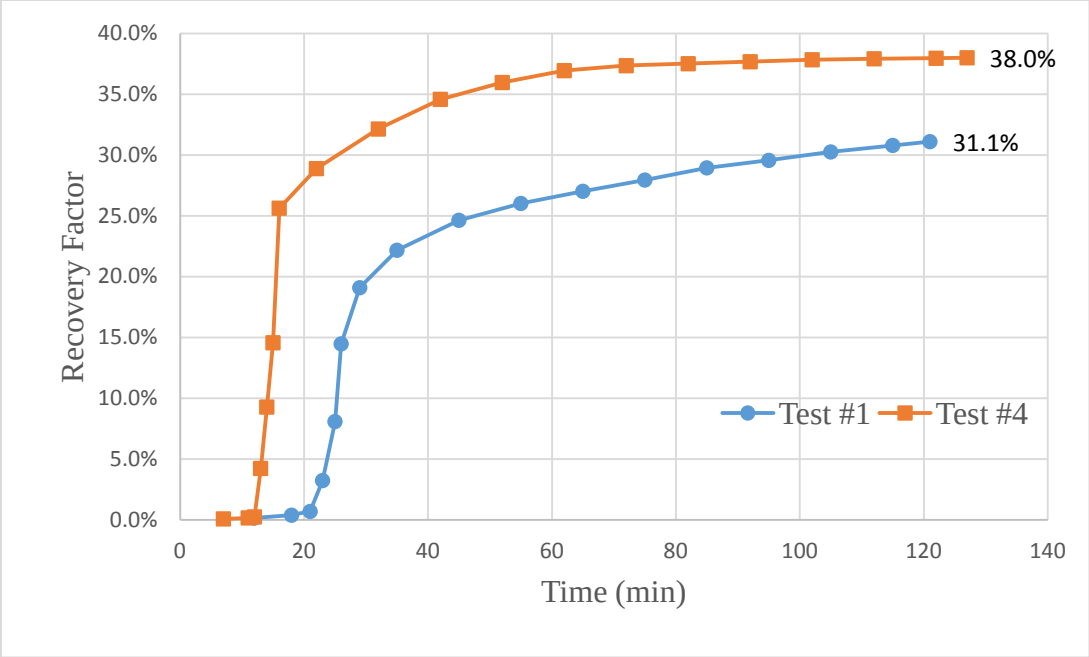

Test#	1	4
Injection Gas	CO_2	CO_2
Injection Volume（PV）	5	5
Injection Rate (ml/min)	7	7
Production Pressure Scheme	Constant 11 MPa	Depletion 11 to 5 MPa

Figure 3-15 Curves of recovery factors for test #1 and test #4

production pressure scheme.

Test #1 had total recovery factor of 31.1% while test #2 yielded 36.7%, which indicates that a smaller gas injection rate has a positive effect on oil production. As the injection rates were different and the total injected gas volumes were about the same (5 PV), time cannot be a comparison standard, so the number of pore volumes that were injected are used.

Figure 3-16 and Figure 3-17 are comparative curves for test #1 and test #2. From the curves, we can see that the oil production rate of test #2 is lower than that of test #1 and the peak rate of test #2 is much lower and comes much later than that of test #1. There is still an obvious difference between the rates of the two tests after the rate peaks. But the rate of test #2 maintained at a relatively high level for a longer time and the production rate decline of test #2 is slower than for test #1 at the later stage.

Because the injection rate in test #2 was small, there was more time for the injected CO_2 to spread and dissolve in the heavy oil in the core before the gas broke through. As a larger spread area was reached, more CO_2 dissolved in the heavy oil in the core, and thus the gas breakthrough time was delayed. And the delayed time had the benefit of allowing more high mobility heavy oil to flow to near the production well area. When a breakthrough is reached, more heavy oil can be produced. After the breakthrough, because of the larger spread area before, more heavy oil was touched by the CO_2 which then dissolved, leading to a higher production rate and maintained for a long time in the

later stage. Because of constant production pressure, neither of the tests had any foamy oil flow.

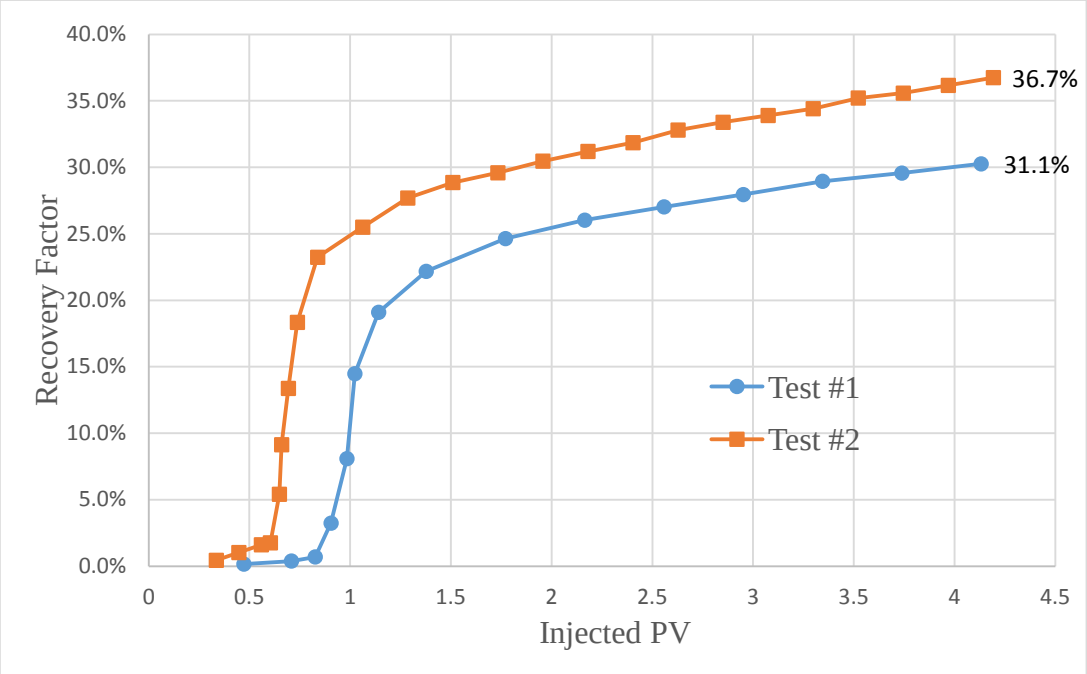

Test#	1	2
Injection Gas	CO_2	CO_2
Injection Volume（PV）	5	5
Injection Rate (ml/min)	7	2
Production Pressure Scheme	Constant 11 MPa	Constant 11 MPa

Figure 3-16 Curves of recovery factors for test #1 and test #2

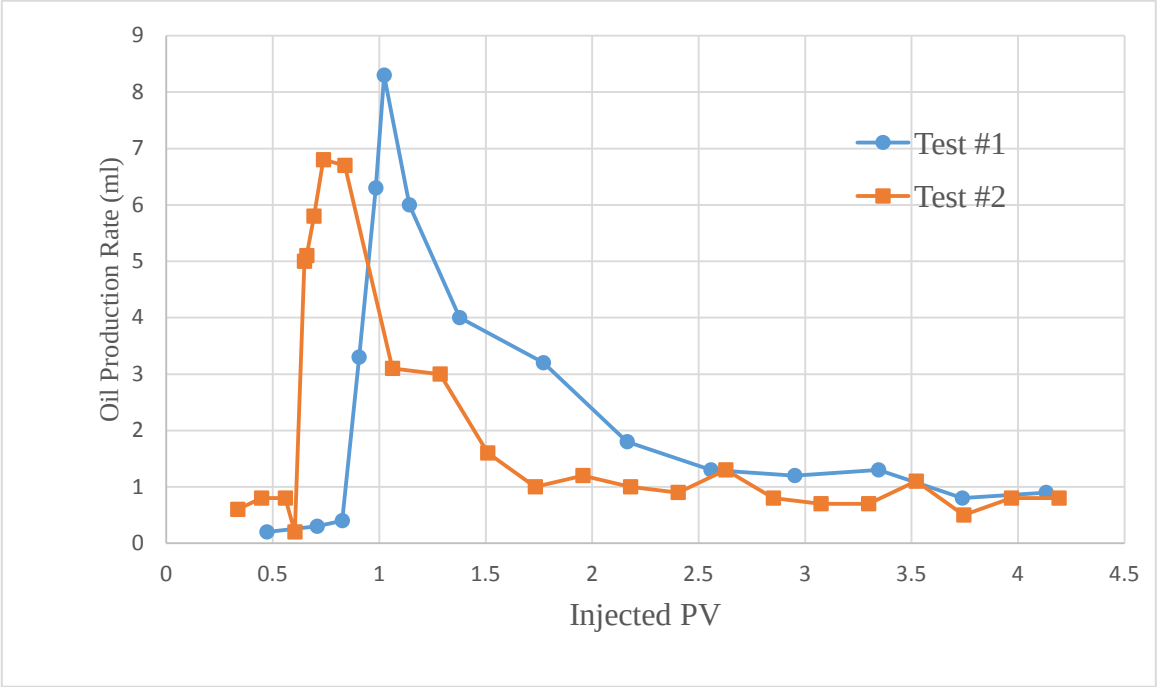

Test#	1	2
Injection Gas	CO_2	CO_2
Injection Volume（PV）	5	5
Injection Rate (ml/min)	7	2
Production Pressure Scheme	Constant 11 MPa	Constant 11 MPa

Figure 3-17 Curves of oil production rates for test #1 and test #2

Test #3 vs. test #4

Test #3 had a gas injection rate of 2 ml/min and test #4 had a rate of 7 ml/min. Both of them had pure CO_2 injected with depleted production pressure. In this comparison, the effect not only came from the injection rate, but also from the foamy oil flow caused by production pressure depletion.

Also, like the last comparison, the times of the tests were different, PV numbers of injected CO_2 were used in the comparison instead of time. Test #3 had a total recovery factor of 39.0% while test #4 yielded 38.0%. The results were too similar to distinguish which was better Curves of recovery factors and oil productions rate are used for the analysis. At the early stage, the oil production rate of test #4 was much higher than that of test #3. And the largest gap appeared at the peak rates. However, at the later stage, right after the rate peaks, the rate decline of test #4 was fast while that of test #3 was gentle. By the end of the tests, the recovery factors of the two tests were almost the same. At the early stage, the CO_2 injection rate of test #3 was much lower, which gave the injected CO_2 more time to spread in the core and it dissolved better in the heavy oil. Also, the breakthrough point was delayed in test #3, and displacement pressure was better held and increased, therefore, more heavy oil was produced before and at the breakthrough point (production rate peak point).On the other hand, test #4 took a shorter time, leading to faster production pressure depletion, which in turn led to better foamy oil flow production performance. Therefore, at the later stage, test #4 maintained higher a rate of production

and then held better oil production. In the combination of the effect of the gas injection rate and production pressure depletions, these two tests had almost the same heavy oil recovery factor.

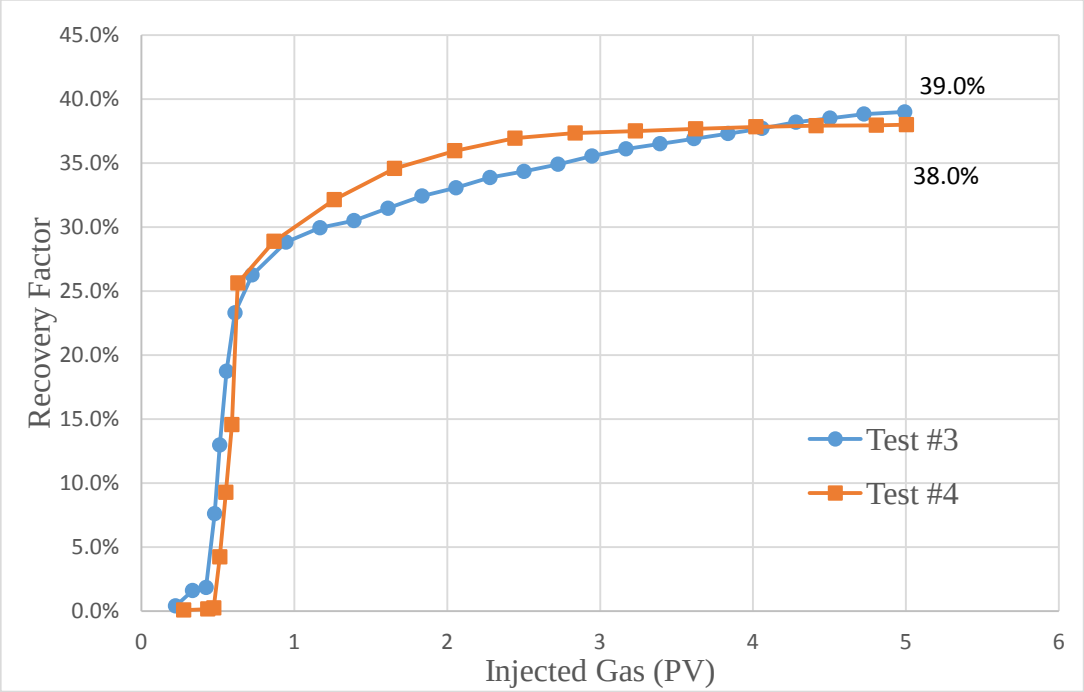

Test#	3	4
Injection Gas	CO_2	CO_2
Injection Volume（PV）	5	5
Injection Rate (ml/min)	2	7
Production Pressure Scheme	Depletion 11 to 8 MPa	Depletion 11 to 5 MPa

Figure 3-18 Curves of recovery factors for test #3 and test #4

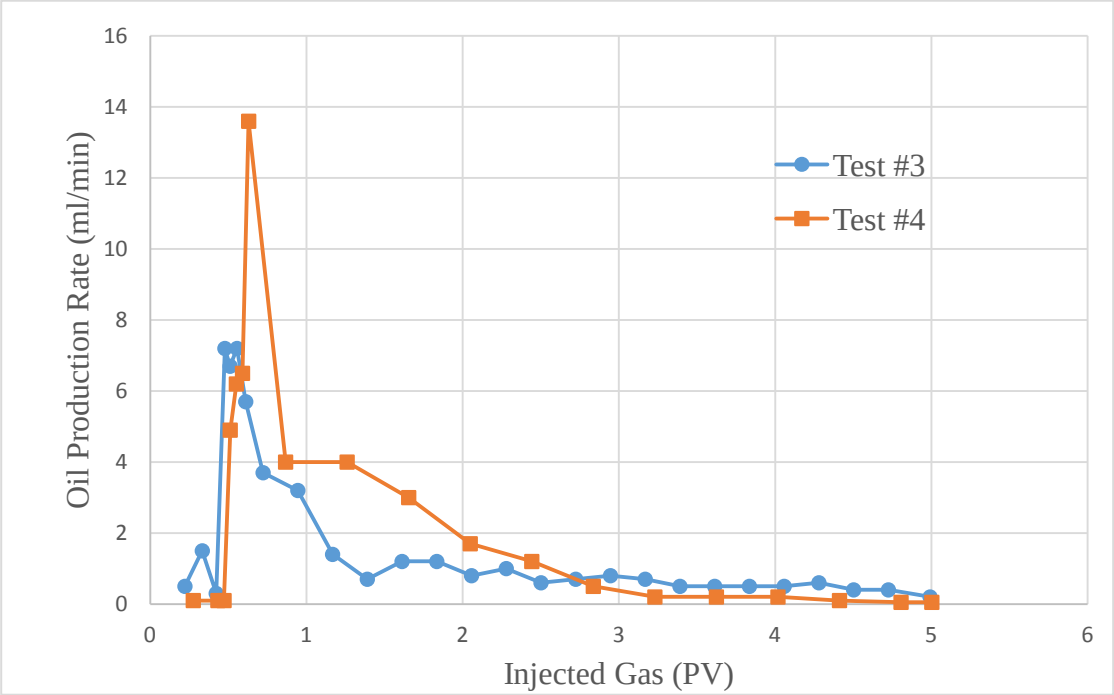

Test#	3	4
Injection Gas	CO_2	CO_2
Injection Volume（PV）	5	5
Injection Rate (ml/min)	2	7
Production Pressure Scheme	Depletion 11 to 8 MPa	Depletion 11 to 5 MPa

Figure 3-19 Curves of oil production rates for test #3 and test #4

3.2.6.5 Comparison of single- and multi-production pressure control schemes

Test #1 vs. test #6

In this comparison, the basic single-production pressure control scheme case (test #1) and the multi-production pressure control scheme case (test #6) are put together for analysis. The basic gas injection rates are all the same, that is, 7 ml/min. 5 PV pure CO_2 were injected in both of the cases. The final result shows a significant difference. Test #1 had a recovery factor of 31.1% while test #6 yielded 42.5%. From Figure 3-20 we can see that the oil recovery performances of the two cases were similar at the early stage. The difference started from the injector shut in and production pressure depletion of the first cycle in test #6. In the early stage of the first cycle, CO_2 spread and dissolved in the heavy oil in the core. In the production pressure depletion period, the heavy oil with CO_2 dissolved and produced by displacement pressure built by pressure depletion. Foamy oil generated at the area near the producer could grow and split stably without disturbing the injected gas flow. Therefore, the scheme of test #6 gave better oil production performance than test #1 and the other tests.

3.2.7 Conclusions of core-flooding experiments

From the core-flooding experiments, several conclusions can be summarized:

(1) CO_2 has large solubility in heavy oil.

(2) The constant production pressure scheme can effectively hold a large displacement

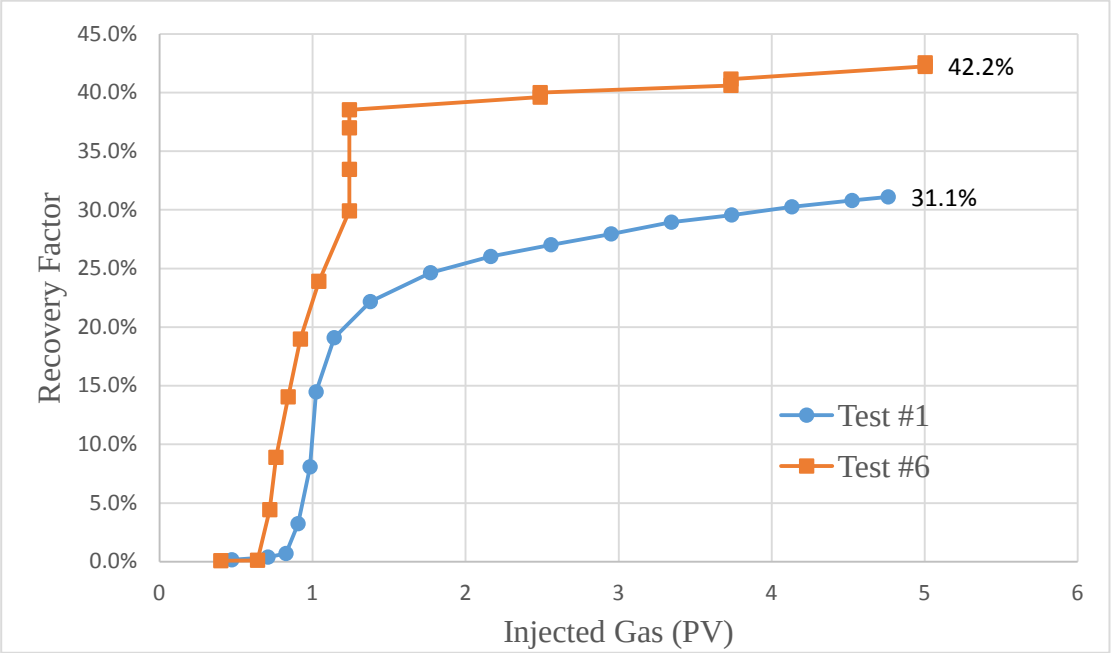

Test#	1	6
Injection Gas	CO_2	CO_2
Injection Volume（PV）	5	5
Injection Rate (ml/min)	7	7
Production Pressure Scheme	Constant	Constant/ Depletion

Figure 3-20 Curves of recovery factor for test #1 and test #6

pressure in the reservoir which has the great benefit that more CO_2 dissolves in the heavy oil.

(3) The constant production pressure scheme can effectively hold a large displacement pressure in the reservoir which has the great benefit that more CO_2 dissolves in the heavy oil.

(4) The production pressure depletion scheme has the function to enlarge the displacement pressure in the reservoir. Moreover, it can generate foamy oil near the producer which can greatly enhance heavy oil recovery.

The multi-pressure-control scheme has both the advantage of the constant production pressure scheme and the production pressure depletion scheme. On the one hand, it can better hold the reservoir pressure in the early stage to have more CO_2 dissolved in heavy oil. On the other hand, foamy oil flow is best utilized at a later stage which avoids disturbing the injection gas flow. This pressure control scheme is proved to be a good method for enhancing heavy oil recovery.

3.3 Cyclic solvent injection (CSI) core test

3.3.1 Introduction

A CSI core test was designed to simulate the single well injection and production scenario.

3.3.2 Materials

The test materials, including heavy oil and brine samples, artificial core and gas, are all the same as for the core-flooding tests.

3.3.3 Experimental setup

The experimental equipment is exactly the same as for the core-flooding tests except that the gas injection port is moved to the same side as the production port on the core holder.

3.3.4 Experimental preparation

The materials were transferred to the transfer cylinders ahead of time. Porosity was measured when the core was saturated with brine and had the value of 29.32%. Permeability was measured after the brine saturation and had the value of 1550 mD. Then the heavy oil sample saturated the core. After the heavy oil saturation, initial oil saturation could be calculated and had the value of 73.17%. After that, the core was flooded by brine to 90% water cut.

3.3.5 Experimental test

The test was designed to have three cycles. Each cycle contained three steps: injection, soaking and production.

During the injection step, CO_2 was injected into the core until the core pressure reached

15 MPa. Then the core was soaking for 30 minutes with all wells shut in. After the soaking step, the production well was opened and produced with pressure depleted from 15 MPa to 8 MPa in the rate of 100 kPa/min. When the production well pressure reached 8 MPa, it would be shut in, and the injection step of the next cycle started.

3.3.6 Results and analysis

The experimental result data was carefully summarized. The total oil production was 7.89 g and the total recovery factor was 6.03%. The first cycle had the most production with 5.4 g and a recovery factor of 4.13%; the second cycle had production of 1.87 g and a recovery factor of 1.43%; the third cycle had oil production of 0.62 g and a recovery factor of 0.47%.

From the result we can see that the overall performance was really poor. Through analysis and speculation, it is concluded that the reason for the poor performance is that the size of the model was too small and the compressibility of the heavy oil and brine in the core was really low with initially high core pressure. Therefore, when gas was injected into the core, the remaining space for the gas to move and transfer was too small. Most of the injected CO_2 was jammed at the injection end of the core and tube. When the production well opened, most of the injected CO_2 was produced as free gas before oil production; only a small amount of gas was effective in oil production.

Although the performance was poor, the data can still be analyzed to give some

conclusions. Figure 3-21 shows the oil production rate, core pressure and GOR. Figure 3-22 shows the oil production rates for each cycle. From the figures, it can be seen that the efficiency of the first cycle is significant compared to other cycles. The GOR of the first cycle is low, which indicates the injected CO_2 made a relatively high contribution to the oil production.

For the second cycle, with some oil and water produced in the first cycle, the space for CO_2 to move in the core became larger. However, the recovery factor obviously decreased with a high GOR. The reason is that when CO_2 was injected, some heavy oil near the well was pushed far away from the production well, and the soaking time was too short for the oil to flow back.

When it came to the third cycle, the GOR rose to a high level in the beginning. The oil production rate remained low during the whole cycle. Therefore, this cycle is worthless and can be ignored in the test.

3.3.7 Conclusions

Although this CSI test was a failure when considering the heavy oil production, information can still be gained from it.

A larger model size experiment could greatly improve the oil production, as a larger space for CO_2 to move and transfer in the model would be provided.

Providing a longer soaking time could give the CO_2 more time to move and dissolve,

which is likely to improve the performance.

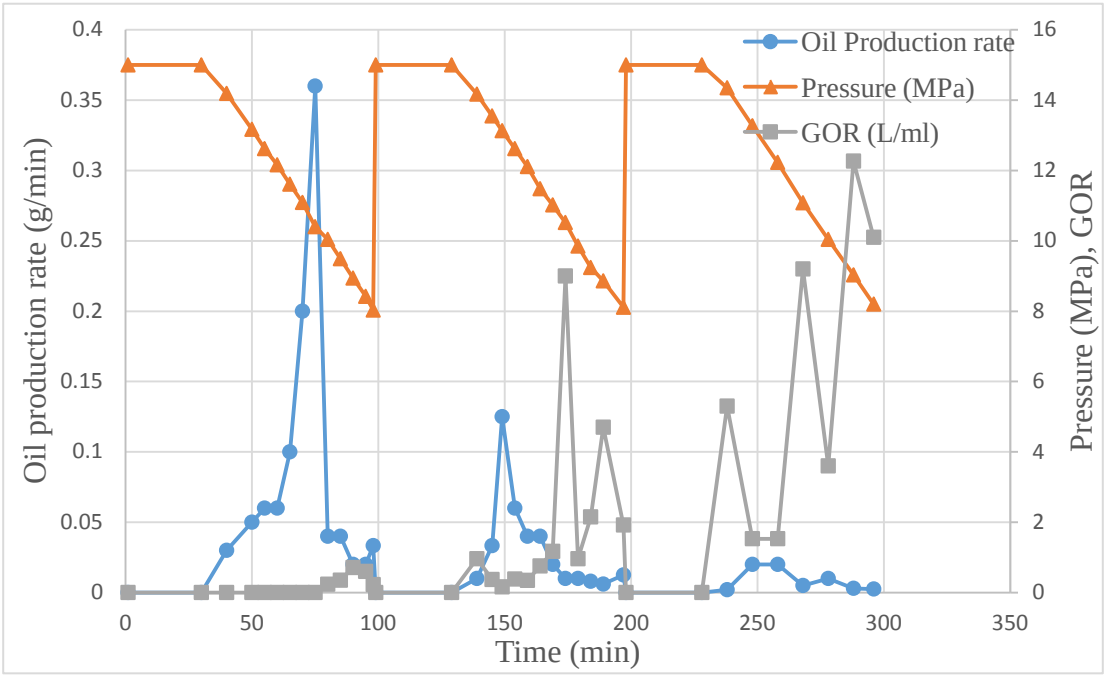

Figure 3-21 Curves of oil production rate, core pressure and GOR for the CSI test

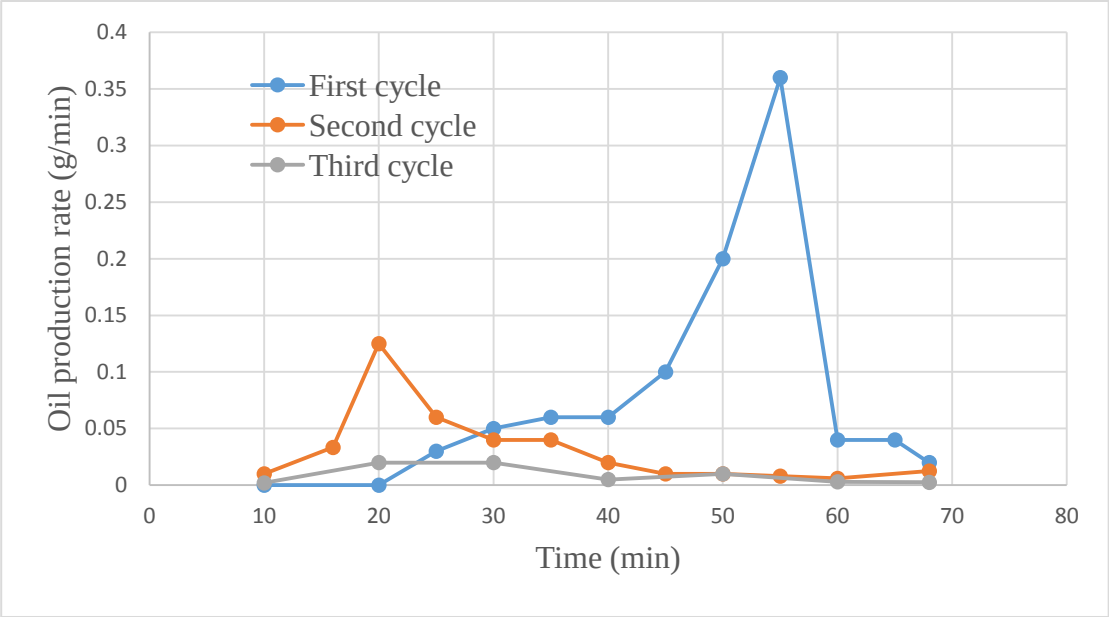

Figure 3-22 Curves of oil production rate of each cycle for the CSI test

CHAPTER 4 NUMERICAL SIMULATIONS

4.1 History matches and predictions for PVT tests

4.1.1 Simulation procedures

The Winprop module in CMG was chosen to history match and predict the PVT tests. The Peng-Robinson equation of state was chosen ahead of time. Two components in live oil were generated, one dead heavy oil and the other CO_2. The properties of these two components were set to default value. The Jossi-Sitel-Thodos Correlation was chosen as the viscosity model type, and correlation parameters were conducted. Experimental results were inserted in the differential liberation, single-phase calculation and saturation pressure tabs to match every single pressure point and pressure range. Three pressure ranges, high, medium and low, were defined in the two-phase flash tabs to predict PVT properties of CO_2 based live oil in these pressure ranges.

4.1.2 Simulation results

By adjusting the regression parameters, correlation parameters, polynomial coefficients and weight factors, the best history match results were obtained. Table 4-1 lists the history match results for the experimental results.

Then the default properties of heavy oil and CO_2 were updated after regressions, which are shown in Table 4-2. With the updated properties, a larger pressure range of properties

Table 4-1 History match result for PVT tests

	Experimental Result Data	After Regression	Error	Weight Factor
Pressure	1.10E+04	1.19E+04	8.18%	1.00E+00
Density	8.17E+02	8.36E+02	2.33%	1.00E+00
Viscosity	2.87E+01	2.65E+01	7.67%	6.00E+00
	Experimental Result Data	After Regression	Error	Weight Factor
Pressure	7.91E+03	7.41E+03	6.32%	1.00E+00
Density	8.58E+02	8.76E+02	2.10%	1.00E+00
Viscosity	5.62E+01	6.26E+01	11.4%	1.00E+01
	Experimental Result Data	After Regression	Error	Weight Factor
Pressure	4.99E+03	4.12E+03	17.4%	2.00E+00
Density	8.75E+02	8.98E+02	2.63%	1.00E+00
Viscosity	1.53E+02	1.45E+02	5.23%	6.00E+00

Table 4-2 Updated dead oil and CO_2 properties

Component	Pc(atm)	Tc(K)	Acentric fact	Mol. weigh	Z	Vc (l/mol)	Omega A	Omega B	SG	Tb (°C)
CO_2	72.8	304.2	0.225	44.01	0.273	0.094	0.288	0.093	0.818	-78.45
Dead Oil	16.734	650	0.45	320	0.297	1.133	0.365	0.075	0.944	430.733

can be predicted. The predicted results are partially shown in Figure 4-1 and Figure 4-2. The predicted results perfectly match the PVT experimental results and obey the physical truth. The predicted results would be used in the following history matches for core-flooding tests and reservoir numerical simulations.

4.2 History match for core-flooding tests

4.2.1 Simulation model

According to the conditions of core-flooding experiments, properties of fluids in the reservoir and properties of CO_2 under reservoir condition, 1-D three phase compositional models were chosen. Because of the existence of complex mass transfer between the different phases, GEM module in CMG were used for simulation.

The model shape was built exactly according to the cores. A cuboid model was divided into 30 grids. Each grid had the parameters of 0.01006m×0.045m×0.045m. The injector was located in the first grid and producer in the 30^{th} grid. Other parameters of reservoir properties were given to the model such as reservoir pressure, reservoir permeability, reservoir porosity, etc. Detailed information is provided in Table 4-3. Fluid and gas properties were inserted with the results obtained from PVT test simulations by the Winprop module mentioned in Chapter 2.1. The water flooding processes before each test were history matched first where an oil-water relative permeability curve for all tests was obtained. The same oil-water relative permeability curve could be used in all tests because

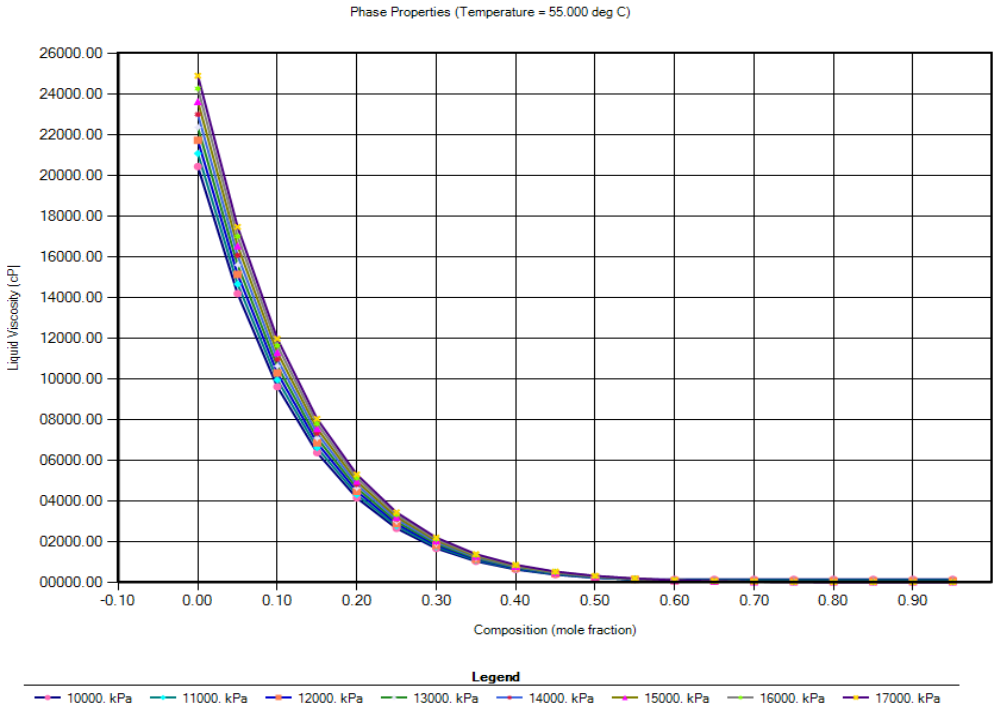

Figure 4-1 Liquid viscosity at different pressures with CO_2 mole fraction in high pressure range

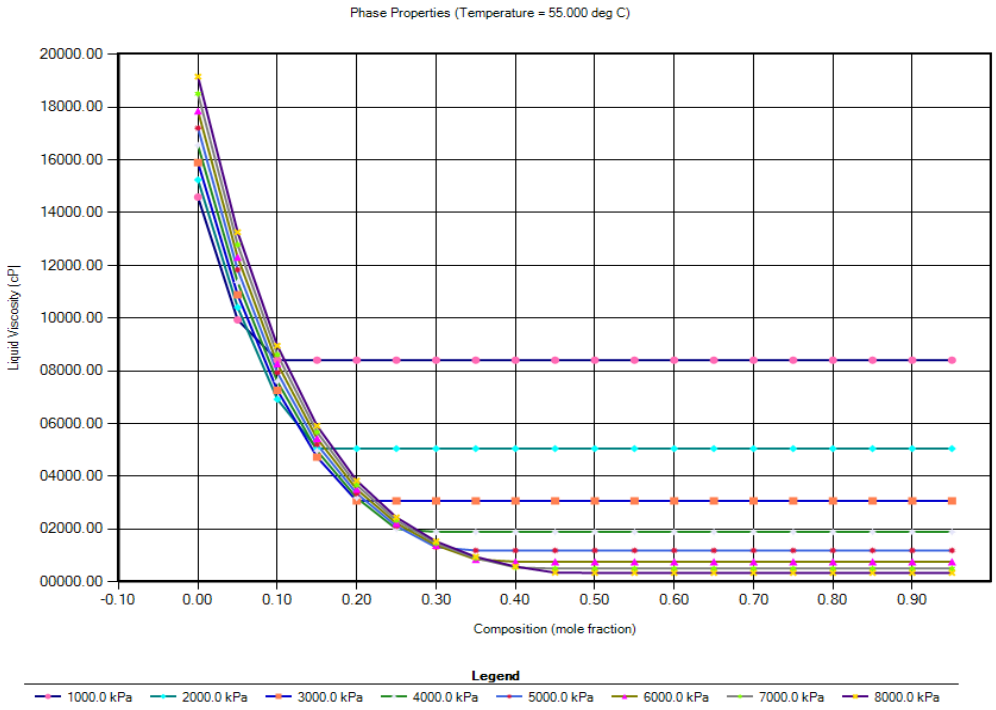

Figure 4-2 Liquid viscosity at different pressures with CO_2 mole fraction in medium pressure range

Table 4-3 Detailed model parameter information

Parameters	Values
Model size	0.3019 m×0.045 m×0.045 m
Grid number	30×1×1
Grid size	0.01006 m×0.045 m×0.045 m
Reservoir pressure	11 MPa
Permeability	1551 mD
Porosity	29.07%
Connate Water Saturation	27 %

the conditions for the water flooding process were all the same. The gas-liquid relative permeability curves are different in different tests due to the different gas injection and production schemes used.

4.2.2 Results and analysis of history matches for core-flooding tests

4.2.2.1 Single test history match results and analysis

Test #1

In the water flooding process, the injection rate was 0.3ml/min under reservoir conditions. In the gas injection process, the injection rate was 7 ml/min. The oil-water relative permeability curves are shown in Figure 4-3. The gas-liquid relative permeability curves will be shown and analyzed later. Figure 4-4 is the history match result of cumulative oil production with time change; the point line is the result data from the experiment, and the solid line is the result of the history match. Figure 4-5 is the history match result of injector pressure change with time; again the point line is the experiment data, and the solid line is the history match result. The numerical simulation result matches the experimental results perfectly with little error (3.25% with cumulative oil production and 0.94% with injector pressure).

In the water flooding process, the highest pressure was only 11.29 MPa due to the low compressibility of water and low injection rate. The oil saturation in the reservoir kept dropping as more and more oil was flooded out and finally dropped below 0.6 at the end

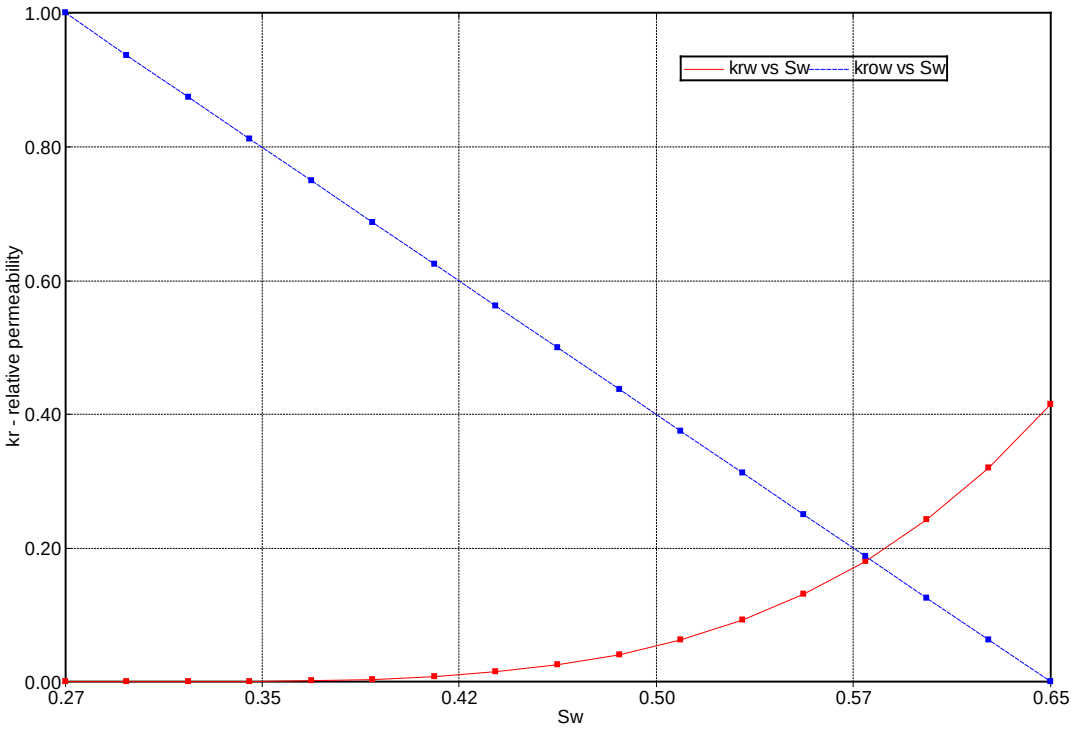

Figure 4-3 Oil-water relative permeability curves for test #1

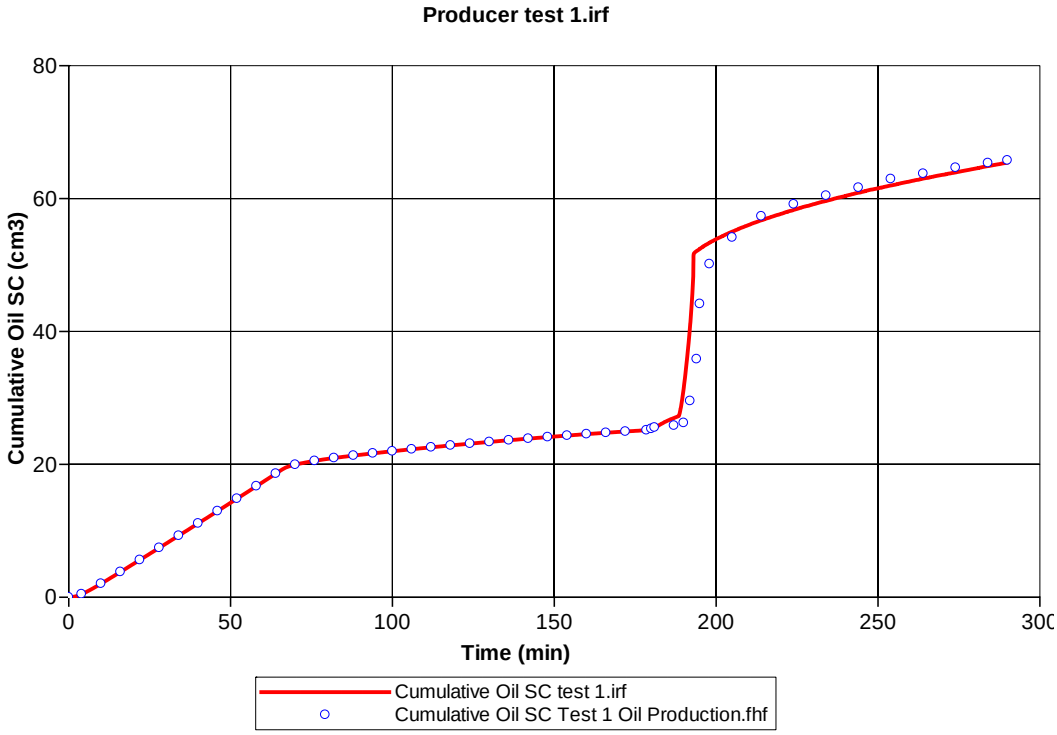

Figure 4-4 History match of cumulative oil production for test #1

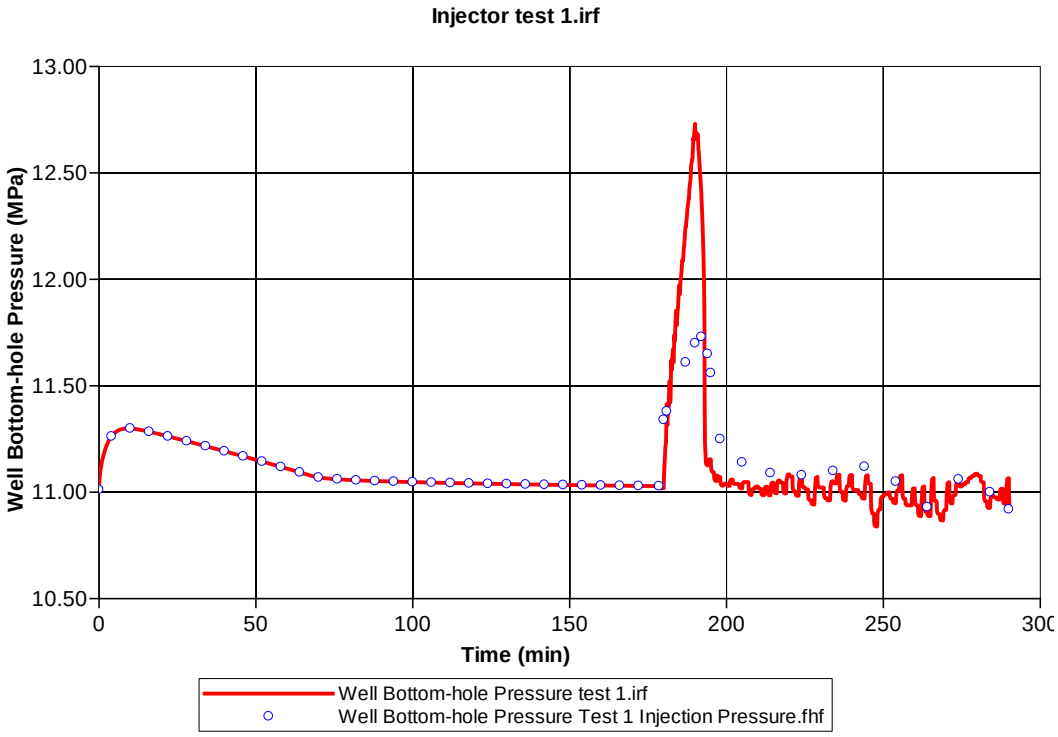

Figure 4-5 History match of injector pressure for test #1

of water flooding process.

In the gas injection process, as the gas was injected into the core, the core pressure rose as high as 12.74 MPa. The oil viscosity in the core decreased from the injector to the producer gradually before the gas breakthrough. Water saturation near the producer rose in this period. Oil saturation rose in the near producer grids and decreased as low as 0.1 in the injector grid due to the gas flooding and pressure differential. Gas saturation in producer grid rose as high as 0.5. When the breakthrough happened, the pressure in the core dropped rapidly. After the breakthrough period the oil viscosity did not change much; it was about 30 cp. However, oil production in this period kept dropping due to oil saturation decrease in the core. At the end of the test, there was no oil remaining in the near injector grids. Gas saturation became high with 0.7 in the injector grid and 0.2 in the producer grid.

Test #2

In this test, the water flooding process was exactly the same as in test #1, so the oil-gas relative permeability was the same, as shown in Figure 4-3. The history match results are shown in Figure 4-6 and Figure 4-7. The numerical simulation result perfectly matches the experimental result data. The error for the cumulative oil production history match is 1.06% and for injector pressure it is 0.47%.

The simulation procedure was exactly the same as for test #1, the only difference being that the gas injection rate changed from 7 ml/min to 2ml/min under reservoir conditions.

The water flooding process phenomenon was exactly the same as test #1. The gas flooding

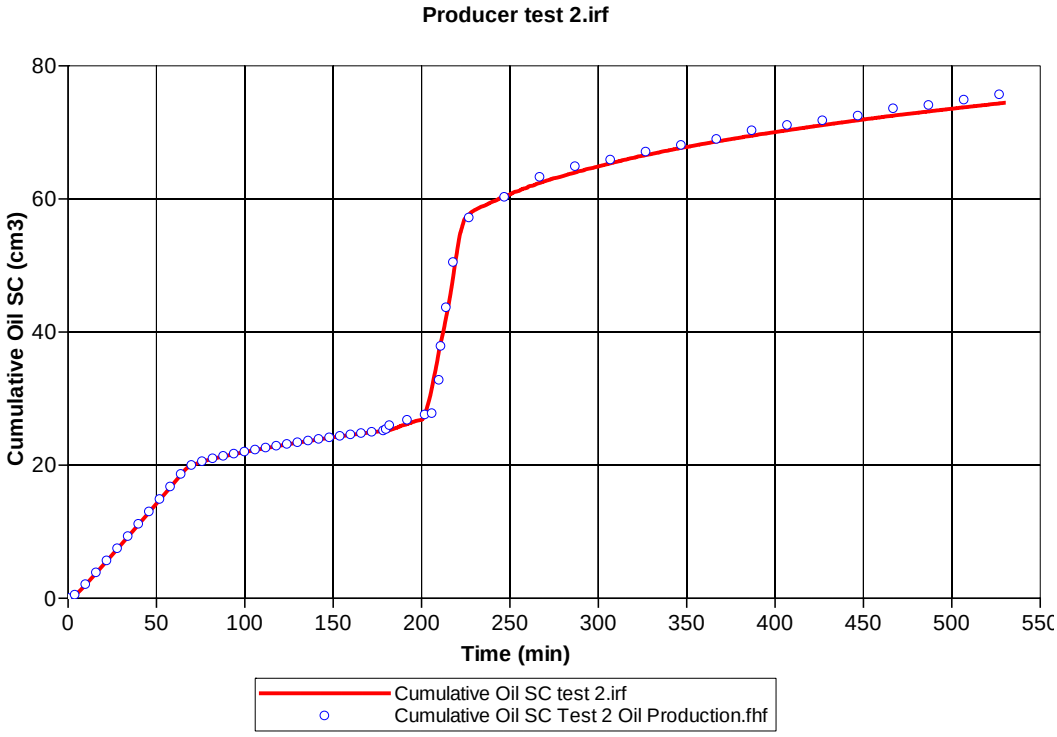

Figure 4-6 History match of cumulative oil production for test #2

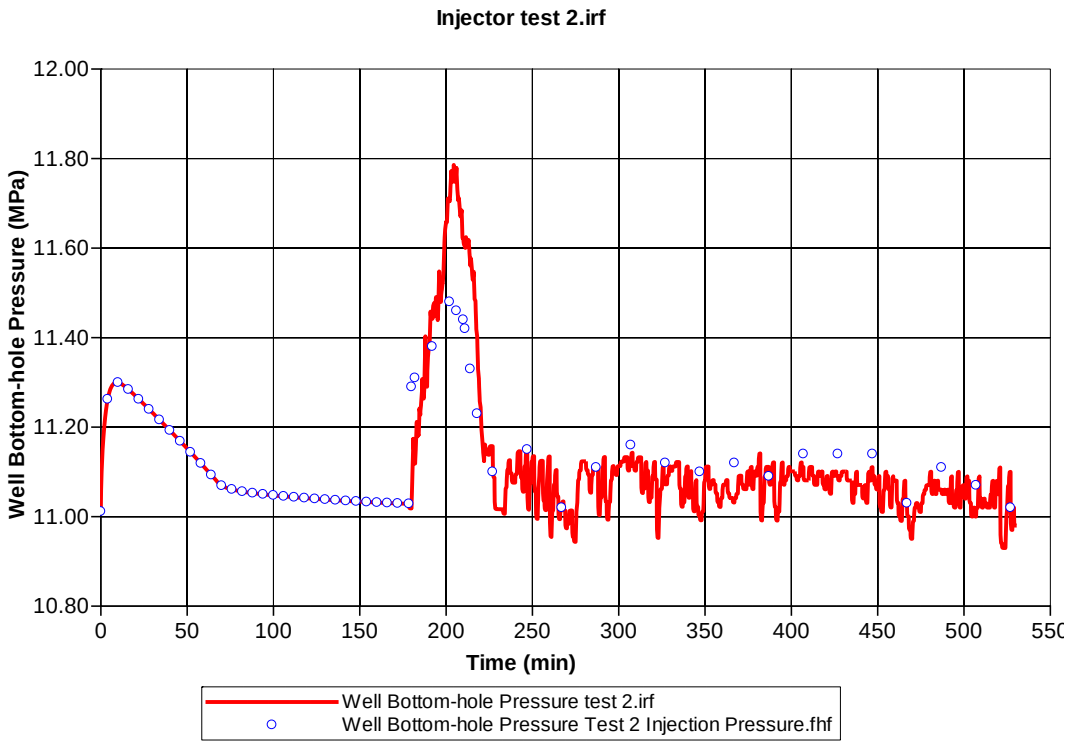

Figure 4-7 History match of injector pressure for test #2

process was similar, with hardly any differences. In the gas injection process, before the breakthrough period, the highest pressure in the core reached 11.78 MPa, which is lower than in test #1 due to the smaller injection rate. Oil viscosity decreased gradually as more gas was injected. At the breakthrough point, pressure in the core dropped rapidly. After breakthrough, oil saturation in the core dropped, and the oil production rate decreased over time. The oil viscosity did not change much compared to before the breakthrough period.

Test #3

In this test, the water flooding process was exactly the same as in the former tests, so the oil-gas relative permeability was the same, as shown in Figure 4-3. The history match results are shown in Figure 4-8 and Figure 4-9. The numerical simulation result perfectly matches the experimental result data. The error for the cumulative oil production history match is 1.41% and for the injector pressure it is 0.37%.

The simulation procedure was exactly the same as for test #2, the only difference being the production pressure depleted from 11 MPa to 8 MPa in the gas flooding time. The water flooding process phenomenon was exactly the same as for the former tests. In the gas injection process, before the breakthrough, although gas continued to be injected into the core, the depleted production pressure made the highest core pressure only reach 11.53 MPa. Oil viscosity was reduced by CO_2 dissolution. Gas injection and depleted pressure led to a large displacement pressure between the injector and producer and

increased the oil production rate. At breakthrough, the pressure dropped rapidly, and the oil production

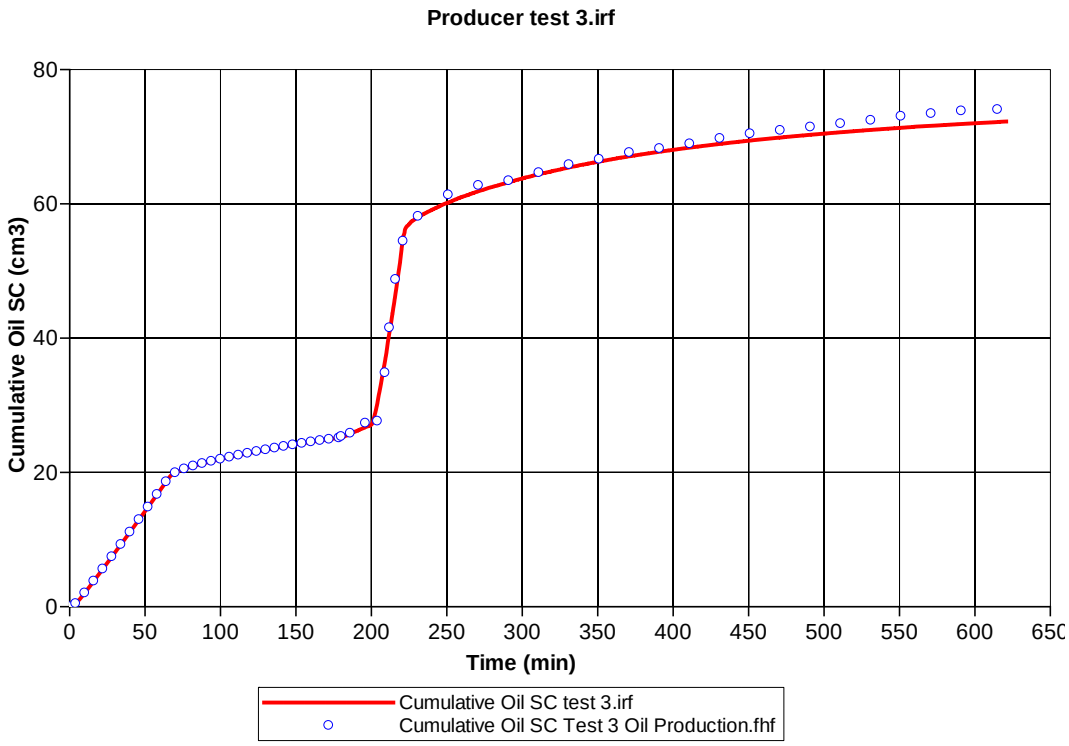

Figure 4-8 History match of cumulative oil production for test #3

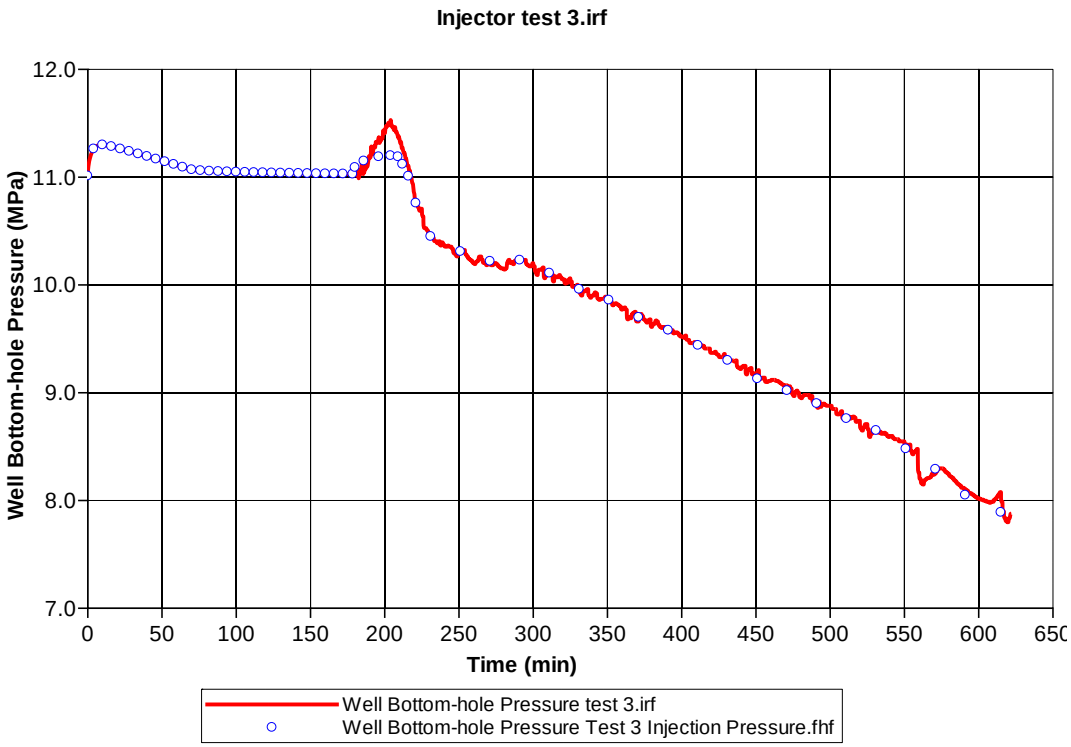

Figure 4-9 History match of injector pressure for test #3

rate reached the highest point. In the period from the beginning of the gas injection to breakthrough, oil saturation in the near producer grids rose and in the near injector grids dropped to 0.1. Gas saturation at the injector grid reached 0.5. After breakthrough, the oil production rate decreased due to the reduced oil saturation in the core. At the end of the test, oil saturation near the producer rose a little due to the gas flooding. Oil saturation in the injector grid decreased to zero. Gas saturation reached 0.7 at the injector and 0.2 at the producer. The water remaining in the core was almost connate water which had 0.29 at the producer grid and 0.3 at the injector grid.

Test #4

In this test, the water flooding process was exactly the same as in the former tests, so the oil-gas relative permeability was the same, as shown in Figure 4-3. The history match results are shown in Figure 4-10 and Figure 4-11. The numerical simulation result perfectly matches the experimental result data. The error for the cumulative oil production history match is 2.26% and for injector pressure it is 2.48%.

The difference between this test and previous one is that the gas injection rate changed from 2 ml/min to 7 ml/min, and this led to the gas injection time being shorter. Another difference is that the production pressure depletion ending the pressure changed from 8 MPa to 5 MPa; these two differences made the pressure depletion rate much greater than in test #3.

The water flooding process will not be introduced here as it was exactly the same as

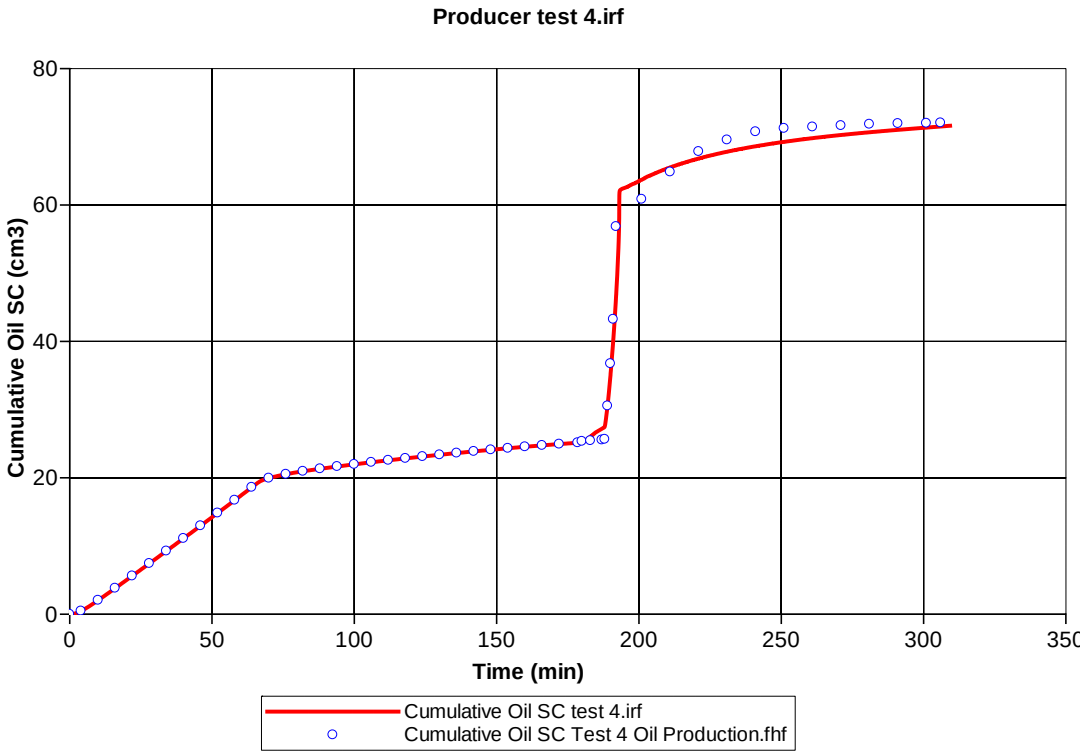

Figure 4-10 History match of cumulative oil production for test #4

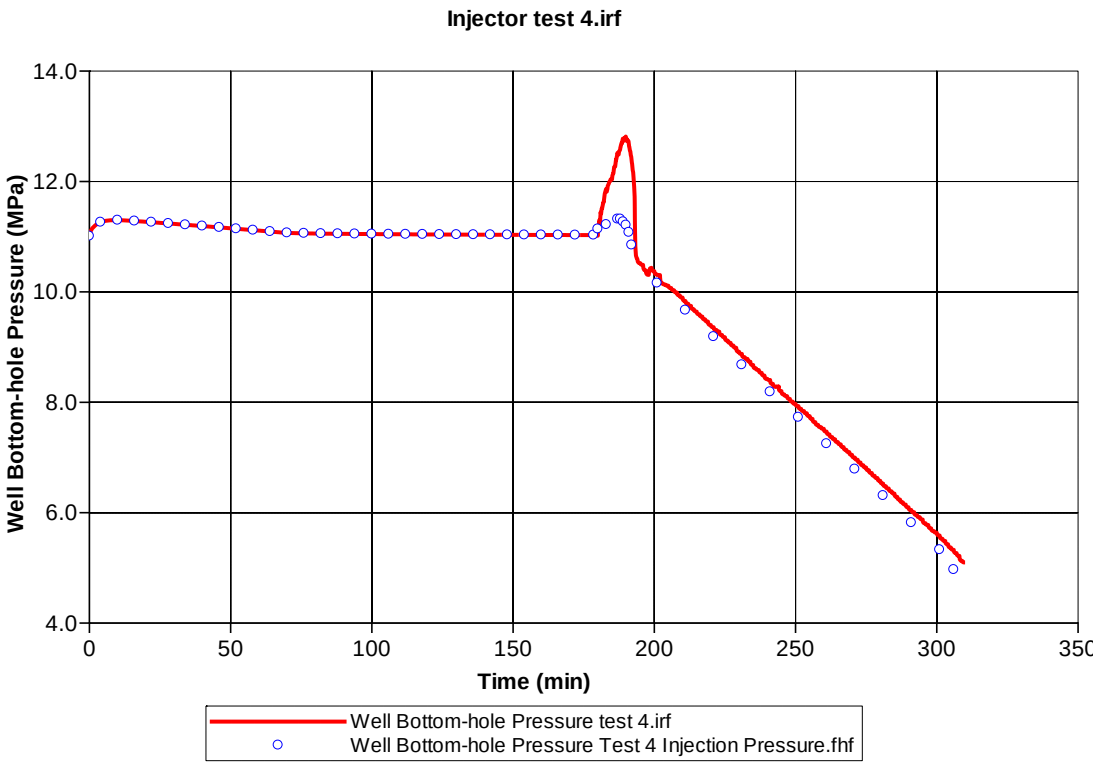

Figure 4-11 History match of injector pressure for test #4

before. In the gas flooding process, before breakthrough, because of the high gas injection rate, the highest pressure in the core could reach 12.82 MPa. Oil viscosity in the core was reduced gradually as more and more CO_2 was injected. Gas injection and production pressure depletion led to a high pressure differential between the injector and producer. Low oil viscosity and high displacement pressure made more heavy oil move towards the producer and produced. The oil production rate reached peak pointat the breakthrough moment. The core pressure dropped rapidly at this point. After breakthrough, the oil production rate dropped due to the reduced oil saturation in the core. When the core pressure dropped below about 7 MPa, oil viscosity in the core rose back to around 100 cp. The reason for this is that when the pressure was lower than the CO_2 saturation pressure, some CO_2 was released from the oil. At the end of the test, oil saturation in the near producer grid rose to a high level, and there was no oil remaining in the injector grid. Gas saturation reached 0.7 in the injector grid and 0.2 in the producer gird.

Test #5

In this test, the water flooding process was exactly the same as in the former tests, so the oil-gas relative permeability was the same, as shown in Figure 4-3. The history match results are shown in Figure 4-12 and Figure 4-13. The numerical simulation result perfectly matches the experimental result data. The error for the cumulative oil production history match is 1.51% and for injector pressure is 1.52%.

The only difference between this test and test #1 is that the injected gas changed from

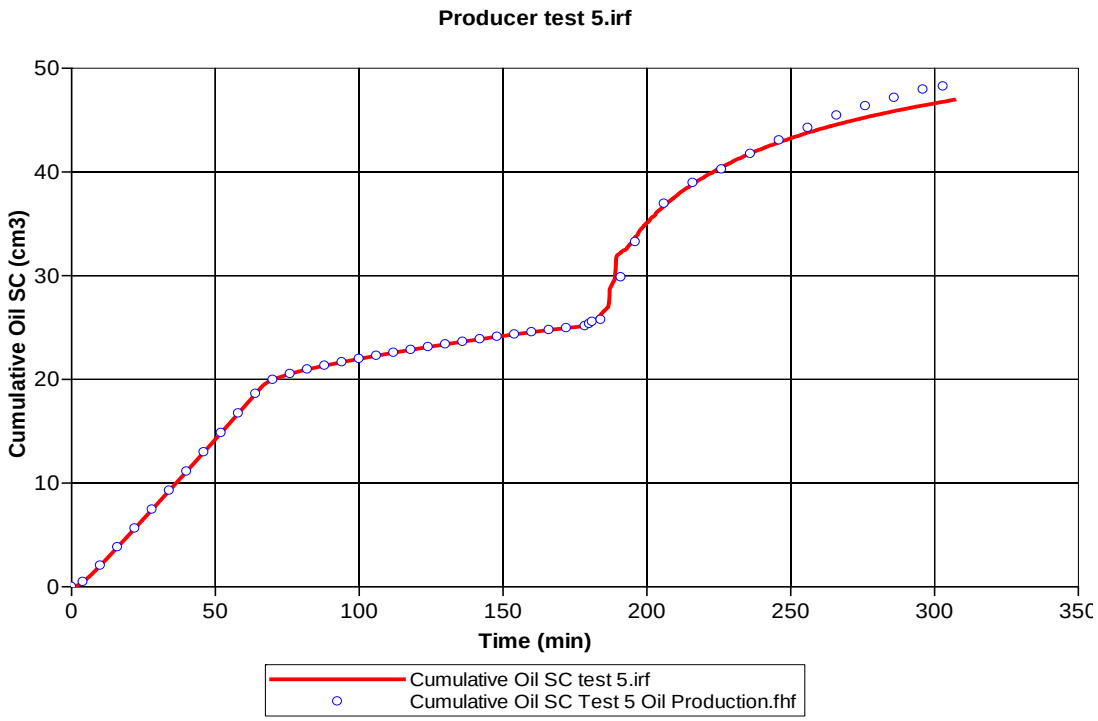

Figure 4-12 History match of cumulative oil production for test #5

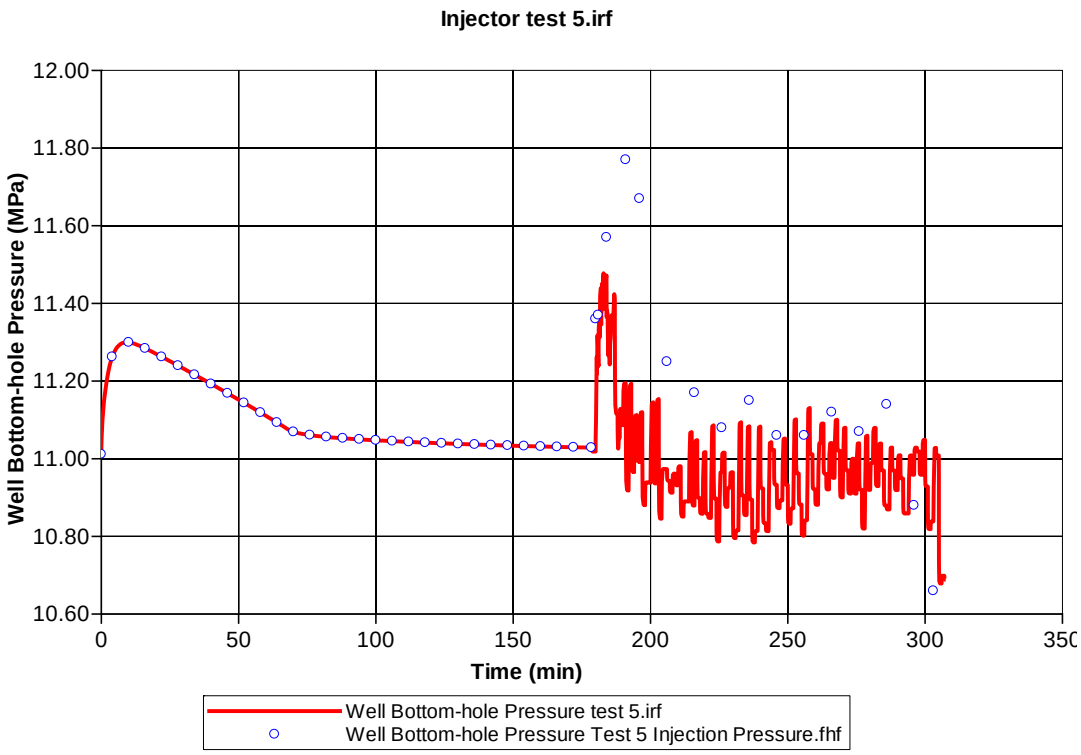

Figure 4-13 History match of injector pressure for test #5

pure CO_2 to flue gas (20% CO_2 and 80% N_2). N_2 was added to the injected component, but because it cannot dissolve in oil, the influence factor of N_2 was set to zero.

The water flooding process will not be introduced here. In the gas injection process, before breakthrough, the pressure in the core rose due to the high gas injection rate. However, only a quarter of the injected gas could dissolve in the oil. That made it easy for the gas to breakthrough, so the highest core pressure only reached 11.47 MPa. Oil viscosity in the core was reduced due to CO_2 dissolution. At the breakthrough point, because 80% of the gas could not be dissolved in the oil, the gas saturation in the near producer grids reached as high as 0.3. After breakthrough, the core pressure dropped rapidly. The oil production rate was reduced. Oil viscosity was reduced to 60 cp. At the end of the test, gas saturation reached 0.16 in the producer grid and 0.7 in the injector grid. No oil remained in the injector grid, and oil saturation reached a high level in the producer grid.

Test #6

In this test, the water flooding process was exactly the same as in the former tests, so the oil-gas relative permeability was the same, as shown in Figure 4-3. The history match results are shown in Figure 4-14 and Figure 4-15. The numerical simulation result perfectly matches the experimental result data. The error for cumulative oil production history match is 2.41% and for injector pressure it is 4.60%.

This is a cyclic process with independent gas flooding and production pressure

depletion processes in each cycle. Detailed information is in 1.2.5.3.

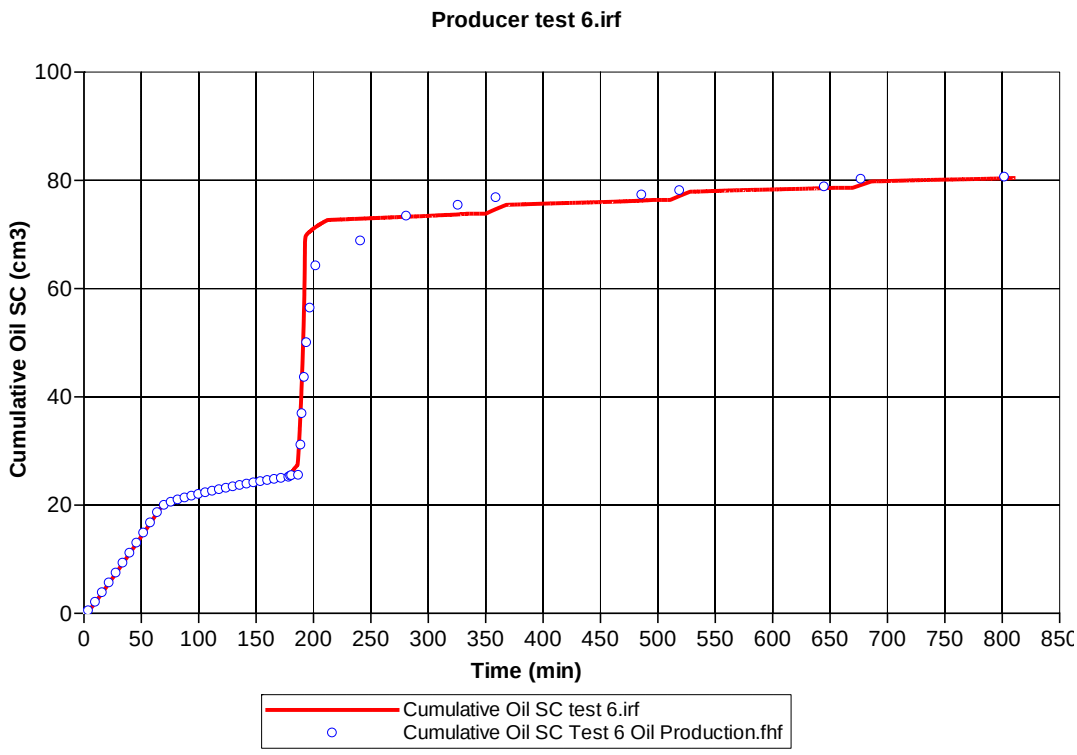

Figure 4-14 History match of cumulative oil production for test #6

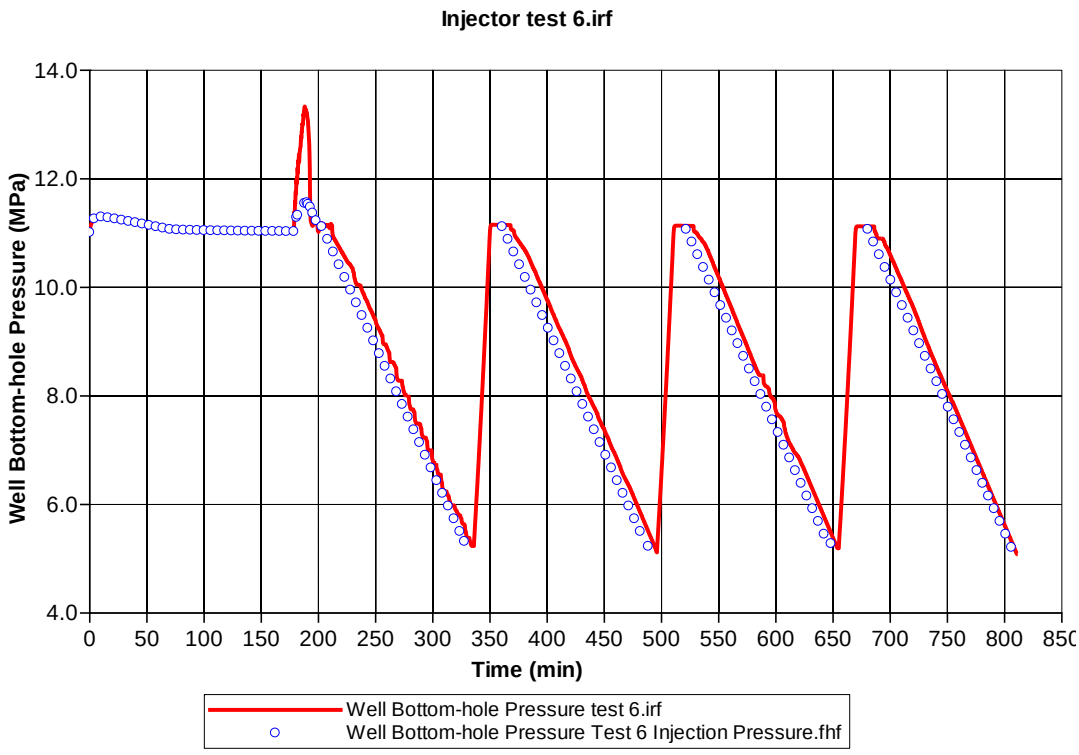

Figure 4-15 History match of injector pressure for test #6

In the first cycle, before breakthrough, gas was injected at a high rate which led to a rise in the core pressure. Oil viscosity was reduced by CO_2 dissolution. The oil production rate increased by viscosity reduction and increased displacement pressure. With the breakthrough, oil saturation in the near producer grids rose and was almost zero in the injector grid. Gas saturation reached 0.3 in the producer grid. After the breakthrough, the oil production rate dropped due to lower oil saturation. When the pressure depletion process began, large amounts of oil and gas were produced. Oil viscosity rose back to 100 cp from 60 cp when the pressure reduced to 7 MPa.

After the first cycle was done, the next cycle started immediately. However, the following three cycle had limited contributions to the whole recovery factor, totaling only 9.4%. From the history match data, the oil saturation change in the core at the end of each cycle was small. The gas saturation at these moments changed slightly. However, as the contact face area of gas and oil did not change much, the performance is not significant.

4.2.2.2 Comparison analysis of history match results between tests

Test #1 vs. test #4

Test #1 was the constant production pressure control scheme while test #4 was the production pressure depletion scheme. The gas injection rates were both 7 ml/min with pure CO_2. This comparison is to discuss the contribution of foamy oil flow in oil production. The major comparison point is the gas-liquid relative permeability curves.

Figure 4-16 shows the gas-liquid relative permeability curves of these two tests. From the curves, we can see that the K_{rg} curve of test #4 is lower than that of test #1. This indicates that the gas in test #4 flowed more slowly than or not as easily as the gas in test #1. The slower CO_2 flow in the reservoir had the positive effect that the CO_2 can had much more time to spread, to make contact and to dissolve in the heavy oil. And test #4 had the foamy oil flow phenomenon, which also affects the relative permeability curve.

Test #3 vs. test #4

Both of these tests are with the production pressure depletion scheme, which means that foamy oil flow occurred in both tests. Test #3 had a lower injection rate and depletion rate. This comparison observes the effect of depletion rate on foamy oil flow. Figure 4-17 shows the gas-liquid relative permeability curves for test #3 and test #4. From the curve, we can see that K_{rg} curve of test #4 is lower than that of test #3. This indicates that the gas in test #4 flowed more slowly than or not as easily as the gas in test #3. In addition to the CO_2 dissolved in oil, the foamy oil flow effect is more important in this comparison. To foamy oil, as the gas bubble remained in the reservoir, the bubbles split into smaller bubbles. The increased number of bubbles swelled the whole volume of the gas-oil phase which led to more oil production.

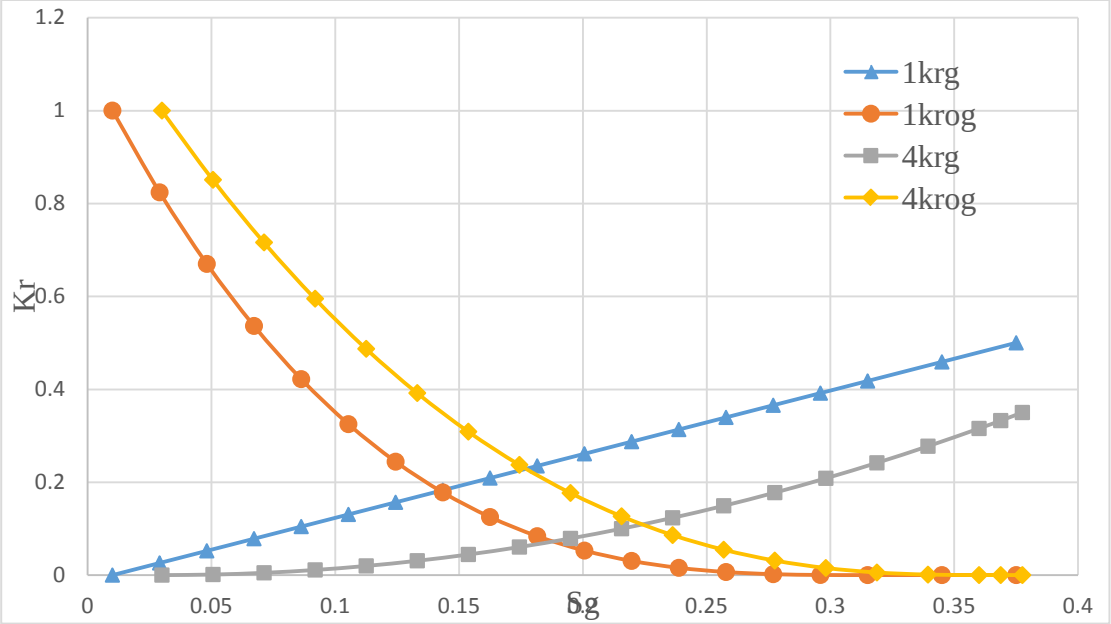

Figure 4-16 Gas-liquid relative permeability curves of test #1 and test #4

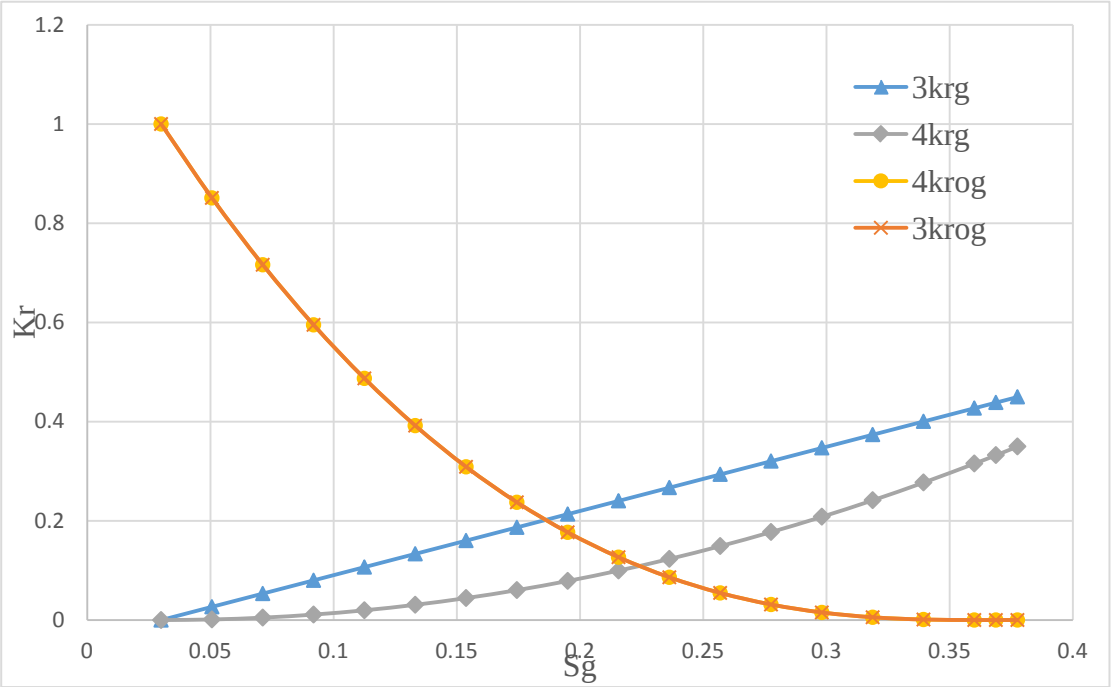

Figure 4-17 Gas-liquid relative permeability curves of test #3 and test #4

Test #4 vs. test #6

Test #4 was the simple production pressure depletion scheme case while test #6 was the multi-pressure control case. Test #4 kept the injected gas when the production pressure depleted. Test #6 separated the injection and production pressure depletion into two connected processes. In test #4, the higher production pressure depletion rate generated high quality and a high quantity of foamy oil at the near producer area. However, the high gas injection rate had a great negative effect on the foamy oil. The strong injected gas flow would destroy and push out the newly generated foamy oil before it developed further. The reason test #6 to had two processes separately was to supply a constant and stable environment for the foamy oil to generate and develop. When foamy oil keeps splitting and swelling in the reservoir, a greater contribution will be made to total heavy oil recovery. The gas-liquid relative permeability curves of test #4 and test #6 (Figure 4-18) support this theory.

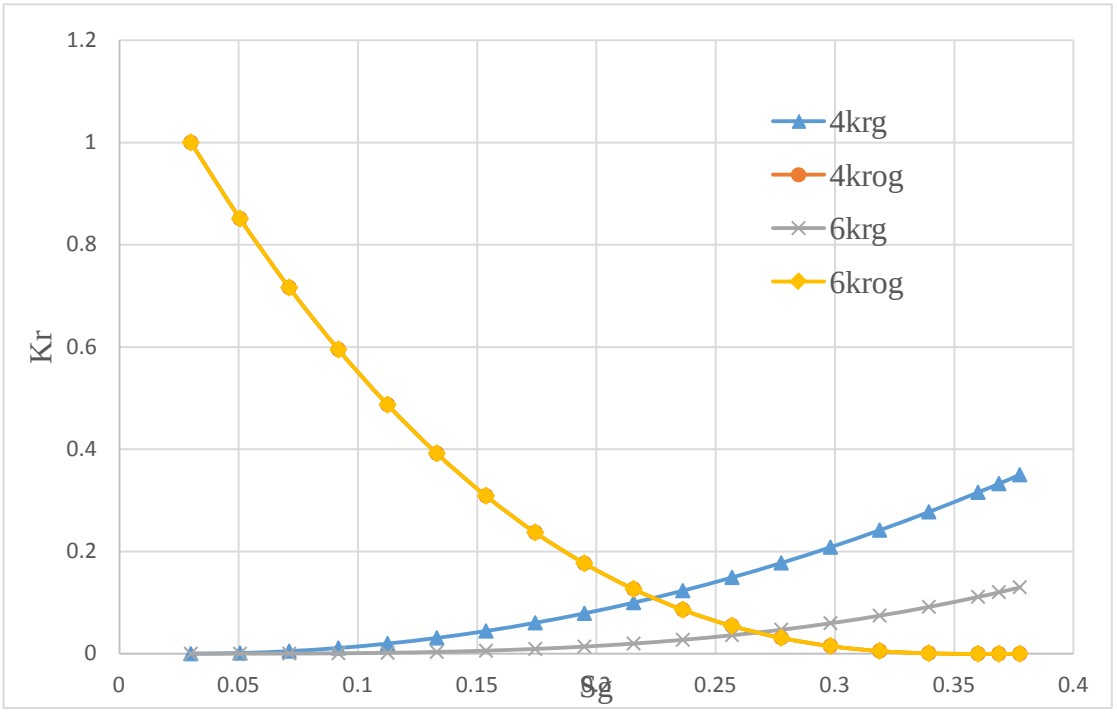

Figure 4-18 Gas-liquid relative permeability curves of test #4 and test #6

4.3 Reservoir model simulation and production prediction

4.3.1 Reservoir model

3-D reservoir model simulation is an important method to predict reservoir original oil in place, EOR method performance, etc. The prediction by 3-D reservoir model simulation is much more accurate than by 2-D simulation.

The target area was about 470 m on each side. The Sequential Gaussian Simulation method in CMG was used in model building. The grid number was set to 45×45×3, and the size of each grid was automatically average interpolated according to the total area. The depth of the reservoir was 1408 m. Well logging data from several wells in the area were chosen to be the sampling points. The data were normalized and plotted on histograms. Figure 4-19 and Figure 4-20 are histograms of the distribution of porosity and permeability data for the target field area. These data were processed by the geostatistics method and given to the reservoir model. The model shape is shown in Figure 4-21. Two wells were placed in the model as injector and producer.

4.3.2 Reservoir model development simulation

Module GEM in CMG was chosen to run the simulation. Three kinds of reservoir development categories were simulated: water flooding followed by CO_2 flooding, CO_2 flooding without water flooding and water flooding followed by flue gas flooding. Each categories has 14 to 16 different schemes which is 44 cases in total. The duration of all

the cases is 20 years. The best scheme case in each category will be introduced here. The data can be checked from Table 4-4 to Table 4-9.

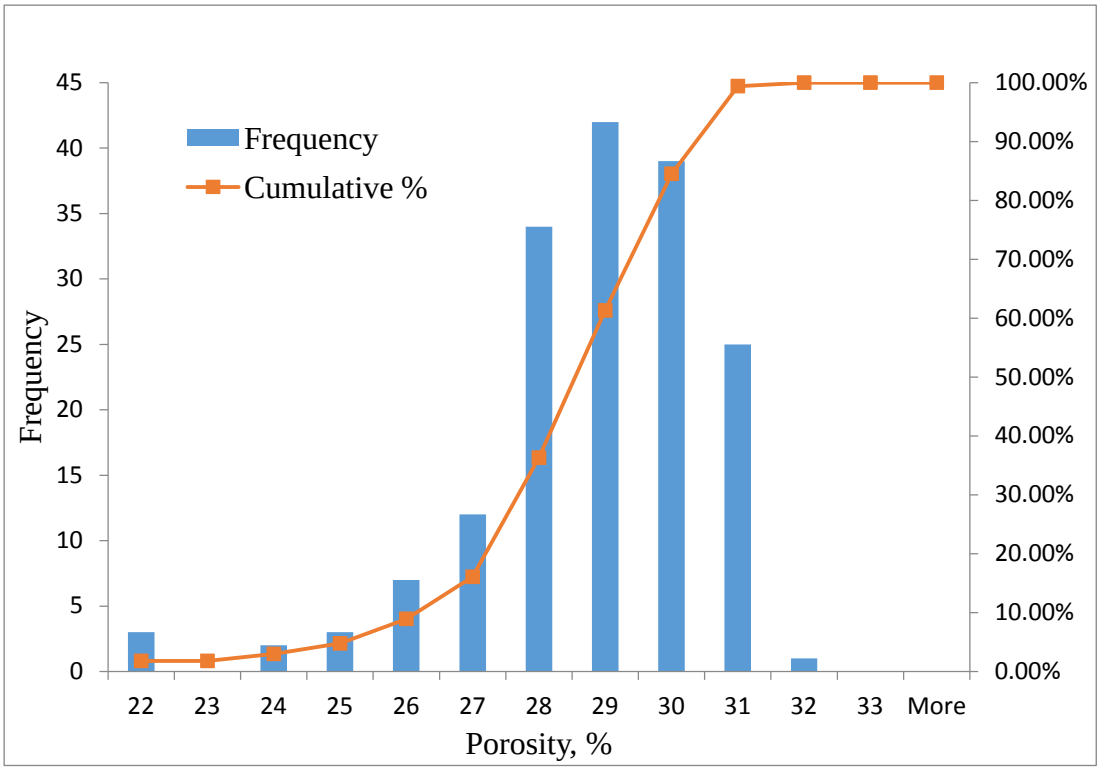

Figure 4-19 Histogram of the distribution of porosity data for target area

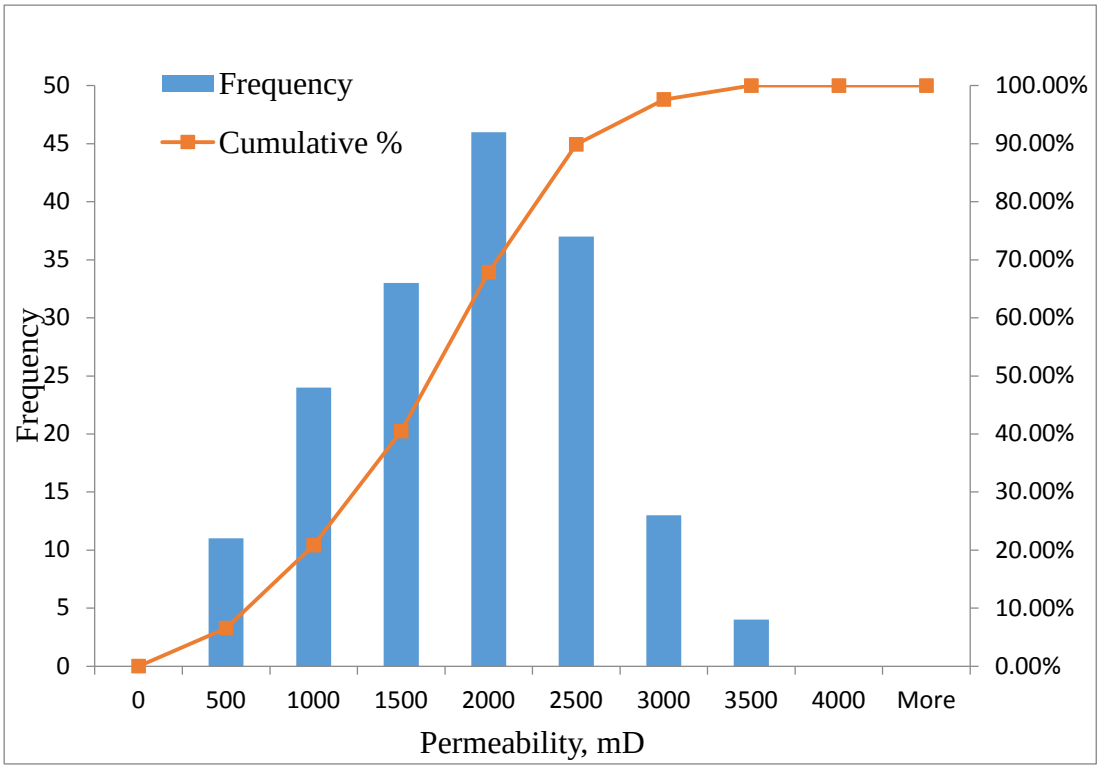

Figure 4-20 Histogram of the distribution of permeability data for target area

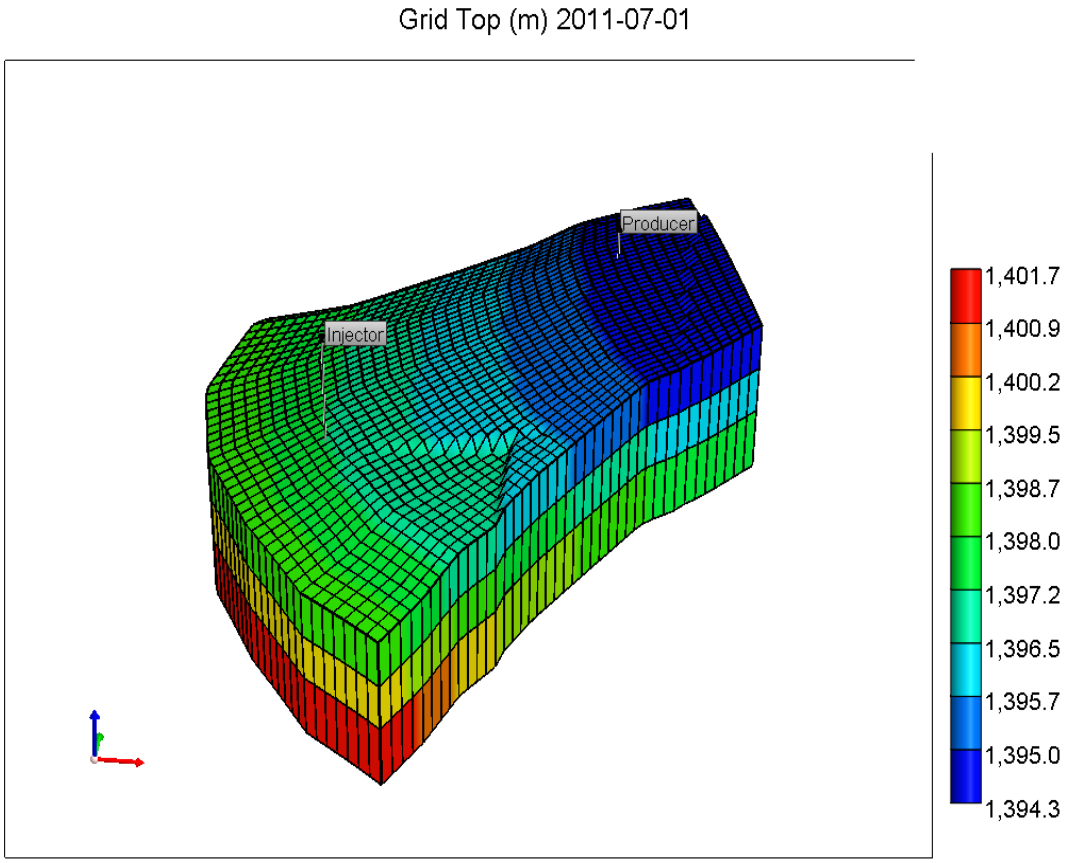

Model size: 470 m × 470 m
Grid number: 45 grids × 45 grids ×3 grids
Depth: 1408 m
Average thickness: 5 m
Average permeability: 1500 mD
Average porosity: 28%
Pressure: 11 MPa
Temperature: 55^{o}C
Oil viscosity: 869.3 cp
Original oil saturation: 72.5%

Figure 4-21 CMG 3D reservoir model grid top

Table 4-4 Different water flooding test schemes followed by CO_2 flooding reservoir development category

Test #	Injection rate (Reservoir condition) m^3/day	Bottom hole pressure scheme	Bottom hole pressure (MPa)	Pressure depletion time (yrs)
1	100	Constant	11	/
2	100		8	/
3	100		5	/
4	50	Constant	11	/
5	50		8	/
6	50		5	/
7	100	Cyclic pressure depletion (pressure base)	11 to 5	1
8				2
9	50	Cyclic pressure depletion (pressure base)	11 to 5	1
10				2
11	100	Cyclic pressure depletion (injected gas volume base 0.1PV)	11 to 5	1
12				2
13	50	Cyclic pressure depletion (injected gas volume base 0.05PV)	11 to 5	1
14				2

Table 4-5 Results of water flooding tests followed by CO_2 flooding reservoir development category

Test #	Recovery factor	Gas efficiency (Gas injection volume/oil production volume m^3/m^3)	PV	Gas injection volume standard condition (MM m^3)	Cumulative gas production standard condition (MM m^3)	Cumulative oil production (M m^3)	Gas efficiency (Gas injection volume/gas production volume m^3/m^3)
1	25.78%	1398.83	2.458	79.876	71.178	57.102	152.32
2	25.32%	1226.49	2.572	68.806	64.347	56.1	79.48
3	27.33%	958.50	2.615	58.024	55.907	60.536	34.97
4	20.30%	938.21	1.358	42.199	35.839	44.978	141.40
5	21.95%	733.44	1.378	35.671	32.498	48.635	65.24
6	25.19%	539.71	1.378	30.118	28.656	55.804	26.20
7	29.42%	1114.84	2.387	72.651	65.674	65.167	107.06
8	29.35%	1111.64	2.385	72.267	64.301	65.009	122.54
9	24.89%	678.81	1.328	37.427	32.926	55.136	81.63
10	24.82%	675.76	1.325	37.15	31.976	54.975	94.11
11	25.11%	517.52	0.7993	28.783	17.682	55.617	199.60
12	23.30%	377.57	0.5558	19.485	12.415	51.607	136.99
13	22.60%	388.88	0.5704	19.466	12.501	50.056	139.14
14	20.65%	278.99	0.3804	12.765	8.0832	45.755	102.32

Table 4-6 Different CO_2 flooding test schemes without water flooding reservoir development category

Test #	Injection rate (Reservoir condition) m3/day	Bottom hole pressure scheme	Bottom hole pressure (MPa)	Pressure depletion time (yrs)
1	100	Constant	11	/
2	100		8	/
3	100		5	/
4	50	Constant	11	/
5	50		8	/
6	50		5	/
7	100	Cyclic pressure depletion (pressure base)	11 to 5	1
8				2
9	50	Cyclic pressure depletion (pressure base)	11 to 5	1
10				2
11	100	Cyclic pressure depletion (injected gas volume base 0.1PV)	11 to 5	1
12				2
13	50	Cyclic pressure depletion (injected gas volume base 0.05PV)	11 to 5	1
14				2
15	100	Constant at 5 MPa before breakthrough and cyclic after breakthrough (pressure base)	11 to 5	1
16				2

Table 4-7 Results of CO_2 flooding tests without water flooding reservoir development category

Test #	Recovery factor	Gas efficiency (Gas injection volume/oil production volume m^3/m^3)	PV	Gas injection volume standard condition (MM m^3)	Cumulative gas production standard condition (MM m^3)	Cumulative oil production (M m^3)	Gas efficiency (Gas injection volume/gas production volume m^3/m^3)
1	29.55%	1540.57	3.229	100.83	87.917	65.45	197.30
2	28.17%	1337.20	3.275	83.449	76.742	62.406	107.47
3	29.79%	1039.50	3.275	68.609	65.386	66.002	48.83
4	7.17%	2499.78	1.638	39.724	35.522	15.891	264.43
5	21.30%	841.39	1.638	39.696	35.294	47.179	93.30
6	25.56%	586.06	1.638	33.184	31.077	56.622	37.21
7	31.79%	1280.69	3.142	90.185	81.508	70.419	123.22
8	31.97%	1264.07	3.14	89.528	81.513	70.825	113.17
9	25.02%	774.12	1.638	42.902	37.263	55.42	101.75
10	25.33%	761.66	1.638	42.737	37.384	56.11	95.40
11	28.14%	721.49	1.287	44.971	30.575	62.331	230.96
12	25.21%	521.82	0.8879	29.142	20.523	55.847	154.33
13	21.50%	500.56	0.7631	23.845	15.52	47.637	174.76
14	19.27%	349.06	0.4962	14.897	9.5703	42.678	124.81
15	31.95%	733.46	1.521	51.92	34.889	70.788	240.59
16	28.28%	518.14	1.03	32.456	22.927	62.639	152.13

Table 4-8 Different water flooding tests schemes followed by flue gas flooding reservoir development category

Test #	Injection rate (Reservoir condition) m3/day	Bottom hole pressure scheme	Bottom hole pressure (MPa)	Pressure depletion time (yrs)
1	100	Constant	11	/
2			8	/
3			5	/
4	50	Constant	11	/
5			8	/
6			5	/
7	100	Cyclic pressure depletion (pressure base)	11 to 5	1
8				2
9	50	Cyclic pressure depletion (pressure base)	11 to 5	1
10				2
11	100	Cyclic pressure depletion (injected gas volume base 0.1PV)	11 to 5	1
12				2
13	50	Cyclic pressure depletion (injected gas volume base 0.05PV)	11 to 5	1
14				2

Table 4-9 Results of water flooding tests followed by flue gas flooding reservoir development category

Test #	Recovery factor	Gas efficiency (Gas injection volume/oil production volume m^3/m^3)	PV	Gas injection volume standard condition (MM m^3)	Cumulative gas production standard condition (MM m^3)	Cumulative oil production (M m^3)	Gas efficiency (Gas injection volume/gas production volume m^3/m^3)
1	13.17%	2457.48	2.756	71.702	68.334	29.177	115.43
2	16.58%	1667.17	2.756	61.242	60.114	36.734	30.71
3	21.26%	1157.51	2.756	54.522	54.324	47.103	4.20
4	9.74%	1627.18	1.378	35.121	32.983	21.584	99.05
5	14.59%	928.82	1.378	30.013	29.22	32.313	24.54
6	19.92%	606.11	1.378	26.745	26.611	44.126	3.04
7	20.96%	1418.62	2.738	65.885	62.637	46.443	69.94
8	21.06%	1412.77	2.733	65.914	61.721	46.656	89.87
9	17.80%	806.13	1.378	31.784	29.721	39.428	52.32
10	17.82%	810.83	1.378	32.006	29.288	39.473	68.86
11	21.77%	677.95	1.155	32.693	27.315	48.223	111.52
12	21.63%	435.25	0.7411	20.857	16.878	47.92	83.03
13	17.90%	438.01	0.6411	17.367	13.897	39.65	87.52
14	17.74%	285.46	0.4159	11.219	8.5864	39.302	66.98

4.3.3 Analysis of the best scheme case in each category

4.3.3.1 Water flooding followed by CO_2 flooding category best scheme case

The best scheme case in this category is case #7 which had continued gas injection when production pressure depleted cyclically. The gas injection rate was 100 m^3/day. Production pressure was depleted from 11 MPa to 5 MPa in one year, and then rose back to 11 MPa to start the next cycle. The duration was 20 years. Relative permeability of test #4 was used to simulate the half flooding and half foamy oil flow scheme. It had a recovery factor of 29.42%. In this category, cases like core-flooding test #6, which had the injector shut in when production pressure depleted, were also tried. But the recovery factors is not as well as this case. The reason for that is simple. A reservoir is much larger than a core, and the injected gas flow hardly have effect on foamy oil in a reservoir compared to in a core; the cases that had the core-flooding test #6 scheme took a longer time to take effect than case #7 which led to a recovery factor lower than case #7 in the test duration of 20 years.

Figure 4-22 shows the curves of time vs. production pressure and cumulative oil production. From the curves, water flooding does not contribute much to the oil production. The slope change point on cumulative oil production curve is at about year 2017. At this time, water in the water channels in the reservoir is flooded out by CO_2 and oil production rate reaches the peak point which is the same phenomenon as in the

core-flooding tests.

Figure 4-23 can prove this theory. Also, at the first several cycles, water production is

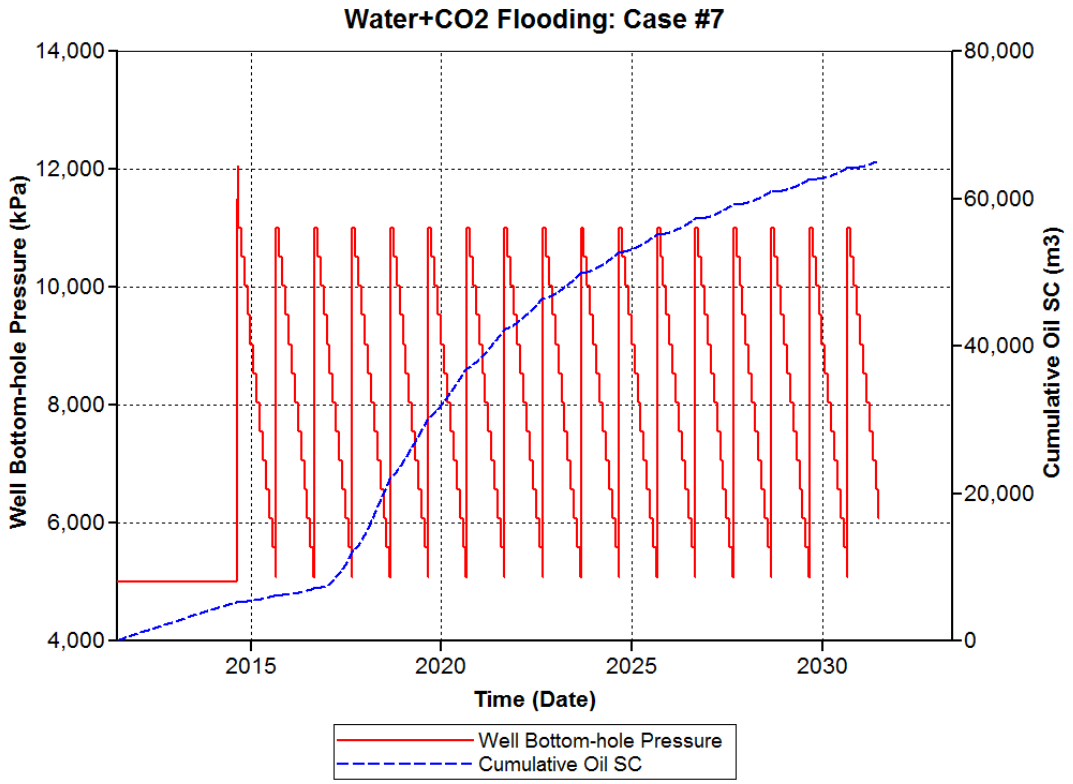

Figure 4-22 Curves of cumulative oil production and production pressure for case #7 in water flooding followed by CO_2 flooding category

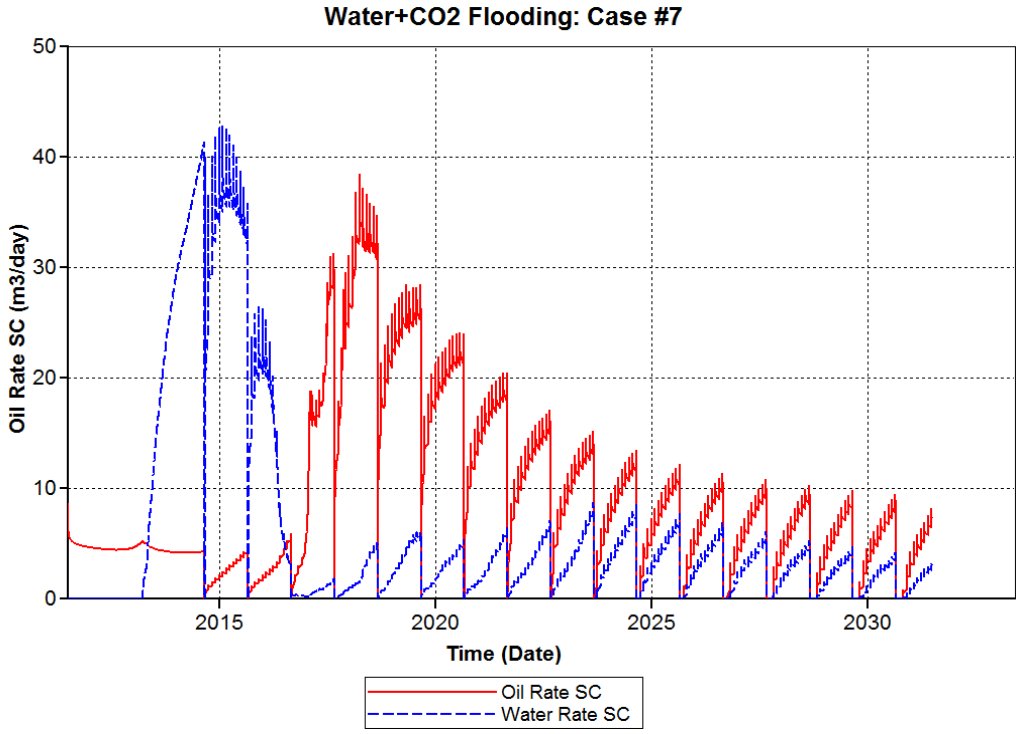

Figure 4-23 Curves of oil production rate and water production rate for case #7 in water flooding followed by CO_2 flooding category

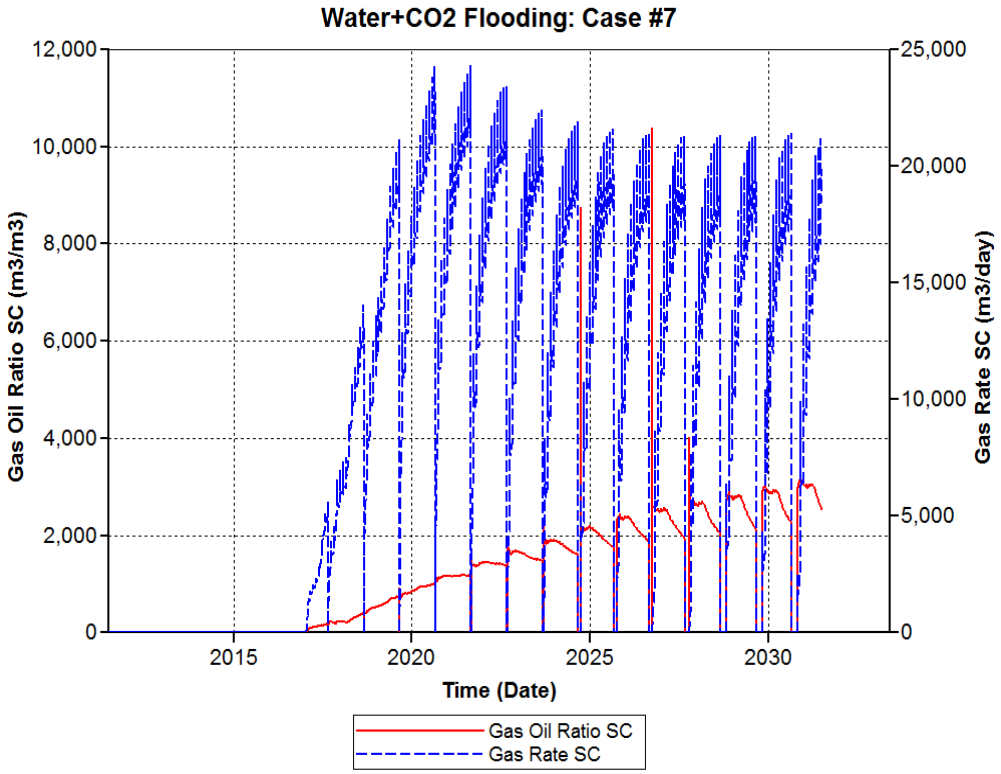

Figure 4-24 Curves of production GOR and gas production rate for case #7 in water flooding followed by CO_2 flooding category

pretty high due to the water in the water channels being flooded out. When almost all the water is gone, a high oil production rate appears and soon reaches the peak point. At peak point, the gas breaks through, and the oil production rate starts to decrease cycle after cycle.

Figure 4-24 is the curves of time vs. production GOR and gas production rate. We can see that when the gas breaks through, the GOR does not go very high. That means the mobility of gas in the oil-gas phase is not high, and the ability to form a continuous gas phase is very low. This is because of foamy oil flow in the reservoir. As CO_2 continues to be injected, the CO_2 in the reservoir meet each other slowly and finally form continuous free gas which leads to the increase of GOR.

4.3.3.2 CO2 flooding without water flooding category best scheme case

In this category, the best performance case is #8. Pure CO_2 was injected into the reservoir without water flooding in advance. The injection rate was 100 m^3/day. At the same time as the CO_2 was injected, the production pressure was depleting from 11 MPa to 5 MPa in two years. Then production pressure was reset to 11 MPa and the next cycle followed. The duration of the whole simulation was 20 years. The recovery factor of this case in 20 years is 31.97%.

Figure 4-25 shows the curves of time vs. cumulative oil production and production pressure for this case. The oil production curve has an upward trend after being flat for a

short time. On the flat curve range, the injected CO_2 spreads and dissolves in the heavy oil

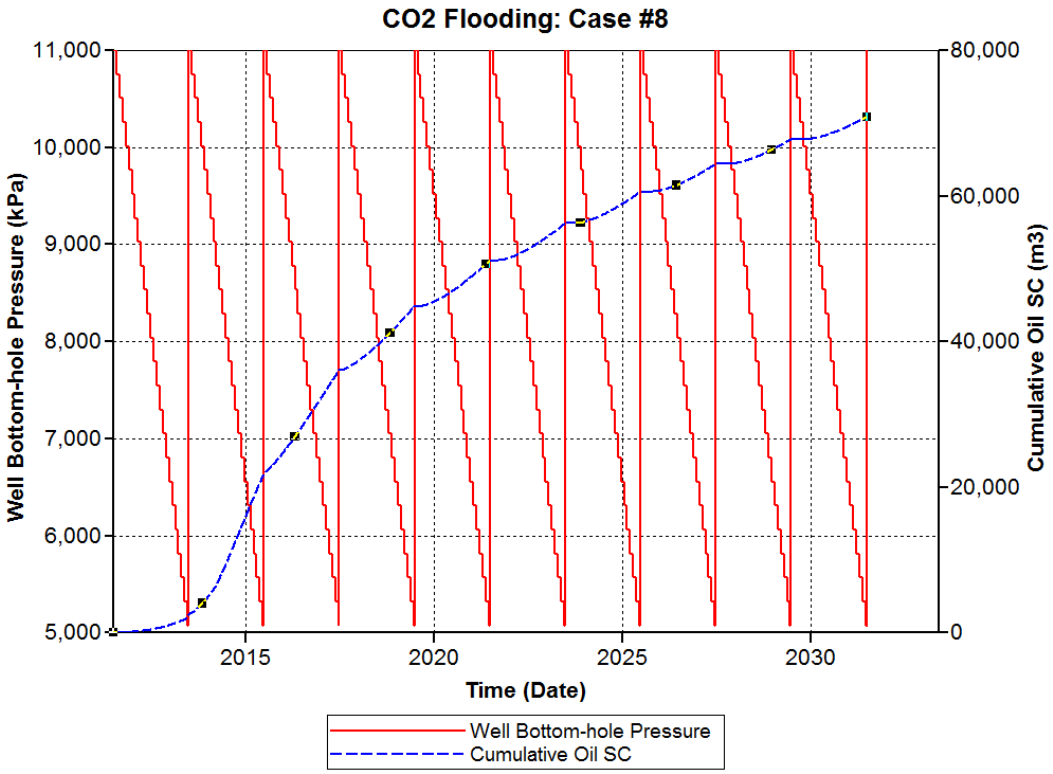

Figure 4-25 Curves of cumulative oil production and production pressure for case #8 in CO_2 flooding without water flooding category

in the reservoir. Only a little heavy oil is produced due to the differential pressure in the reservoir resulting from the gas injection and production pressure depletion. As there was no water flooding in advance, there is no water channel in the reservoir. The gas can spread and come into contact with the heavy oil more efficiently and it is not that easy for the gas to breakthrough compared to the category with water flooding in advance. However, as there is no need to flood water out of the reservoir, the gas breakthrough time is earlier than in the category with water flooding. As the gas breaks through, not only is the mobility of the heavy oil gained by CO_2 dissolution, but also foamy oil flow occurs, and the oil production rate reaches a peak point, as Figure 4-26 shows.

Because of the foamy oil flow, low gas production, low GOR and a high recovery factor are observed at the earlier stages. As more and more CO_2 is injected into the reservoir, the ability of the CO_2 to form a continuous gas phase increases. Moreover, oil is produced in large pores in the reservoir and is occupied by CO_2, which makes it flow easily. These two facts lead to higher and higher gas production rates and production GOR and have a negative effect on foamy oil flow performance, as shown in Figure 4-27.

4.3.3.3 Water flooding followed with flue gas flooding category best scheme case

In the water flooding followed by flue gas flooding category, the case with the best performance is #11. This case has a similar scheme to core-flooding test #6. The water

flooding process was done first. As water cut at the producer reached 97%, the water

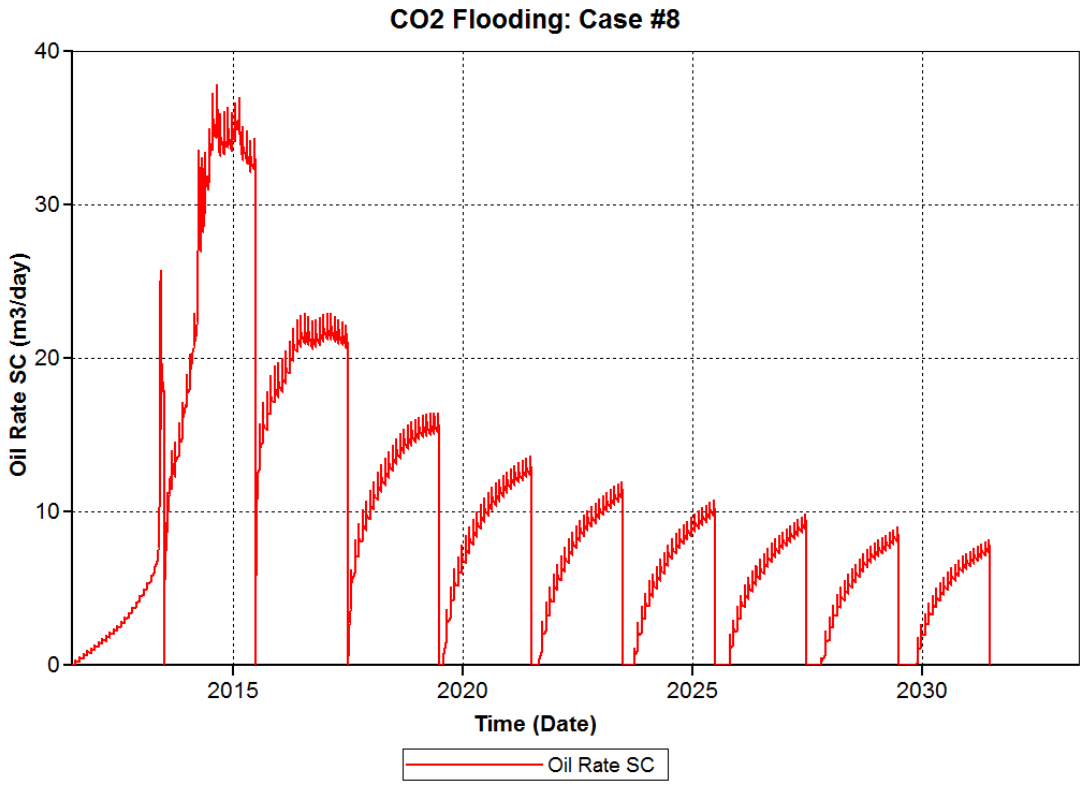

Figure 4-26 Curve of oil production rate for case #8 in CO_2 flooding without water

flooding category

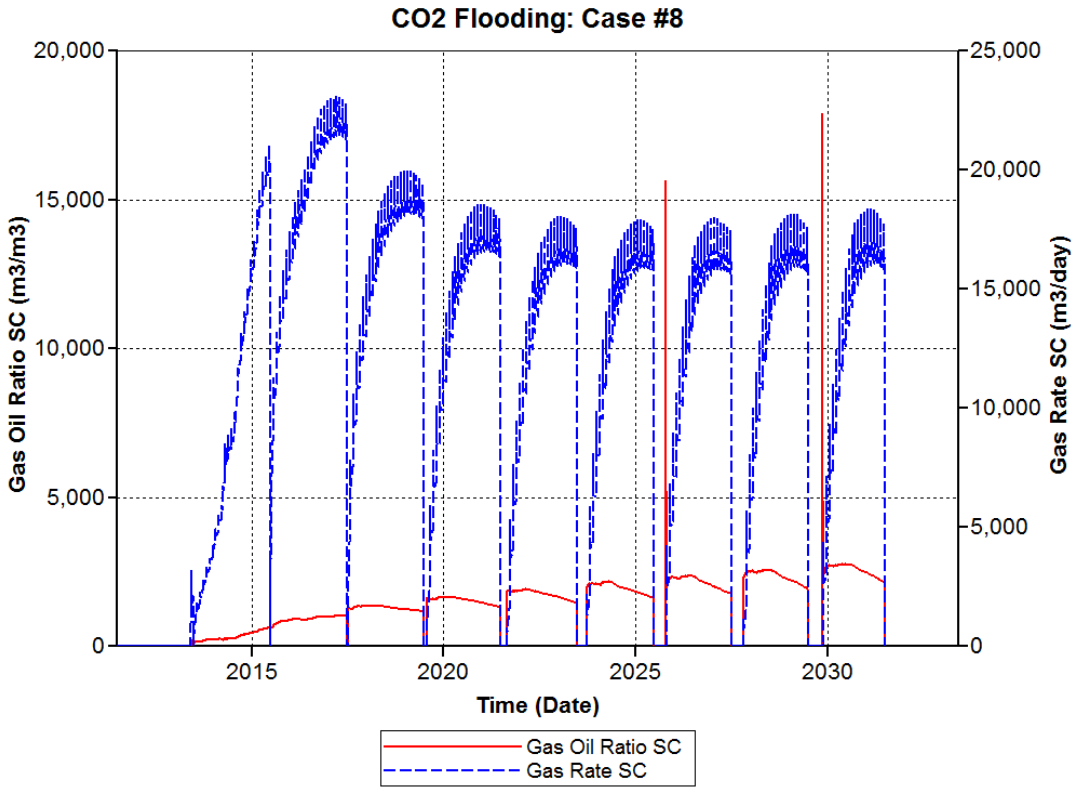

Figure 4-27 Curve of production GOR and gas production rate for case #8 in CO_2 flooding without water flooding category

flooding process ended and gas flooding began. Flue gas consisting of 80% N_2 and 20% CO_2 was injected into the reservoir with an injection rate of 100 m^3/day. As 0.1 PV flue gas was injected, the injector was shut in. The production pressure depletion process followed, starting from 11 MPa to 5 MPa, and duration was one year. Then the production pressure was reset to 11 MPa. Gas injection started again to resume the reservoir pressure to 11 MPa and the next cycle began. The duration of the whole simulation was 20 years. The total recovery factor of this case is 21.77%.

The performance of the flue gas injection was obviously not as good as that of the CO_2 injection. N_2 is a stable gas which almost never dissolves in heavy oil, so only 20% of the injected gas can take effect on dissolution. The other 80% can only maintain the pressure. From Figure 4-28 we can see that the oil production rate is very low compared with the CO_2 flooding cases. The gas production rate is extremely high. Water production rates in the earlier cycles are high because the water in the water channels formed in the water flooding process is flooded out by gas injection. As water is being flooded out, CO_2 in the flue gas dissolves in the heavy oil. When all the water is flooded out, viscosity reduced heavy oil starts to be produced and soon reaches the peak rate.

At the peak rate, gas breakthrough occurs. Although there is no injection gas flow to influence the foamy oil flow due to the injector being shut in when pressure depletes, the performance of foamy oil is still limited. The dissolved CO_2 in heavy oil is too little, and N_2 in the flue gas can still have a negative influence on foamy oil development just like

injection gas flow does. Therefore, when we check production GOR from Figure 4-29, we can clearly see the peak GOR in each cycle.

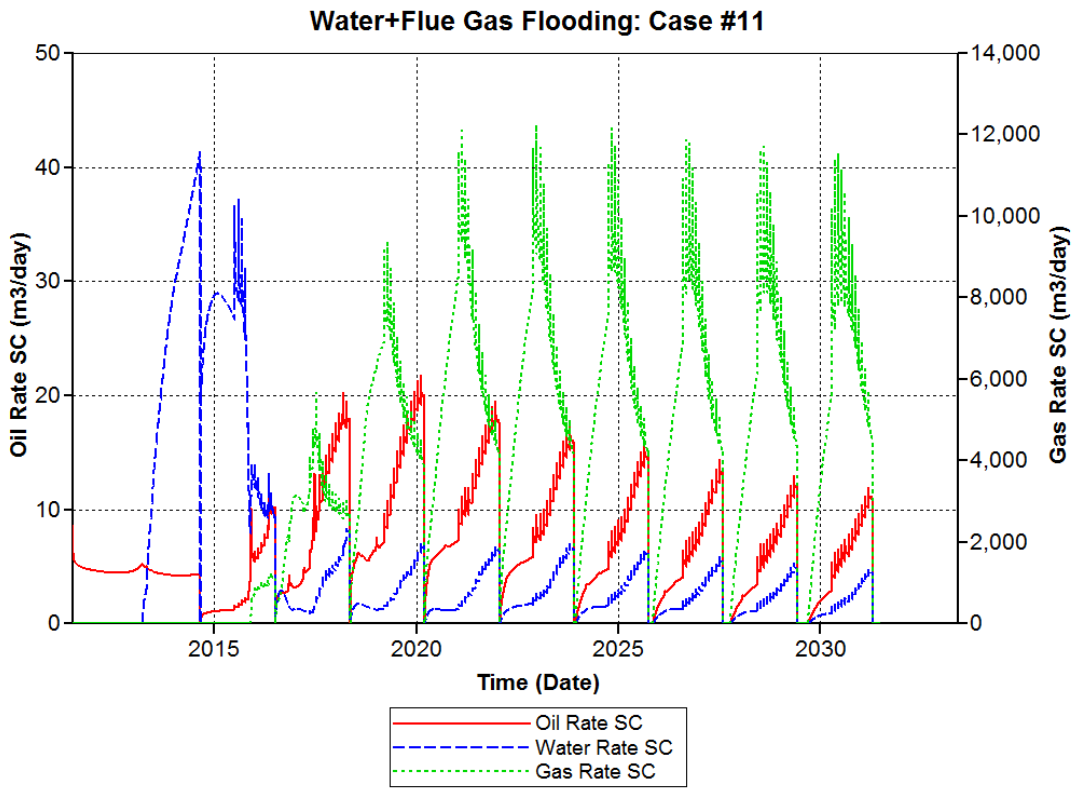

Figure 4-28 Curves of oil, water and gas production rates for case #11 in water flooding followed by flue gas flooding category

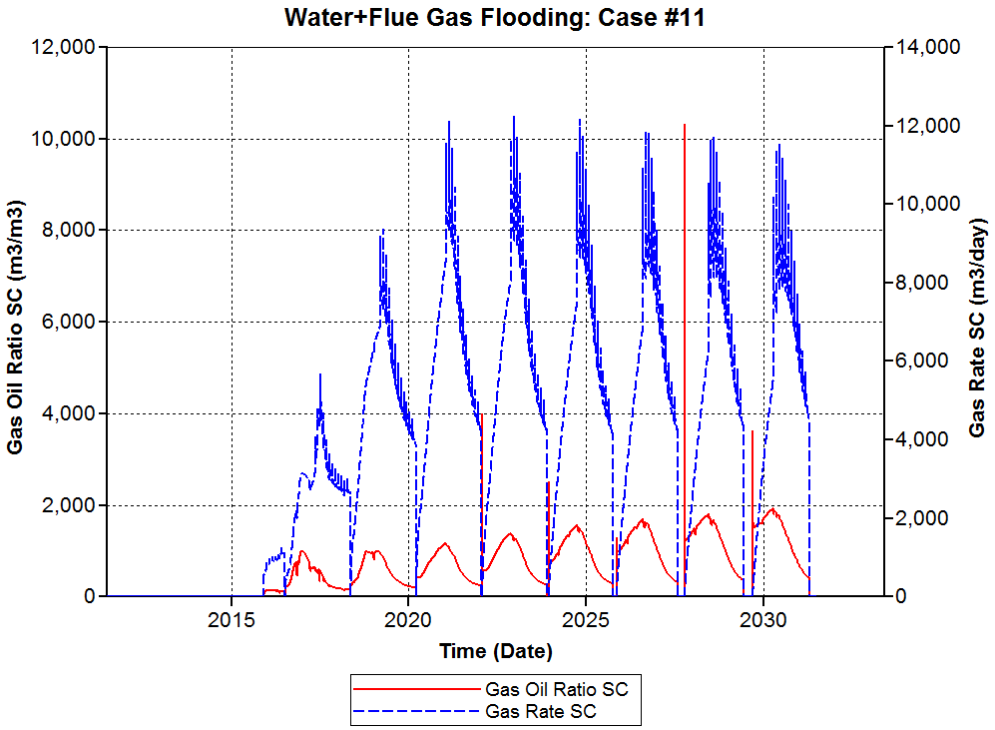

Figure 4-29 Curves of production GOR and gas production rate for case #11 in water flooding followed by flue gas flooding category

CHAPTER 5 CONCLUSIONS AND RECOMMENDATIONS

5.1 Conclusions

In this study, comprehensive studies have been done on the utilization of the CO_2 injection method in heavy oil reservoirs to enhance oil recovery. PVT tests were done to test the properties of oil when CO_2 is dissolved in. Six core-flooding tests were done to test the performance of different CO_2 injection categories, including different injection rates, different production pressure control schemes, and different CO_2 purity. After that, numerical simulations were performed to history match the core-flooding results and the characteristics of the relative permeability were analyzed. Finally, a numerical reservoir model was built, and different CO_2 injection categories were tried on the model to test the performance on a large scale.

Some major conclusions were obtained during the thesis study and are summarized here:

1. From the PVT tests, the performance of CO_2 dissolution in heavy oil to reduce the heavy oil viscosity is proved. The viscosity is largely reduced as CO_2 saturated in the heavy oil. And when pressure is higher, the solubility of CO_2 in the oil is higher, and the viscosity is further reduced.
2. From the core-flooding tests, the results of test #1 with pure CO_2 injected and test #5 with flue gas injected were compared. The pure CO_2 case performed

much better than the flue gas, which is another proof of the effect of CO_2 in heavy oil recovery. And the comparison of the results also indicates that the performance is better when CO_2 has higher purity.

3. The constant production pressure scheme can effectively hold a large displacement pressure in the reservoir which greatly helps more CO_2 dissolve in heavy oil.

4. The results of two constant production pressure tests with different gas injection rates were compared. The lower gas injection rate case has better results, which indicates that a low gas injection rate is beneficial for oil recovery.

5. The production pressure depletion scheme has the function to enlarge the displacement pressure in the reservoir, and moreover, can generate foamy oil near the producer which can greatly enhance heavy oil recovery.

6. Two production pressure depletion scheme cases with different depletion rates and depletion ending pressure were tests and compared. The faster depletion rate case had better results because the faster rate generates foamy oil with better quality for CO_2.

7. A comparison between constant production pressure scheme cases and production pressure depletion cases indicates that foamy oil flow has a positive effect and can greatly enhance heavy oil recovery.

8. A multi-production pressure control scheme case was conducted to test the

performance. The result yielded the highest recovery factor compared to other tests. The result indicates that better CO_2 saturation and a stable foamy oil flow without any interference is beneficial for heavy oil production.

9. From the results of the history matches of the tests by numerical simulation, gas relative permeability of the cases with foamy oil flow is much lower than other cases. This finding is in line with investigations of the literature and proves that foamy oil leads to lower gas mobility.

10. From the results of the tests on the reservoir model, the performance of the CO_2 injection method in a heavy oil reservoir is proved again. Also, a simply constant CO_2 injection rate with a cyclic production pressure depletion scheme case yields the highest recovery factor. The lab scale tests cannot fully reflect all the properties and performances of a method. A numerical field reservoir model or pilot is necessary.

5.2 Recommendations

There are a few recommendations for future work:

1. PVT tests should be redone with higher accuracy. And also, the density of sampled data should be enhanced to give a more sensitive curve which can be used in the investigations of pseudo bubble point and supersaturation in foamy oil.

2. Several more core-flooding tests should be designed without the water flooding process beforehand to compare the different performances of CO_2 flooding acts with and without the effect of water channels.

3. Several more core-flooding tests should be done with different proportions of CO_2 in flue gas to further test the effects of CO_2 purity.

4. Heavy oil samples with different viscosities should be used in the core-flooding tests to test the performance of CO_2 in viscosity reduction in different dead oil viscosities.

5. Real cores collected from the field should be used in core-flooding tests to compare with the artificial cores because the wettability of the two kinds of cores may be different and may affect the relative permeability of the fluids and gases.

REFERENCES

Alomair, O., Iqbal, M. CO_2 Minimum Miscible Pressure (MMP) Estimation using Multiple Linear Regression (MLR) Technique. Society of Petroleum Engineers, 2014

Alshmakhy, A., Maini, B. B. Viscosity of Foamy Oil. In Canadian Unconventional Resources and International Petroleum Conference. Society of Petroleum Engineers, 2010

Arora, P., Kovscek, A. R. Mechanistic Modeling of Solution Gas Drive in Viscous Oils. Paper SPE 69717, 2001

Beeson, D. M., Ortloff, G. D. Laboratory Investigation of the Water-Driven Carbon Dioxide Process for Oil Recovery. Journal of Petroleum Technology, 11(04), 63-66, 1959

Beggs, H. D., Robinson, J. R. Estimating the Viscosity of Crude Oil Systems. Journal of Petroleum Technology, 27(09), 1-140, 1975

Bon, J., Sarma, H. K., Theophilos, A. M. An Investigation of Minimum Miscibility Pressure for CO_2-Rich Injection Gases with Pentanes-Plus Fraction. In SPE International Improved Oil Recovery Conference in Asia Pacific. Society of Petroleum Engineers, 2005

Bora, R., Maini, B. B., Chakma, A. Flow Visualization Studies of Solution Gas Drive Process in Heavy Oil Reservoirs Using a Glass Micromodel. Society of Petroleum

Engineer, 1997

Brook, G., Kantzas, A. Evaluation of Non-thermal EOR Techniques for Heavy Oil Production. In Annual Technical Meeting. Petroleum Society of Canada. 1998

Butler, A. M., Mokrys, I. J. Recovery of Heavy Oils using Vaporized Hydrocarbon Solvents: Further Development of the Vapex Process. Petroleum Society of Canada, 1992

Butler, R. M., McNab, G. S., Lo, H. Y. Theoretical Studies on the Gravity Drainage of Heavy Oil During In-Situ Steam Heating. The Canadian Journal of Chemical Engineering, 59(4), 455-460, 1981

Chew, J. N., Connally Jr, C. A. A Viscosity Correlation for Gas-Saturated Crude Oils, 1959

Chung, F. T. Oil Recovery by Immiscible CO_2 Flooding: Topical report (No. FC22-83FE60149). IIT Research Institute National Institute for Petroleum and Energy Research Bartlesville, Oklahoma, 1988

Chung, F. T., Jones, R. A., Nguyen, H. T. Measurements and Correlations of the Physical Properties of CO_2/Heavy-Crude-Oil Mixtures. SPE Reservoir Eng, 3(3), 822-828, 1988

Claridge, E. L., Prats, M. A Proposed Model and Mechanism for Anomalous Foamy Heavy Oil Behavior. In International Heavy Oil Symposium, pp. 9-20, 1995

Craig, D. R., Bray, J. A. Gas Injection and Miscible Flooding (No. CONF-710677-). Alberta Oil Gas Conser Bd., 1971

Danesh, A. PVT and Phase Behavior of Petroleum Reservoir Fluids (Vol. 47). Elsevier, 1998

Dong, M., Huang, S., Hutchence, K. Methane Pressure Cycling Process with Horizontal Wells for Thin Heavy Oil Reservoirs. In SPE Asia Pacific Oil and Gas Conference and Exhibition. Society of Petroleum Engineers, 2004

DU, Z., Chan, C., Zeng, F. An Experimental Study of the Post-CHOPS Cyclic Solvent Injection Process. Society of Petroleum Engineers, 2013

Dusseault, M. B. (2001). Comparing Venezuelan and Canadian Heavy Oil and Tar Sands. In Canadian International Petroleum Conference, Calgary, Alberta, Canada pp. 2001-061, 2001

Dyer, S. B., Farouq Ali, S. M. The Potential of the Immiscible Carbon Dioxide Flooding Process for the Recovery of Heavy Oil. In 3rd Technical Meeting of the South Saskatchewan Section, the Petroleum Society of CIM, Regina, 1989

Emera, M. K., Sarma, H. K. A Genetic Algorithm-Based Model to Predict CO_2-Oil Physical Properties for Dead and Live Oil. Journal of Canadian Petroleum Technology, 47(2), 52-61, 2008

Enayati, M., Heidaryan, E., Mokhtari, B. New Investigations into Carbon Dioxide Flooding by Focusing on Viscosity and Swelling Factor Changes. In Canadian International Petroleum Conference/SPE Gas Technology Symposium, pp. 17-19, 2008

Garcia, F. M. A Successful Gas-Injection Project in a Heavy Oil Reservoir. Society of Petroleum Engineers, 1983

Geilikman, M. B., Dusseault, M. B., Dullien, F. A. L. Dynamic Effects of Foamy Fluid Flow in Sand Production Instability. In SPE International Heavy Oil Symposium, Calgary, Alberta, Canada, pp. 19-21, 1995

Ghedan, S. Global Laboratory Experience of CO_2-EOR Flooding. In SPE/EAGE Reservoir Characterization & Simulation Conference, 2009

Hall, H. N., Geffen, T. M. A Laboratory Study of Solvent Flooding. Society of Petroleum Engineers, 1957

Hatzignatiou, D. G., Lu, Y. Feasibility Study of CO_2 Immiscible Displacement Process in Heavy Oil Reservoirs. In Annual Technical Meeting, Calgary, Alberta, Canada, 1994

Holm, L. W. Carbon Dioxide Solvent Flooding for Increased Oil Recovery, 1959

Holm, L. W. Miscibility and Miscible Displacement. Journal of Petroleum Technology, 38(08), 817-818, 1986

Holm, L. W., O'Brien, L. J. Carbon Dioxide Test at the Mead-Strawn Field. Society of Petroleum Engineers, 1971

Holm, W. L. Evolution of the Carbon Dioxide Flooding Processes. Journal of Petroleum Technology, 39(11), 1-337, 1987

Huang, S. S., Pappas, E. S., Jha, K. N. The Carbon Dioxide Immiscible Recovery Process and its Potential for Saskatchewan Reservoirs. In Technical Meeting/Petroleum

Conference of the South Saskatchewan Section. Petroleum Society of Canada, 1987

Istchenko, C. M., Gates, I. D. The Well-Wormhole Model of Cold Production of Heavy Oil Reservoirs. In SPE Heavy Oil Conference and Exhibition. Society of Petroleum Engineers, 2011

Jhaveri, B. S., Brodie, J. A., Zhang, P., Daae, V. Review of BP's Global Gas Injection Projects. Society of Petroleum Engineers, 2014

Johnson, W. E., Macfarlane, R. M., Breston, J. N., Neil, D. C. Laboratory Experiments with Carbonated Water and Liquid Carbon Dioxide as Oil Recovery Agents. Prod. Monthly, 17, 1952

Kantar, K., Karaoguz, D., Issever, K., Varana, L. Design Concepts of a Heavy Oil Recovery Process by an Immiscible CO_2 Application. Journal of Petroleum Technology, 37(02), 275-283, 1985

Kehn, D. M., Pyndus, G. T., Gaskell, M. H. Laboratory Evaluation of Prospective Enriched Gas-Drive Projects. Journal of Petroleum Technology, 10(06), 45-48, 1958

Kraus, W. P., McCaffrey, W. J., Boyd, G. W. Pseudo-Bubble Point Model for Foamy Oils. Paper, 1101, 93-94, 1993

Lederer, E. L. Mischungs-and Verdünnungsviscosität. In 1st World Petroleum Congress. World Petroleum Congress, 1933

Lim, G. B., Kry, R. P., Harker, B. C., Jha, K. N. Cyclic Stimulation of Cold Lake Oil Sand with Supercritical Ethane. In International Heavy Oil Symposium, pp. 521-528, 1995

Lobe, V.M. A Model for the Viscosity of Liquid-Liquid Mixture. MASc. Thesis, University of Rochester, Rochester, NY, 1973

Mai, A., Bryan, J., Goodarzi, N., Kantzas, A. Insights into Non-Thermal Recovery of Heavy Oil. Journal of Canadian Petroleum Technology, 48(3), 27, 2009

Maini, B. B. Foamy Oil Flow in Primary Production of Heavy Oil under Solution Gas Drive. Paper SPE 56541, 1999

Maini, B. B. Foamy-Oil Flow. Journal of Petroleum Technology, 53(10), 54-64, 2001

Maini, B. B. Effect of Depletion Rate on Performance of Solution Gas Drive in Heavy Oil Systems. In SPE Latin American and Caribbean Petroleum Engineering Conference. Society of Petroleum Engineers, 2003

Maini, B. B., Sarma, H. K., George, A. E. Significance of Foamy-oil Behavior in Primary Production of Heavy Oils. Petroleum Society of Canada, 1993

Masters, C. D., Attanasi, E. D., Dietzman, W. D., Meyer, R. F., Mitchell, R. W., Root, D. H. World Resources of Crude Oil, Natural Gas, Natural Bitumen, and Shale Oil. World Petroleum Congress, 1987

Mastmann, M., Moustakis, M. L., Bennion, D. B. Predicting Foamy Oil Recovery. In SPE Western Regional Meeting. Society of Petroleum Engineers, 2001

Mehrotra, A. K., Svrcek, W. Y. Correlations for Properties of Bitumen Saturated with CO_2, CH_4 and N_2, and Experiments with Combustion Gas Mixtures. Journal of Canadian Petroleum Technology, 21(06), 1982

Meyer, R. F. World Heavy Crude Oil Resources. In Proceedings of the 15th World Petroleum Congress. New York: John Wiley & Sons, 1997

Meyer, R. F., Attanasi, E. D. Heavy Oil and Natural Bitumen-Strategic Petroleum Resources. World, 434, 650-7, 2003

Miller, J. S., Jones, R. A. A Laboratory Study to Determine Physical Characteristics of Heavy Oil after CO_2 Saturation. Society of Petroleum Engineers, 1981

Moortgat, J. B., Firoozabadi, A., Li, Z., Espósito, R. O. CO_2 Injection in Vertical and Horizontal Cores: Measurements and Numerical Simulation. SPE Journal, 18(02), 331-344, 2013

Moritis, G. EOR Oil Production up Slightly. Oil & Gas Journal, 96(16), 49-49, 1998

Nasehi Araghi, M., Asghari, K. Use of CO_2 in Heavy Oil Water flooding. In SPE International Conference on CO2 Capture, Storage, and Utilization. Society of Petroleum Engineers, 2010

Or, C., Sasaki, K., Sugai, Y., Nakano, M., Imai, M. Experimental Study on Foamy Viscosity by Analyzing CO_2 Micro-Bubbles in Hexadecane Gas, 4, 1, 2014

Ostos, A., Maini, B. Capillary Number in Heavy Oil Solution Gas Drive and its Relationship with Gas-Oil Relative Permeability Curves. In SPE/DOE Symposium on Improved Oil Recovery. Society of Petroleum Engineers, 2004

Pooladi-Darvish, M., Firoozabadi, A. Solution-Gas Drive in Heavy Oil Reservoirs. Journal of Canadian Petroleum Technology, 38, 54-61, 1999

Ramey, H. J. In Situ Combustion. World Petroleum Congress, 1971

RoJa, Q. A., Tao Zhu, S. P. E., Dyer, S. B. Scaled Model Studies of CO_2 Floods. SPE Reservoir Engineering, 1991

Sahin, S., Kalfa, U., Celebioglu, D. Bati Raman Field Immiscible CO_2 Application--Status Quo and Future Plans. SPE Reservoir Evaluation & Engineering, 11(04), 778-791, 2008

Sarma, H., Maini, B. Role of Solution Gas in Primary Production of Heavy Oils. In SPE Latin America Petroleum Engineering Conference. Society of Petroleum Engineers, 1992

Sheng, J. J., Hayes, R. E., Maini, B. B., Tortike, W. S. A Dynamic Model to Simulate Foamy Oil Flow in Porous Media. In SPE Annual Technical Conference, pp. 687-699, 1996

Sheng, J. J., Maini, B. B., Hayes, R. E., Tortike, W. S. Critical Review of Foamy Oil Flow. Transport in Porous Media, 35(2), 157-187, 1999

Shi, R., Kantzas, A. Enhanced Heavy Oil Recovery on Depleted Long Core System by CH_4 and CO_2. In International Thermal Operations and Heavy Oil Symposium. Society of Petroleum Engineers, 2008

Shu, W. R. A Viscosity Correlation for Mixtures of Heavy Oil, Bitumen, and Petroleum Fractions, 1984

Simon, R., Graue, D. J. Generalized Correlations for Predicting Solubility Swelling and

Viscosity Behavior of CO_2-Crude Oil Systems. Journal of Petroleum Technology, 17(01), 102-106, 1965

Smith, G. E. Fluid Flow and Sand Production in Heavy-Oil Reservoirs under Solution-Gas Drive. SPE Production Engineering, 3(02), 169-180, 1988

Spivak, A., Chima, C. M. Mechanisms of Immiscible CO_2 Injection in Heavy Oil Reservoirs, Wilmington Field, CA. Paper SPE 12667, 15-18, 1984

Srivastava, R. K., Huang, S. S., Dong, M. Laboratory Investigation of Weyburn CO_2 Miscible Flooding. Journal of Canadian Petroleum Technology, 39(2), 41-51, 2000

Stone, H. L., Crump, J. S. The Effect of Gas Composition upon Oil Recovery by Gas Drive. Society of Petroleum Engineers, 1956

Tang, G. Q., Firoozabadi, A. Gas and Liquid-Phase Relative Permeability for Cold Production from Heavy Oil Reservoirs. In SPE Annual Technical Conference, 1999

Teja, A. S. A Corresponding States Equation for Saturated Liquid Densities. Applications to LNG. AIChE Journal, 26(3), 337-341, 1980

Holm, L. W., Josendal, V. A. (1974). Mechanisms of Oil Displacement by Carbon Dioxide. Journal of Petroleum Technology, 26(12), 1427-1438, 1974

Vittoratos, E., Scott, G. R., Beattie, C. I. Cold Lake Cyclic Steam Stimulation: A Multi-Well Process, 1990

Wang, M., Lawal, A., Stephenson, P., Sidders, J., Ramshaw, C. Post-Combustion CO_2 Capture with Chemical Absorption: A State-Of-The-Art Review. Chemical

Engineering Research and Design, 89(9), 1609-1624, 2011

Welker, J. R. Physical Properties of Carbonated Oils. Journal of Petroleum Technology, 15(08), 873-876, 1963

Whorton, L. P., Kieschnick, W. F. A Preliminary Report on Oil Recovery by High-Pressure Gas Injection. American Petroleum Institute, 1950

Zhang, F., Fan, X., Ding, J. Field Experiment of Enhancing Heavy Oil Recovery by Cyclic Fuel Gas Injection. In International Oil and Gas Conference and Exhibition in China. Society of Petroleum Engineers, 2000

Zhang, Y. P., Sayegh, S., Huang, S. Enhanced Heavy Oil Recovery by Immiscible WAG Injection. In Canadian International Petroleum Conference. Petroleum Society of Canada, 2006